Effectiveness of adaptation measures to make the urban rainwater distribution more robust after short intense rainfall events

R. G. Wiebing

December 2023

UNIVERSITY OF TWENTE.

Nelen & Schuurmans

"All models are wrong, but some are useful"

George E. P. Box (1974)

Effectiveness of adaptation measures to make the urban rainwater distribution more robust after short intense rainfall events

Master Thesis

University of Twente

Faculty of Engineering Technology
Department of Water Engineering & Management

Author: R.G. (Rutger) Wiebing

Date: December 1, 2023
Version: Final

Supervisors:

Dr. ir. M.J. (Martijn) Booij	Head of the committee	University of Twente
Dr. ing. T.H.M. (Tom) Rientjes	Daily Supervisor	University of Twente
N. (Noortje) Oosterhoff, MSc	Daily Supervisor	Nelen & Schuurmans
Ir. R. (Ria) Löschner – Wolleswinkel	Supervisor	Nelen & Schuurmans
R. (Remo) van Tilburg, MSc	Supervisor	Nelen & Schuurmans

Preface

In front of you lies my thesis which I wrote as final part of the master *Water Engineering and Management* at the University of Twente. It is written during my graduation internship at Nelen & Schuurmans in 2023.

First of all, I would like to thank my supervisors at Nelen & Schuurmans. Weekly meetings with Noortje Oosterhoff, the daily supervisor, helped me a lot by giving guidance, receiving feedback, discussing content related questions, and to find my way within the company. When complex questions about QGIS or model implementations arose, Remo van Tilburg was there to get me started whereafter I could proceed. During the thesis, Ria Löschner always maintained the general overview, and provided me with valuable feedback and guidance. In addition, I would like to thank all colleagues for their warm welcome and contributions to a pleasant working atmosphere.

Secondly, I would like to thank Martijn Booij and Tom Rientjes, supervisors from the university. Monthly meetings were always pleasant and informative. Their knowledge about hydrodynamic and hydrological processes allowed for in depth discussions, as well as setting the right scope for this thesis project and improving it by their valuable feedback.

Lastly, I would thank Rudie Tempels and Bas Berends, who work at the municipality of Doetinchem. They are experts who are already working on water related topics in the area for numerous years. Both have provided valuable input as experts, as well as granting me access to documents and historic measurements.

I am grateful for all encountered enthusiasm when I asked questions or asked for information, and I hope you enjoy reading my thesis.

Rutger Wiebing
Utrecht, December 2023

Summary

Higher frequencies of short and increasingly intense rainfall events as well as prolonged periods of limited rainfall are expected due to the changing climate. Particularly in urban areas, this can result in both insufficient and excessive quantities of water, as well as water quality issues. Therefore, a robust spatial rainwater distribution is needed to retain (i.e., store) rainwater in desired locations, while also preventing excessive amounts of rainwater in locations where it results in damage, hindrance, and sewage overflows.

Hence, the research aim was to study the effectiveness of adaptation measures to increase the robustness of the spatial rainwater distribution. This is done by quantifying effects of measures using a fully distributed 1D-2D hydrodynamic model *3Di*. As a first step, the overall performance of the used model was evaluated when subjected to historic short and intense rainfall events. It showed good performance when its results were compared to measurements and expert judgement. The second step was to establish *base scenarios* for short and intense design rainfall events with varying cumulative rainfall depths (i.e., varying *extremeness*), predicted for climate conditions in 2050. These base scenarios are used to assess the spatial rainwater distribution of the current urban area when subjected to future rainfall events. Lastly, proposed measures are separately implemented into the model, to study their isolated effectiveness to increase the robustness of the spatial rainwater distribution. The effects of measures are quantified in reference to the base scenarios using the following four metrics: relative increase in retained rainwater, relative decrease of vulnerable buildings and inaccessible roads, and relative decrease in sewerage overflows.

Four measures have been implemented on municipal scale. Two on private properties, being: storing roof runoff at 50% of the buildings (*Storepp*), and reducing impervious surface with 50% (*Erf50p*). The other two are implemented in the public space, being: lowering verges to 10 cm under adjacent road section elevation (*Road10*), and implementing 30 cm deep wadis (*Wadi30*, internationally called *bioswales*). Measures showed varying effectiveness for assessed rainfall events and metrics. It was found that measure *Erf50p* was least effective for all assessed events and metrics. *Storepp* shows consistent effectiveness for all rainfall depths, becoming the second most effective to retain rainwater and reduce sewerage overflows for larger rainfall depths. *Road10* is most effective for all metrics during smaller rainfall depths. In addition, it is the most effective to reduce inaccessibility of roads for all assessed depths. *Wadi30* is most effective to retain rainwater, reduce vulnerable buildings, and reduce overflows for larger rainfall depths. Yet, geographical features within urban areas are found to be significantly affecting the effectiveness of measures, stressing the importance of its location and implementation and thus the use of a high-resolution 1D-2D model.

To increase confidence and familiarity with adaptation measures, results of a quantitative study as described should be shared with persons related to urban climate adaptation. Subsequently, it helps policy makers to establish adaptation plans and designers to make resilient urban development designs. Consequently, urban areas can become more resilient to changing rainfall patterns, ensuring liveability in future climate conditions.

Content

1 Introduction

1.1 Problem context

Future meteorological conditions in the Netherlands will change due to the changing climate, resulting in more extreme weather. Effects will be particularly large in the summer period, where both average and maximum temperatures will increase, and periods without rainfall will be prolonged (Bessembinder et al., 2023). Furthermore, rainfall events will become more extreme, consisting of larger amounts of rainfall in shorter time periods, i.e., contain higher rainfall intensities (Bessembinder et al., 2023; KNMI, 2022). Due to the increasingly unequal occurrence of rainfall over time, focus has shifted from *swiftly draining rainwater* to *retaining rainwater* (Ministry of I&W, 2022; Stumpe & Tielrooij, 2000). The additionally retained rainwater can thereafter for instance be used by vegetation, to mitigate drought stress. Retention is particularly important for areas in the higher-elevated sandy parts of the Netherlands, which are solely rainfed since water inlet is often infeasible (Hoogvliet et al., 2021; Mondeel & Drost, 2022; Veraart & Voskamp, 2022). Rainwater which is drained out of the area is therefore irreversible *lost*.

The retention of rainwater is particularly challenging during short and intense rainfall events. Rainfall intensities during these events commonly exceed the infiltration capacities of surface areas, generating *excess* rainwater (i.e., rainwater available for surface runoff). This process is exacerbated within urban areas due to high percentages of impervious surfaces and limited storage capacities for excess rainwater. Hence, excess rainwater is rapidly drained by waterways and a dense sewerage system. Yet, the draining capacity of the urban water system is limited which can thus be exceeded during intense rainfall events. Consequently, the sewerage system will overflow into surface waters or pluvial flooding occurs, or both. Sewerage overflows contribute to degrading water qualities, while pluvial flooding induces hindrance and damage (Beersma et al., 2019; Guo et al., 2021; KNMI, 2021).

Limiting sewage overflows and pluvial flooding, as well as increasing rainwater retention are three municipal objectives to ensure high urban living standards (Dolman & Brolsma, 2023; VNG, 2017). Urban areas should thus adapt to mitigate negative effects induced by higher frequencies of short and increasingly intense rainfall events due to climate change, making it more *climate resilient*. To increase this resilience, it is needed to implement adaptation measures to aim for a robust urban rainwater distribution with increased rainwater retention, while also preventing excessive amounts of rainwater where it leads to damage, hindrance, and sewage overflows.

Ideally, adaptation measures should have a positive effect on all three mentioned municipal objectives to create a robust urban rainwater distribution efficiently, since municipal resources and available urban spaces are scarce. A lot of interest for this topic is also seen in literature, where rainwater is increasingly seen as a resource instead of solely a nuisance which has to drained as fast as possible (Dolman & Brolsma, 2023; Zeleňáková, 2021; Zischg et al., 2018). Yet, no best practices have been established on how to assess the effectiveness of measures to increase the robustness of an urban rainwater distribution, stressing the complexity of such areas. *Section 1.2* gives an overview of present state-of-the-art methods.

1.2 State-of-the-art to assess effects of measures on a robust rainwater distribution

A first division in evaluating measures for a robust spatial rainwater distribution can be made between qualitative and quantitative methods. Qualitative approaches are based on multi-criteria analysis (MCA) which support a ranking of the effectiveness of measures based on multiple criteria. Expert judgement is often involved to assess the effects of measures on different criteria, as well as the relative importance of criteria. de Oliveira Campos et al. (2020) and He et al. (2019) show systematic approaches to perform a MCA for urban resilience measures regarding the spatial rainwater distribution. An advantage is that measures can be assessed on a large range of different criteria which are not necessarily linked. This enables the assessment of measures' effects on a range of objectives and *co-benefits* to increase urban resilience. Despite the systematic approaches, these methods remain partly subjective and susceptible to manipulation since expert judgement is involved to a large extent (Cea & Costabile, 2022). Therefore, results of quantitative studies, using models, are considered to be more precise and objective.

Hydrodynamic models attempt to simulate the distribution of rainwater through the urban area with the help of physically based equations regarding the motion of fluid (Teng et al., 2017). Modelling the distribution of water through the urban area can be done in 1D, 2D, 3D or coupled models (e.g., 1D-2D). Traditionally, 1D modelling is used for sewer network and channel modelling based on cross sections. In addition, flood inundation planes can be added (Bulti & Abebe, 2020; Cea & Costabile, 2022; Guo et al., 2021; Kuiry, Sen, & Bates, 2010; Teng et al., 2017). An advantage of these models is that they tend to be computationally inexpensive and do not require extensive input data. A large number of studies can be found using 1D models such as SWMM or MUSIC, for instance in Li et al. (2016, 2018), Gong & Xu (2016), Qin et al. (2013), Xiong et al. (2020), and Zischg et al. (2018). Within these studies, high similarities between modelled and measured discharges are found. In these model, urban areas are split in sub-catchments (i.e., lumped catchment model). Each sub-catchment produces an amount of excess rainwater, based on calibrated parameters characterising each catchment. At a defined point in the catchment area, excess rainwater is thereafter drained by waterways or sewerage system. However, interactions of rainwater flow between catchments (surface or sewerage flow) are excluded (Xiong et al., 2020). In addition, rainwater routing (flow directions) and ponding within the sub-catchment is not studied, i.e., inundation depths of pluvial flooding cannot be determined precisely (Bulti & Abebe, 2020; Cea & Costabile, 2022; Guo et al., 2021). Moreover, this method is less suited to study effects of differing climate conditions and implementation of measures since the sub-catchments are calibrated for the present situation. Consequently, it is not known whether those calibrated parameters are valid for changed conditions, such as changed meteorological conditions for future climate scenarios or changes within the study area due to implemented measures.

2D models are capable of modelling water movement in two directions, assuming shallow water conditions for the third direction, i.e., the height of water columns (Shallow Water Equations,

SWE). Hence, 2D models do not account for friction caused by 3D objects, such as a wall (Volp, Van Prooijen, & Stelling, 2013). However, 3D modelling of flow dynamics is deemed unnecessary when modelling inundation depths and spatial rainwater distributions within urban areas, particularly when assessing it on large spatial scales (Teng et al., 2017).

High spatial variation within the urban surface area (e.g., elevated sidewalks) can be explicitly represented in 2D models as long as the modelling grid is fine enough. This results in a *fully distributed model*, which calculates the distribution of rainwater on every ground surface cell. While computational costs are higher for 2D models compared to 1D models, 2D-models have the capability to simulate timing and duration of inundation with high accuracy (Cea & Costabile, 2022; Guo et al., 2021; Teng et al., 2017). Within 2D SWE-based models, a distinction between simplified and full SWE-models can be made. Simplified SWE-based models omitted one or more terms from the SWE to save computational costs. Yet, 2D models based on the full SWE are most effective for studying the overland distribution of rainwater across an urban area as of now (Cea & Costabile, 2022; Guo et al., 2021; Xing et al., 2021). But these models do not incorporate sewerage systems or narrow waterways, which can have significant effects on rainwater distributions across an urban area (Haghighatafshar et al., 2018; Wei et al., 2022). Therefore, a 2D model is most suited to study the effects of measures when a dense drainage network is absent, or when its contribution to rainwater drainage is insignificant compared to the assessed rainfall event (Bulti & Abebe, 2020). Urban areas generally do have a dense drainage network of sewerage pipes however, limiting the effective use of 2D models in an urban context to study the effects of measures as for instance shown in Folkesson (2020) and Zischg et al. (2018). These show that outcomes of inundation depths and drained volumes are disputable since limited interaction (i.e., only overland flow) of a sub-catchment under study with its upstream and downstream sub-catchments is present. Yet, those interactions are very important to make urban areas more resilient as a whole (Folkesson, 2020; Haghighatafshar et al., 2018; Wei et al., 2022). Therefore, studying the effectiveness of measures to make the urban area more robust on catchment scale is limited when using a 2D model.

A 1D-2D model or the coupling of a 1D and 2D model can significantly improve the quality of rainwater distribution modelling within an urban area, accurately estimating timing and maximum discharges of peaks, run-off volumes, and inundation depths and extents (Cea & Costabile, 2022; Guo et al., 2021; Patra, Kumar, & Mani, 2016). Consequently, these models are also effective in assessing the effects that adaptation measures have on the urban rainwater distribution, as shown in Ahiablame & Shakya (2016), Costa et al. (2021), and Haghighatafshar et al. (2018). The main difficulty to apply 1D-2D modelling is that information about the sewerage network must be available in detail (Cea & Costabile, 2022; Guo et al., 2021). In addition, 1D-2D modelling is computationally more expensive than 1D or 2D modelling, and it can make computations instable.

General data availability is high and accurate within the Netherlands. This includes detailed information about soil types, digital elevation maps (DEM), surface waters, and sewer system dimensions. Therefore, a fully distributed 1D-2D hydrodynamic model can generally be used to its full potential when studying a Dutch urban area. Yet, computational time can still be a limitation when such detailed input data is available.

Some modelling software overcome the drawback of increased computational costs by implementing sophisticated modelling techniques. For example, some modelling software include local refinements in grid sizes to speed up calculation time by modelling areas of less interest in coarser resolution, such as HEC-RAS, D-Hydro, TUFLOW, 3Di, MIKE FLOOD, and InfoWorks ICM. Another innovative technique to reduce computational times is the *subgrid technique*, implemented in HEC-RAS 5.0, TUFLOW, and 3Di modelling software (W. Schuurmans & van Leeuwen, 2017). It allows for incorporation of high-resolution spatial data without averaging it within computational grid cells. Therefore, the subgrid technique allows for lower computational times while maintaining high accuracy outcomes (De Bruijn et al., 2018; W. Schuurmans & van Leeuwen, 2017; Volp et al., 2013). Both HEC-RAS 5.0 and 3Di are considered amongst the best 1D-2D hydrodynamic models available as concluded in Henckens & Engel (2017). Yet, 3Di has better performance when modelling (very) shallow water flows or full sewerage pipes in comparison to HEC-RAS 5.0 (Henckens & Engel, 2017). In addition, 3Di model computations are cloud-based (Henckens & Engel, 2017; W. Schuurmans & van Leeuwen, 2017). This makes it very suitable for scenario analysis since multiple scenarios can be computed parallel to each other. Hence, state-of-the-art 1D-2D hydrodynamic modelling software 3Di will be used within this study. General model characteristics and its setup for this study are described in *Section 2.2*.

1.3 Research gap

Comprehensive studies on the urban water balance are not commonly performed in the Netherlands (Hoogvliet et al., 2013), but needed to assess rainwater retention. When it is attempted, it is often conceptually solved on larger timescales as found in Brolsma et al. (2016), and Hoogvliet et al. (2013). Yet, it would also be beneficial to assess if adaptation measures are effective to increase rainwater retention after short and intense rainfall events, which are typical for the summer period when rainwater is scarce. In addition, those events cause most overflows, as well as damage and hindrance due to pluvial flooding. Therefore, measures which are effective to retain rainwater, limit pluvial flooding and sewerage overflows can have a large contribution to a robust spatial rainwater distribution. Effects of measures on all mentioned aspects of a more robust rainwater distribution, while incorporating interconnectedness of urban sub-catchments, can be modelled by a high-resolution 1D-2D model. As of now, such research on larger urban scales is not commonly performed due to computational limitations, resulting in the lack of quantitative data about the effectiveness of adaptation measures (Costa et al., 2021; Haghighatafshar et al., 2018). Studies about the effectiveness of adaptation measures are needed however, to implement effective measures needed for a resilient and liveable urban area in the future.

1.4 Research aim and questions

1.4.1 Research aim

The aim of this research is to assess which adaptation measures are effective to make the spatial rainwater distribution more robust after short and intense rainfall events. Their effectiveness on making the spatial rainwater distribution more robust will be assessed by quantifying them in terms of increasing rainwater retention, limiting pluvial flooding, and limiting sewerage overflows. This will be assessed on municipal scale.

1.4.2 Research questions

The setup and input data of the used 3Di model is described in more detail in *Section 2.2*. Although data sources within the Netherlands are often open source and of high quality, uncertainties are present in both input data as well as the model itself. Therefore, it is useful to evaluate a model's performance with reference to reality, for the intended use of the model. Thus, an evaluation of model outcomes with reference to historic rainfall events is performed, leading to Question 1:

Question 1: How does the model perform in replicating the spatial rainwater distribution across the study area after historic short intense rainfall events?

After the model performance has been evaluated, it will be used to set base scenarios where outcomes of model runs with implemented measures are compared to. To establish base scenarios, rainfall events which will be used as model input have to be chosen. For scenario analysis, *design rainfall events* are commonly used within the Netherlands. Those will be investigated, after which a choice is made which events are useful to achieve the study objective. Model runs with these chosen design rainfall events will function as base scenarios, to answer Question 2 about the present functioning of the urban area:

Question 2: How does the urban area presently function when subjected to selected design rainfall events?

Next, it will be assessed what measures presently applied within the Netherlands to enhance a robust spatial rainwater distribution. Due to the limitation of time, a selection of the measures will made which will be assessed. The selected measures will be assessed on their effectiveness to retain rainwater, limit pluvial flooding as well as sewerage overflows within the urban context. This helps fulfilling the research aim of this study, leading to the 3rd and final question:

Question 3: Which proposed measures are effective to achieve a robust spatial rainwater distribution after short intense rainfall events?

1.5 Scope

For this study, a calibration of model parameters is out of scope. This would take a lot of time and computational resources since a lot of parameters are present and a large study area is modelled in high detail. Furthermore, calibration can be performed for present conditions, but those calibrated parameters can interfere with effects occurring for future scenarios or when measures altering the urban area are implemented.

The study also excludes hydrological processes within the subsoil. Modelling (slower) components of the hydrological cycle are not a priority within the 3Di modelling software, so the level of detail regarding hydrological processes is much lower than that of hydrodynamic processes. Besides, processes of the subsoil are more challenging to evaluate, since measurements are scarce.

Since hydrological processes working on longer scales (e.g., groundwater seepage) are excluded and assessed rainfall event will be short and intense, the time scale which is modelled will be in the order of a day. When the modelling starts, it will be assessed if a day is long enough to establish stable model outcomes.

For this study, predicted design rainfall events for climate conditions present in 2050 will be assessed. The year 2050 is chosen since adaptive measures generally have a lifespan of several decades, and the Royal Dutch Meteorological Institute (KNMI) has predicted changes in meteorological conditions for this year. Moreover, design rainfall events are deducted from these predictions (Beersma et al., 2019). STOWA & RIONED (2020) suggest using the *KNMI 2050WH scenario* when applying analyses on urban areas within future conditions. When needed, this scenario is also used within this study.

1.6 Thesis structure

The structure of this thesis is as follows. Firstly, *Section 2* gives a more elaborate description of study area whereafter general information about the used modelling software 3Di is given. Thereafter, the model setup is explained and to a limited extent discussed, complemented by a model verification. *Section 3* presents the followed methods needed to answer the research questions. This includes the selection of used rainfall events as well as selecting measures which will be studied. *Section 4* presents the results of this study as well as an interpretation of found results. *Section 5* provides a more general discussion of the results, as well as the potential of this study. Lastly, conclusions are presented in *Section 6*, together with recommendations for future research and practices.

2 Study area and model setup

2.1 Study area

The study area comprises the north-eastern part of the city Doetinchem and is situated in two sub-catchments of the rivers *IJssel* and *Oude IJssel* (WRIJ, 2023b). The total study area has a surface area of 9.6 square kilometres. Doetinchem is situated in a relatively high-elevated, sandy part of the Netherlands (see Figure 1). The average height is 13.41 metres above Normal Amsterdam Level (m+NAP). m+NAP represents the Dutch ordnance datum, where 0m+NAP approximates mean sea level. North-eastern parts of the study area are higher elevated compared to the south-western parts (along the Oude IJssel). Phreatic groundwater tables within the study area have been obtained from a database of the Geological Service Netherlands (Geologische Dienst Nederland, 2023). Annual average groundwater tables per measuring well are given in Figure 1, with an annual average of 2.2 m below surface. Fluctuations of water tables during seasons vary between 0.19 and 1.36 metres (Geologische Dienst Nederland, 2023). Groundwater tables within the study area are relatively deep in reference to the surface level compared to other (lower elevated) parts of the Netherlands. Waterways as given by the water board *Rijn and IJssel* (WRIJ, 2023b), including the river Oude IJssel, are shown in Figure 1.

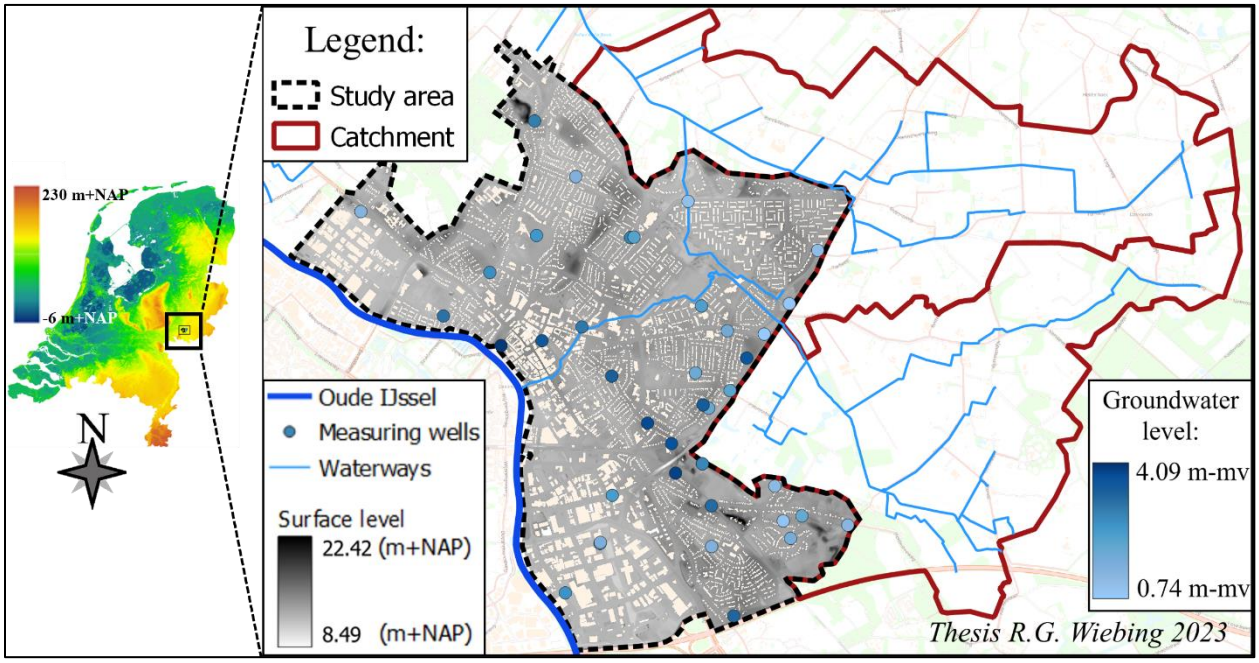

Figure 1: Study area and its upstream catchment. Buildings are cut out of surface height map. Groundwater levels are given in m-mv, meaning metres below surface level.

Next to surface waters, a sewerage system is part of the water system within an urban area. An overview of the sewerage system is given in Figure 2. For the larger part the flow of sewage and rainwater in the sewerage system is governed by gravity-forces, flowing from higher elevated parts to lower elevated parts. Consequently, the *gravity drained* sewerage system drains towards the Oude IJssel. At the lowest elevated parts of the study area, the system is drained by two

drainage pumps of water board Rijn and IJssel. These drainage pumps discharge the water to wastewater treatment plants outside the study area.

However, not all sewerage pipes of the sewerage system are drained by these pumps. Figure 2 shows that multiple types of sewerage pipes are present, indicated by different colours. *Red* pipes represent sanitary sewerage pipes which are solely used for dry weather flow (DWF), i.e., wastewater from buildings. *Blue* pipes represent storm drains which are solely used to discharge rainfall run-off (i.e., excess rainwater), and are not necessarily drained by pumps of the water board. Some storm drains drain the excess rainwater to surface water. *Orange* pipes represent mixed sewerage pipes, used to discharge both DWF as well as excess rainwater. Due to the fact that a sewerage systems' capacity can be insufficient during extreme rainfall events, sewerage overflows are constructed. These overflows are weirs with a connection to sewerage pipes, where sewage or rainwater can overflow when water levels at the overflow location reach a (critical) level. These overflows can be internal, i.e., overflowing into an internal storage tank where it is temporarily stored. It is pumped back into the sewerage system when water levels have dropped to non-critical levels. Overflows are however most commonly external, i.e., discharging surplus sewage out of the sewerage system into surface waters. This can create water quality issues, but it is preferred over the situation where sewage flows onto streets or into buildings.

Measurement locations within the sewerage system are depicted in Figure 2, with different shapes for different constructions within the sewerage system. Access was granted by the municipality to a database called *Telecontrolnet,* containing measurements of water levels within the sewerage system at the measurement locations. Those are identified by two codes in Figure 2, the first being the code used within *Telecontrolnet* (based on geographical location), the second being an introduced code for this study (based on structure type).

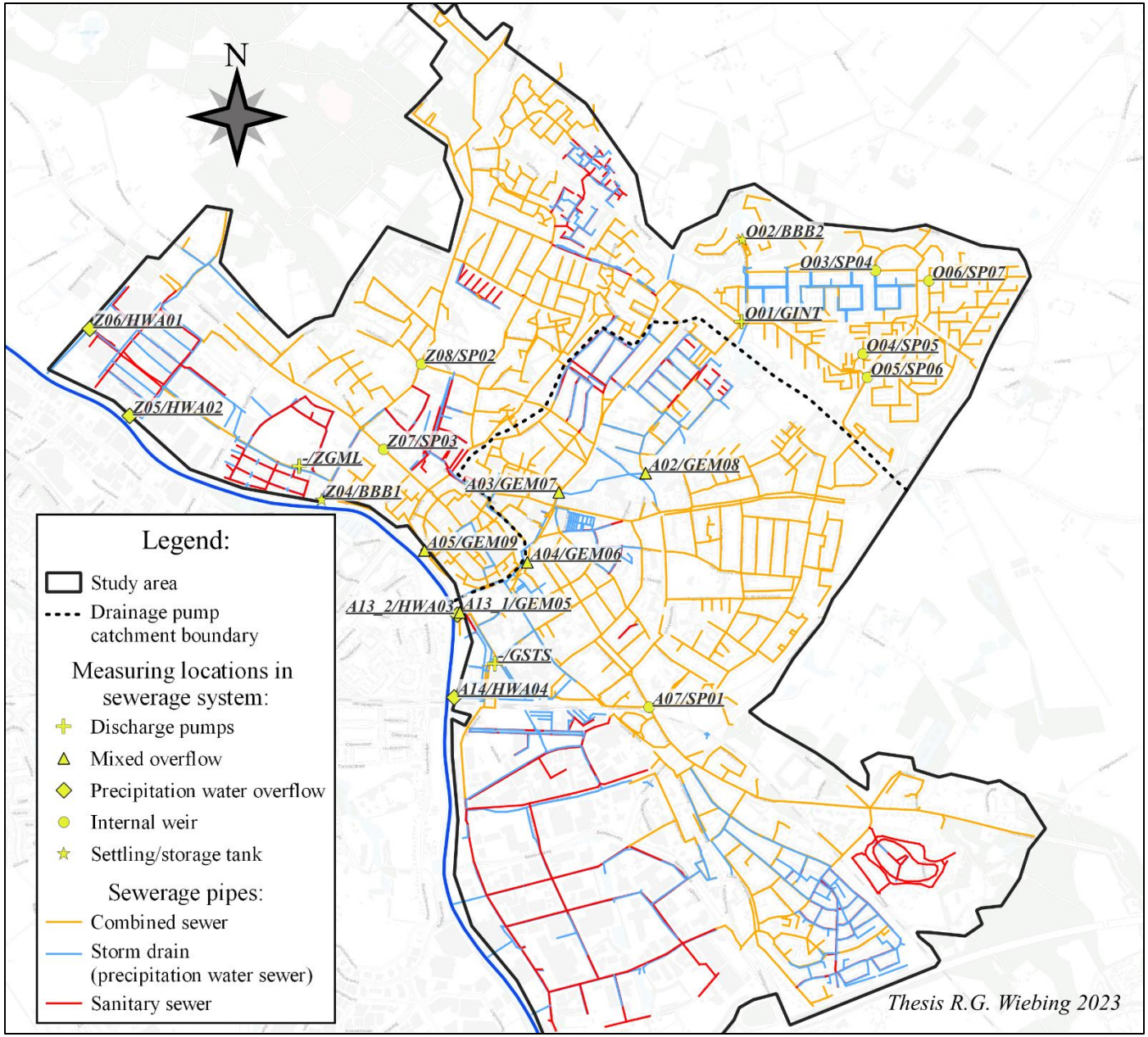

Figure 2: Overview of sewerage system within the study area, including measured locations with codes: {Telecontrolnet}/{this study}

2.2 3Di model setup

2.2.1 3Di modelling software

The 3Di modelling software complies with two basic laws of physics, namely the conservation of mass and the conservation of momentum. Those are solved for each computational cell at every time step. These computational cells are square, making up the so-called *quad-tree* computational grid. The resolution of the computational grid can be refined locally if higher computational accuracy is required, while areas of less interest use coarser computational grid resolutions to limit computational costs. The mass (i.e., the water volume when assuming a constant density for water) is defined at the centre of a computational cell. A change in mass within a cell is the sum of all incoming and outgoing flows from a computational cell, satisfying the conservation of mass. The conservation of momentum is accounted for by the full shallow water equations (SWE), solved in the domain between adjacent computational cells.

The 3Di modelling software's computational grid cell resolution is comparable to conventional hydrodynamic models (Volp et al., 2013). Yet, a *subgrid* is used containing surface area data (e.g., surface level, friction values) in a higher resolution than the computational grid, based on the fact that surface area characteristics show variability on smaller spatial scales compared to the more gradual varying water levels (Volp et al., 2013). This higher resolution subgrid is used for volume and SWE calculations, thus incorporating more detailed geographical input data of the study area in mass and momentum balance calculations. The resolution of the subgrid can be as high as the highest resolution of available input data. Regarding hydrodynamic modelling, quad-tree subgrid modelling gives more accurate results for shallow water flows, while using less computational resources than conventional models without a sub-grid (Volp et al., 2013).

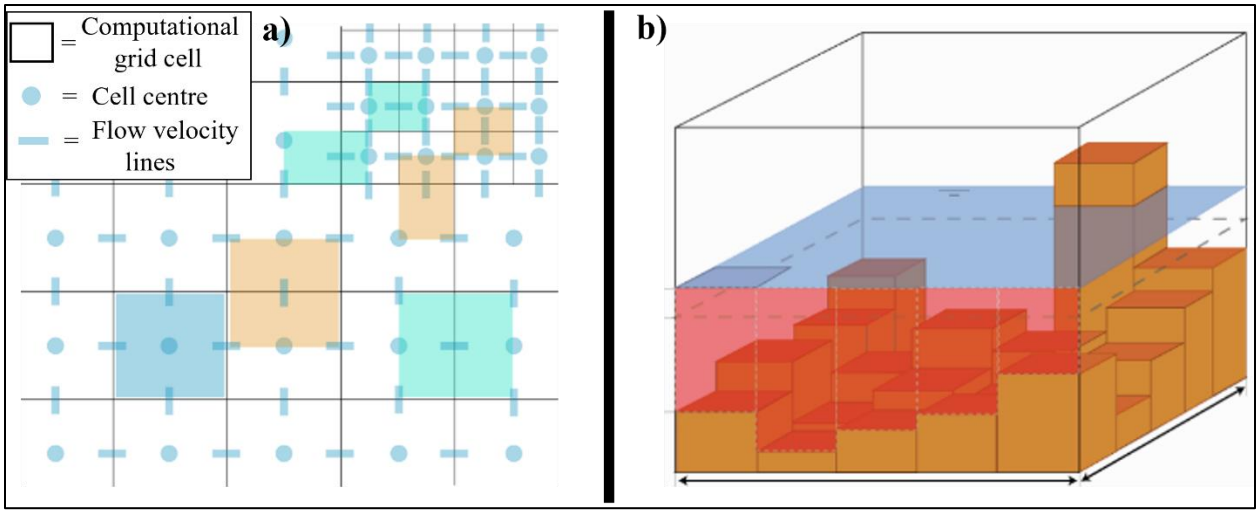

Figure 3a: Computational grid with a refinement in the upper-right corner, conservation of mass domain (dark blue), conservation of momentum domains (cyan blue and orange). Figure 3b: a computational cell (black cube) with underlying higher resolution subgrid (orange cuboids). Source: (Nelen&Schuurmans, 2023).

So, the subgrid technique implies a higher-resolution informational *subgrid* complementing the conventional computational grid. Water levels within a computational grid cell are uniform, defined in the cell centre (shown in Figure 3a and b). Yet, the computation of water volumes within computational cells is based on the higher-resolution surface level data present in the higher-resolution subgrid. Consequently, this results in a non-linear relation between the water level and water volume within a computational cell. In contrast, models without a subgrid use averaged surface level heights within computational cells. Therefore, volume calculations will be more accurate with a subgrid technique compared to conventional models.

Contrarily to models without a subgrid, flow velocities are also calculated at higher resolutions than the computational grid. This higher-resolution velocity grid is used for SWE calculations, incorporating higher-resolution input data to for instance establish depth-dependent friction coefficients. Furthermore, the subgrid is also used to calculate cross sectional areas where water volumes can be exchanged between adjacent computational cells (shown as the red surface in Figure 3b). More in-depth descriptions of those techniques can be found in Volp et al. (2013).

Despite the fact that the subgrid technique generally provides more accurate results with lower computational times, it gradually loses its advantage when higher resolution computational grids are required (Henckens & Engel, 2017). This is caused by the fact that a higher resolution computational grid contains fewer subgrid cells. A higher computational grid resolution can for example be required when the surface elevation map contains a high spatial variability.

In addition, the primary focus of 3Di modelling software is to model hydrodynamic flows both overland and within the sewerage system, to model the extent and depth of inundation caused by for instance extreme rainfall events. Hence, hydrological processes of overland flow and discharge via waterways and sewer pipes are incorporated in high detail due to their hydrodynamic character. Rainfall can also be incorporated in high detail, since it can be distributed over a high-resolution computational grid. Nevertheless, modelling of hydrological processes is not the focus of 3Di, causing an imbalance between the level of detail of hydrodynamic and hydrological processes. Processes such as infiltration, evaporation, water motion in the unsaturated zone, groundwater flow, percolation, transpiration by vegetation, and interception are incorporated with less detail within the 3Di modelling software. Concluding, 3Di is state-of-the-art software for modelling hydrodynamic processes in urban areas, but it is less detailed regarding hydrological processes.

Figure 4 shows the flowchart to generate a simulation for a study area using 3Di modelling software. First, all needed input data that is not variable during a model run is gathered and compiled, including both raster- and vector-based data. Together with the schematisation settings this is called a *schematisation* of the study area. This schematisation is used to generate a 3Di model. Next, input data which can be variable during a model run is included in the *scenario information*. A 3Di simulation can thereafter be started by combining the scenario information with the generated 3Di model.

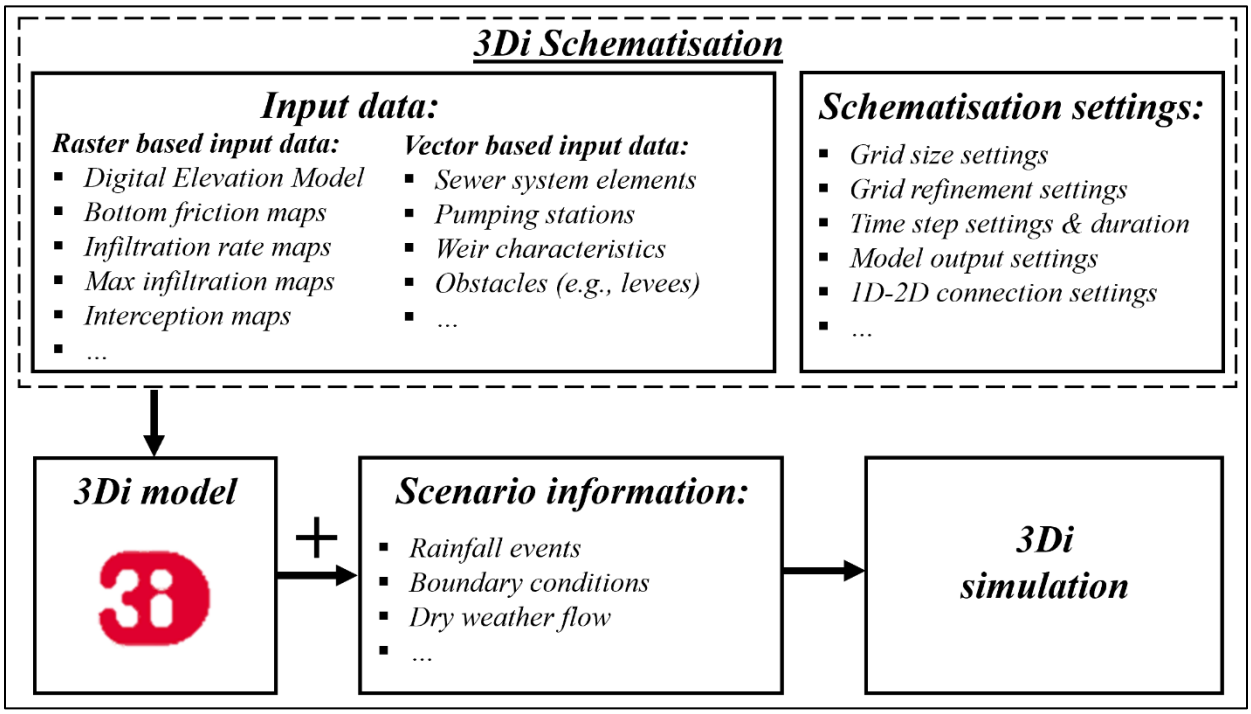

Figure 4: Steps to run a simulation with the 3Di modelling software.

The most recent 3Di model of the study area (not open source, updated in 2022) is used as a basis, managed by a water engineering firm (*Civicon*) based in Doetinchem. It does not include subsoil (ground)water flows. The model setup and used data are described in the following sections. For more detailed information about model setups, an online documentation is available: 3Di Documentation (2023).

2.2.2 Rainfall event input

Rainfall input is the most influential input regarding outcomes of water depth, propagation, and extent of pluvial floods (Alipour, Engeland, & Leal, 2021; Xing et al., 2021). Rainfall inputs used for modelling in this study are described in the method section, since multiple rainfall events are used as input for different research questions.

2.2.3 Computational grid and time step settings

The choice of computational grid resolution is particularly important in urban areas for hydrodynamic modelling since the spatial variability in elevations and land covers is high (Mitsopoulos et al., 2022; Xing et al., 2021). Computational grids of conventional full SWE models within urban areas (excluding the sewerage system) typically have a resolution of 10 m, sometimes with locally refined or coarsened resolutions of 1 up to 50 metres (de Arruda Gomes et al., 2021; Hu et al., 2019; Mitsopoulos et al., 2022; Nash et al., 2018; Xing et al., 2021). Yet, since model outputs are dependent on factors such as inaccurate input data and modelling choices, a very high-resolution computational grid can create a false impression of accuracy (Viero, 2019).

Moreover, conventional models do not incorporate a subgrid, losing the underlying high-resolution data governing water flows in an urban area. Thus, the use of the subgrid technique within 3Di allows for a coarser computational grid than conventional models while maintaining a high accuracy (Casulli & Stelling, 2011; de Arruda Gomes et al., 2021; Volp et al., 2013). In addition, since multiple scenarios and measures will be modelled, computational time should be taken into account. Therefore, the used computational grid size of 8 by 8 m in the provided 3Di model, complemented by a subgrid with a resolution of 0.5 by 0.5 m seems adequate to accurately model water flows in the area. This computational grid resolution results in over 141.000 computational cells for the study area.

The set computational time step is 5 seconds. Nonetheless, 3Di modelling contains an automatic method to reduce the computational time step. This is done to ensure accurate calculations of the full SWE and reduce volume errors. The computational time step can be reduced up to 0.01s.

2.2.4 Digital Elevation Model

A digital elevation model (DEM) is one of the most important model inputs for hydrodynamic modelling (de Arruda Gomes et al., 2021). It gives the elevation of the surface area at the spatial resolution of the DEM, important for calculating the direction and volumes of water flows. The 4th Elevation Map of the Netherlands from 2022 (AHN4) is used as DEM within the model (PDOK, 2022a). This DEM has a resolution of 0.5 by 0.5 m, with a systemic and stochastic inaccuracy of both 5 cm at maximum (AHN, 2022).

A significant part of an urban area consists of buildings. Those do influence water flows and are thus important to incorporate (Iliadis et al., 2023; McClean et al., 2020; Mitsopoulos et al., 2022). Buildings can be incorporated as areas with an increased friction coefficient (impeding water flow), as an elevation in the DEM (obstructing water flow), or left out of the DEM (preventing water flow). Erasing surfaces identified as buildings from the DEM gives the most accurate results in terms of water flows (Glenis et al., 2018; Iliadis et al., 2023). Moreover, this method saves computational resources since no computational cells are needed at the locations of buildings. This is also used in the provided 3Di model, where buildings are erased from the DEM. Buildings are however incorporated as surfaces where rainwater falls onto, whereafter this rainfall is discharged into the sewerage system. If a building has a flat roof, an interception value of 4 mm is implemented on the roof surface, based on the commonly used NWRW tables (RIONED, 2019c). Approximately 22% of buildings in the study area have a flat roof, obtained via the BAG3D data source (3DBAG, 2023).

2.2.5 Landcover map

A landcover map is essential for hydrodynamic and hydrological studies, since it influences overland water flows, interception, evaporation, and infiltration. For this study, a landcover map with a spatial resolution of 0.25 by 0.25 m is used. To attain a landcover map of the full study area, it is composed of multiple data sources from Dutch governmental institutions. Data gaps within a

landcover map are complemented with additional data sources. This is done in the following order: the Base Registration Addresses and Buildings (BAG (PDOK, 2022b)), Base Registration Topography (BGT (PDOK, 2022c)), National Road Database (NWB (PDOK, 2022f)), and the Topographic Base Map (BRT (PDOK, 2022d)). Those data sources have a classification accuracy of respectively 99.99%, 99%, unknown, and 95.9% (Rijksoverheid, 2023).

Friction (Manning) and interception values are based on the landcover map. Standardly used parameters within the 3Di software are shown in Table 1, per landcover type present in the study area. Here, the *pervious factor* represents the supposed ratio of pervious area present within a land cover class. Interception values are based on the commonly used NWRW tables (RIONED, 2019c).

Table 1: Parameters used within 3Di per land cover category.

Land cover	***Friction value***	***Interception value***	***Pervious factor***
	(s/m$^{1/3}$)	*(m)*	*(-)*
Unpaved	0.03	0.003	1
Paved	0.013	0.0025	0
Passable pavement	0.03	0.0025	0.25
Open pavement	0.016	0.0025	0.5
Bushes	0.03	0.003	1
Forest	0.058	0.01	1
Other vegetation	0.03	0.003	1
Agriculture	0.034	0.003	1
Water	0.026	0.0	0

Landcovers in the public domain are documented on a high level of detail. In Figure 5 it is observed that 1.1% of the study area is covered by surface water, 22.2% is classified as vegetated area, 19.5% is covered by buildings, 18.5% by road segments (including pavements, parking spaces et cetera). Contrarily, while private properties (other than buildings) cover 38.7% of the total study area, landcovers within it are not documented. Within this study the landcover of private properties is differentiated in the landcovers *vegetated* and *paved* on neighbourhood scale. This is done by classifying vegetated surfaces within the private property with the Normalised Difference Vegetation Index (NDVI). A detailed description of the index and the followed method can be found in *Appendix A*.

Percentages of paved surface cover on private properties show high variations between neighbourhoods, as shown in Figure 5. On average, private properties within the study area are paved for 61% and vegetated for 39%. This is consistent with findings of Mulder (2020), who calculated an average paved surface cover of 60% within private properties in Dutch municipalities.

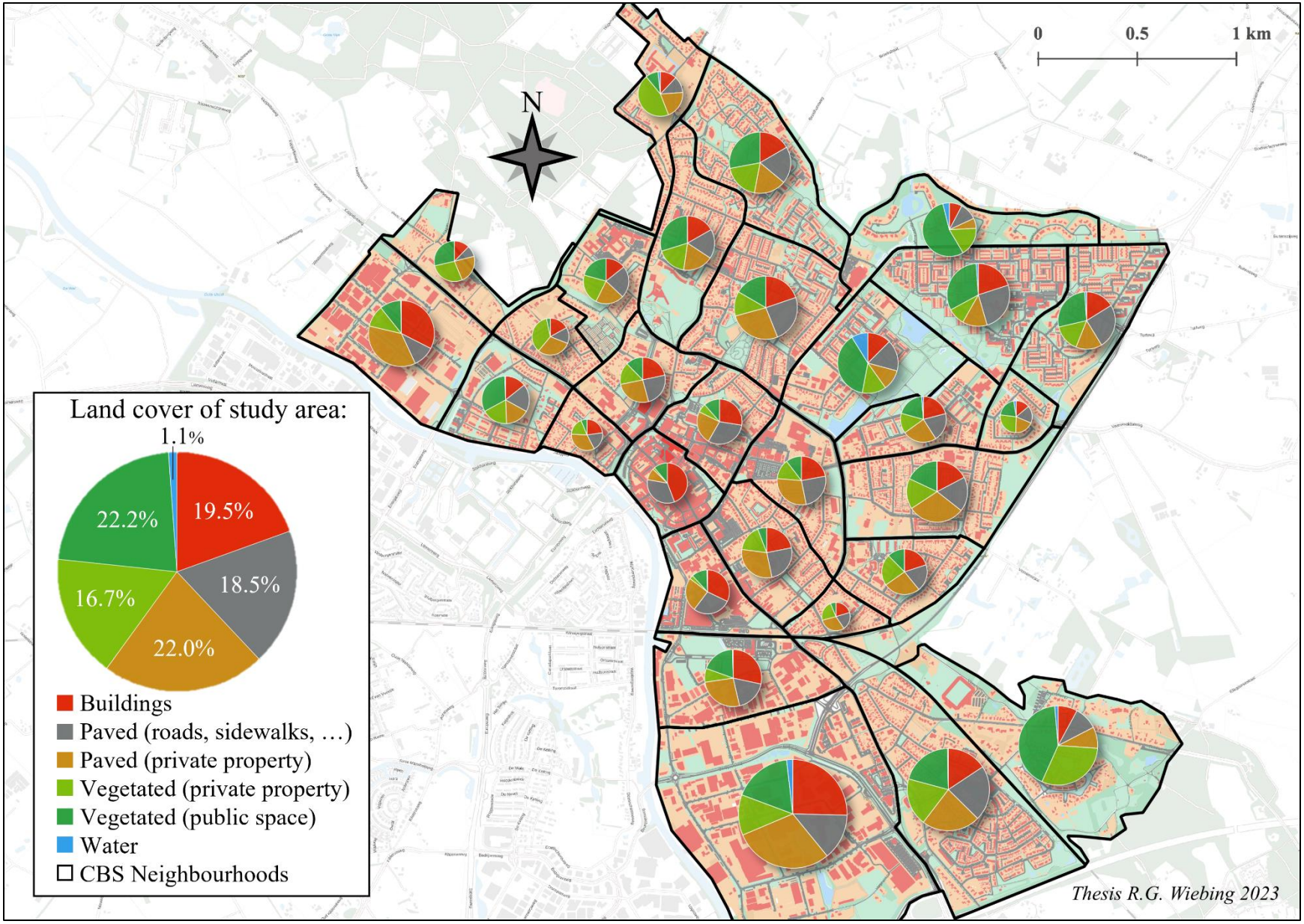

Figure 5: Landcover statistics of the study area within Doetinchem.

2.2.6 Soil type map

Soil types present in the study area were deducted from the Base Registration of the Subsoil of the Netherlands (BRO Bodemkaart (PDOK, 2022e)), based on BOFEK2020 (Heinen et al., 2021). It gives information about the type of subsoil within the first 1.20 m under the surface. Corresponding infiltration rates are given in Table 2. Nonetheless, used infiltration rates contain multiple sources of uncertainty. First of all, the infiltration rate is modelled as a constant value. This results in uncertainty in the amount of *excess* rainwater, since in reality it is a consequence of an events' rainfall intensity and the infiltration rate which are both variable during a rainfall event. When rainfall intensity exceeds the infiltration rate of a surface, excess rainwater is generated. Yet, the infiltration rate depends on subsoil conditions (e.g., soil characteristics, compaction, saturation front, antecedent moisture conditions) and landcover characteristics (e.g., type of vegetation, imperviousness). Yet, particularly in urban areas, detailed data about subsoil characteristics and conditions as well as maximum infiltration rates of landcovers are generally absent. Therefore, it is challenging to accurately represent infiltration rates in any model.

Table 2: Soil types present in study area and its infiltration rates.

Soil type	***Infiltration rate value***	
(present in study area)	*(m/d)*	*(mm/h)*
Podzol; mildly loamy to loamy fine sands	0.48	20
Enkeerd; mildly loamy to loamy fine sands	0.12	5

Within the urban area, paved surfaces influence infiltration rates. For modelling purposes, infiltration rates of surfaces (Table 2) are multiplied by its pervious factor (Table 1). For instance, an asphalt road (i.e., paved surface as land cover: pervious factor of 0) on top of an Enkeerd soil type (infiltration rate of 5 mm/h) gets an infiltration rate of 5*0=0 mm/h. A grassy playground (i.e., grass as land cover: pervious factor of 1) on top of an Enkeerd soil type (infiltration rate of 5 mm/h) gets an infiltration rate of 5*1=5 mm/h. Pervious factors of private properties are based on the amount of paved surface on neighbourhood scale, as shown in *Section 2.2.5*.

2.2.7 Maximum rainwater storage in subsoil

The maximum storage of rainwater in the soil is dependent on subsoil characteristics, subsoil moisture conditions and phreatic groundwater levels and flows. Groundwater levels in Doetinchem are relatively deep in reference to the surface level, creating a large storage capacity in the subsoil. This is particularly true for the summer period. Hence it is expected that the infiltration rate will be the limiting factor during assessed rainfall events instead of the storage capacity in the subsoil.

Yet, ponding of excess rainfall can be substantial when assessing short and intense rainfall events. This can thereafter be infiltrated in the modelled time period after the rainfall events and

can thus theoretically exceed the storage capacity of the subsoil. Therefore, a maximum storage capacity of the subsoil is implemented.

This maximum storage capacity in the subsoil is based on voids of subsoil types and average annual phreatic groundwater tables within the study area. The average annual phreatic groundwater tables are obtained from the Geological Service Netherlands (Geologische Dienst Nederland, 2023). This database includes 39 measurements points within the study area, which measure daily phreatic groundwater tables. The annual average phreatic groundwater table for the study area is 2.2 m below the surface, indicating that the groundwater table can maximally increase 2200 mm. The average storage capacity coefficient of both Podzol and Enkeerd soil types when groundwater tables are deeper than 1.5 metres is 0.17, as seen in the reports of Cultuurtechnische vereniging (1988, p. 462) and Luijmes (2023). This coefficient indicates the volume of voids in the soil above the groundwater table which can theoretically be filled with rainwater. This results in a maximum storage capacity of 374 mm (2200mm*0.17), which is implemented in the model.

2.2.8 Evaporation from the surface

Evaporation of water which ponded on surface areas is assessed within the used model. It is implemented into the model as a constant value in millimetre per second which is subtracted from a computational cell if and only if water is ponding onto it.

The average reference evaporation value for the region of Doetinchem in summer conditions is 3.05 millimetre per day for current climate conditions (KNMI, 2020). A 11% increase in this reference evaporation value is predicted for the KNMI 2050WH climate scenario (Klein Tank et al., 2014). In addition, open water evaporation is circa 1.3 times the amount of the reference evaporation (STOWA, 2021). Given this information, a daily evaporation value of (3.05 * 1.11 * 1.3 =) 4.4 mm/d, i.e., $5.09*10^{-5}$ mm/s, is implemented. This evaporation is only occurring when rainwater is ponding on the surface.

2.2.9 Boundary conditions

As shown in Figure 1, there are three waterways flowing into the study area. The river *Oude IJssel* and two waterways coming from two upstream catchment areas. Boundary conditions have to be set for incoming discharges. Within the model, a constant water level of 10.2 m+NAP is set at the beginning of the Oude IJssel. This is the maximum recorded water level at Doetinchem in summer conditions, according to data of water board Rijn and IJssel (WRIJ, 2023a).

To establish boundary conditions for the two waterways coming from the upstream catchment areas, two separate models of the upstream catchment areas were made. Those were setup in the same way as the 3Di model of the study area. No baseflows are implemented in waterways within the upstream catchment models, since baseflows are absent in the upstream catchments during present and future summer conditions (‘Klimaatatlas Doetinchem’, 2022). The separate models are used to calculate discharges coming into the study area via the two waterways, when an assessed rainfall event is used as rainfall input into the models of the upstream catchments.

Model boundaries with respect to the modelled area are carefully set to minimise impact on model results within the study area. The modelled area is bounded by the river Oude IJssel in

the south, by an elevated provincial road in the east, by the stream called *Zelhemsche Beek* in the north, and catchment area boundaries in the west.

2.2.10 Sewerage system

Sewerage system components within Doetinchem are shown in Figure 2. These components are schematised as 1D elements within the model schematisation. They can however interact with the 2D surface area via overflows and (street) wells (Dutch: (straat)kolken). So, when the sewerage system has to process more sewage and rainwater than it is designed for, it can exit the sewerage system via overflows and (street) wells (i.e., when hydraulic heads are higher than the surface level). Opposite to this, when water is ponding on the surface, it can also flow into the sewerage system via (street) wells if those are present in the computational cell. This water can thereafter be discharged. Sewerage pipes with their street wells are generally schematised in the middle of the road.

Dry weather flow (DWF), i.e., wastewater of buildings which have to be discharged by the sewerage system can be incorporated into the model. It is based on the number of inhabitants per building and amounts of DWF per inhabitant per day. It can be modelled as a constant value or varying over time. A constant DWF is used within this study with a cumulative daily volume of 120 litres per person, which is and commonly assumed average value (RIONED, 2019b).

2.3 3Di model verification

In this study *verification* is interpreted as the process of verifying whether the model is correctly functioning as intended regarding the modelling concepts and assumptions, to find model errors and correct them (Carson, 2002; Thacker et al., 2004). So, multiple checks and tests are performed to verify if input data about the water system in the urban area, coming from governmental databases, is implemented correctly in the used 3Di model. This is needed since a 3Di model is largely automatically generated from input data and the input data is obtained via governmental databases, inevitably containing inaccuracies. Errors that were found while conducting the described verification checks and tests have been updated in the model with the help of expert judgement from modelling and water system experts.

To begin with, the municipal database called *Telecontrolnet* (not open source) was used to check whether characteristics of constructions within the model's sewerage system were implemented correctly. Locations, crest heights, and crest widths of weirs (internal and external overflows) were checked and updated if needed. Maximum pumping capacity of the internal discharge pump managed by the municipality were also checked. Dimensions and height levels of culverts and orifices were also checked and updated. Dimensions and height levels of sewerage pipes were not verified since those were not present in the used database.

Following comparisons of municipal databases, open-source data from the water board Rijn and IJssel was used to check constructions within waterways (WRIJ, 2023b). Locations, crest heights, and crest widths of weirs were checked and updated if needed. Locations, height levels, and dimensions of culverts were also checked and updated if needed. In addition, check valves

indicated by the WRIJ database were implemented into the model schematisation to ensure that water can only flow in one direction within culverts or pipes. Maximum pumping capacities of discharge pumps managed by the water board were checked via e-mail contact with a water board employee.

Next, a 3Di model test run was performed with no other source of water input than the boundary condition on the river Oude IJssel (i.e., no rainfall and no DWF). With this check it is verified whether the boundary condition on the Oude IJssel does for instance not flood the urban area, since this is not occurring in reality. In addition, the sewerage system should not be filled with water from the river since check valves are present.

After that, a test run was performed with no other waterflow input than DWF coming from buildings. The sewerage system has a draining capacity which is significantly higher than inflows originating from DWF. Therefore, with this test no wastewater should be flowing onto the surface area, discharge pumps should turn on and off (since their maximum drain capacity is significantly higher than the produced DWF), and storm drainpipes should be free of water flow.

In another test a uniform rainfall event of 5 mm in one hour was used as rainfall input, which is approximately 25% of the rainfall depth where the drainage capacity of the sewerage system has been dimensioned for. Hence, this test is to verify that the sewerage system is capable of draining rainwater (e.g., functioning connections between 1D sewer system and 2D surface area). Yet, no pluvial flooding or sewerage overflows should occur in such an event with limited rainfall depth.

Lastly, a test was conducted with a rainfall event of 19.8 mm in one hour, which is the rainfall event where the maximum capacity of the sewerage system is dimensioned for to drain. So, no excessive pluvial flooding should occur on roads or at buildings, discharge pumps should be constantly pumping at maximum capacity until about 10-20 hours after the event (van Wieringen, 2009), and overflows may be active.

When used design precipitation events were selected in Step 2 to establish base scenarios, it was determined which modelling time had to be implemented. The selected design precipitation events last for 1 hour, whereafter additional modelling time is needed to calculate the distribution of that rainwater across or out of the study area. A modelling time of 24 hours was assessed first. It was found that approximately all rainwater had been distributed after this period, i.e., was either discharged out of or stored within the study area (but was not still flowing). In the last simulation hour, only minor changes occurred in the water balance terms: 0.17%, 0.18%, and 0.20% of total rainfall input was not yet static for events T002, T010, and T100 respectively. Hence, a modelling time of 24 hours is sufficient to study effects on the water balance of the study area. It was also found that the constant water balance terms of interception and DWF decrease proportionally to an increasing rainfall depth. Those are thus implemented correctly into the model.

3 Methods

3.1 Evaluation of model performance for historic rainfall events

3.1.1 Rainfall events input for evaluation

Evaluation of model performance will be based on expert judgement and comparisons between measured and modelled data during and after historic rainfall events. Since short intense rainfall events are the focus of this study, the model performance after such events should be assessed. In addition, to be able to evaluate the functioning of all components of the sewerage system (e.g., sewerage overflows too), the rainfall event should contain a significant cumulative depth. The sewerage system is dimensioned to drain a rainfall event of 19.8 mm in one hour, so the assessed rainfall events should preferably contain a depth of approximately that amount or more.

To select such events multiple steps were taken. First of all, historic KNMI rainfall data with a daily interval was gathered from rainfall gauge *STN-667 Doetinchem*, located 250 m north of the study area (Lizard, 2023a). With the help of a Python script, all days with a recorded cumulative rainfall depth of more than 15 millimetres in a day were selected, to filter out days with less amounts of rainfall. Next, the National Rain Radar (NRR (Lizard, 2023b)) was used to assess how rain on the selected days was distributed, to select short and intense rainfall events.

The NRR has a spatial resolution of 1 by 1 kilometre which results in 20 tiles (partly) overlapping the study area. The NRR has a temporal resolution of 5 minutes. For Doetinchem, rainfall data of four radars, 2 Dutch, 1 Belgian, and 1 German radar, are combined to reconstruct historic rainfall events (H. Schuurmans & van Vossen, 2013). From 2020 onwards, NRR rainfall data is calibrated by the KNMI, using 32 weather stations and 322 rainfall gauges where rainfall depths are measured. Using a Python script and NRR data, rainfall events were selected which contained more than 15 mm/h for at least 1 tile in the NRR data.

These conditions were satisfied for 2 historic events, which occurred on the 4th and 15th of July 2021. The events respectively contained a cumulative depth of on average 20 mm and 26 mm, where about 16 and 21 mm fell in one hour respectively. So, the historic events are slightly under and above rainfall event characteristics where the sewerage system's maximum drainage capacity is designed for (19.8 mm in one hour) in terms of rainfall intensity and rainfall depth.

3.1.2 Evaluation of the model performance

Figure 2 displays all measurement locations within the sewerage system. Compared to other municipalities, Doetinchem has a dense measuring network with its sewerage system. Nevertheless, it is seen that the southern section of the sewerage system contains almost no measuring points. The most southern measuring point was not active during the assessed historic events. Yet, 18 points measured water levels at the 4th and 15th of July 2021. Those measurements are obtained via the municipal database (*Telecontrolnet*) to compare them to water levels as calculated by the model at the measurement locations. One figure for different structures (fulfilling different

purposes) within the sewerage system will be shown in *Section 4.1* to save space in the results section. These will be a mixed sewer overflow, a storm drain overflow, an internal discharging pump, and a storage facility. The other figures will be presented in *Appendix B*.

Comparing measured and modelled values regarding the water balance is impossible due to the absence of discharge measurements out of the study area. Despite relatively dense measuring network, a lot of storm drain outflows are not measured. Moreover, measured water levels cannot be converted to discharges straightforwardly since velocities are not measured. Furthermore, no measurements are conducted on the amount of rainwater which is drained via waterways.

Likewise, no data is available about flooding depths and extents after the assessed events. Consequently, evaluating the model performance regrading pluvial flooding is challenging. To evaluate this to some extent, a hindrance map after assessed events will be established. The method of establishing a hindrance map is described in *Section 3.1.3*. Thereafter, hindrance locations will be discussed with two experts working in the field of the water system within Doetinchem. The first expert is Rudie Tempels, who is working on topics regarding the development of the public space, the water system, and climate adaptation in Doetinchem for over 30 years. The second expert is Bas Berends, working on topics regarding the water and sewerage system within Doetinchem for over 20 years.

3.1.3 Pluvial flood indicators

Hindrance due to rainfall is a result of rainfall event characteristics as well as storage and drainage capacities of an urban area (Ten Velden et al., 2022). When storage and drainage capacity are insufficient to store fallen rainwater, pluvial flooding (i.e., ponding) occurs which can lead to hindrance. Locations and depths of this ponding can be estimated with the help of the model. This results in a map with the maximum water depth for every grid cell during the simulation. In the case of this study, it results in a maximum water depth with a spatial resolution of the DEM thus 0.5 by 0.5m. Although a general directive to quantify hindrance is absent in the Netherlands, Ten Velden et al. (2022) suggest the vulnerability of buildings and accessibility of roads as *pluvial flood indicators* for quantification of hindrance. This is also previously used in Doetinchem when assessing hindrance caused by pluvial flooding (‘Klimaatatlas Doetinchem’, 2022). For recognisability, these flood indicators are also used in this study. Buildings are identified as vulnerable on the basis of the maximum flood depth against its facades, and the accessibility of roads are assessed based on the maximum flood depth on the road surfaces. Used thresholds, based on the Klimaatatlas Doetinchem (2022), are shown in Table 3.

Table 3: Used flood indicators and their threshold values.

Pluvial flood indicator	***Category***	***Pluvial flood depth***
	(-)	*(m)*
Vulnerability of Buildings:	*Low vulnerability*	< 0.10
	Moderate vulnerability	0.10 – 0.25
	High vulnerability	> 0.25
Accessibility of Roads:	*Fully accessible*	< 0.15
	Only accessible for emergency vehicles	0.15 – 0.30
	Not accessible	> 0.30

3.2 Base scenarios

To compare effects of measures, each measure will be compared individually to the current situation where no measures are yet implemented (i.e., the base scenarios). Regarding rainfall event input for the base scenarios, a selection will be made from *design rainfall events* currently used within the Netherlands. Design rainfall events are commonly used for scenario modelling as well as identifying sections of the urban area which are prone to pluvial flooding.

3.2.1 Design rainfall events in the Netherlands

Design rainfall events called *Bui08 (Rainfall event 08)*, *Bui10 (Rainfall event 10)*, and *Blokbuien (Block rainfall events)* are commonly used within the Netherlands (RIONED, 2019b). More recently established, and not commonly used yet, are *Composietbuien (Composite rainfall events)*. The events show variety in the characteristics of duration, rainfall depth, and intensity distributions.

Bui08 and Bui10 became the standard design rainfall events to test the hydraulic functioning of sewerage systems (RIONED, 2019a). Municipal policy objectives are often referring to Bui08 and Bui10, such as the requirement that no pluvial flooding should occur when the urban area is subjected to Bui08. Durations and rainfall depths of Bui08 and Bui10 are derived from a rainfall data set recorded by the Royal Dutch Meteorological Institute (KNMI) in De Bilt between 1955 and 1979, with a temporal resolution of 15 minutes.

Blokbuien are commonly used in so-called *stress-tests* (STOWA & RIONED, 2020; Ten Velden et al., 2022). These stress-tests are performed to determine the extent of pluvial flooding when an urban area is subjected to an *extreme* rainfall event (i.e., a large *stress* is put on the system). The duration and rainfall depth of Blokbuien are based on latest insights presented in Beersma et al. (2019). The insights are based on extensive statistical analyses on historic rainfall events, using multiple rainfall data sets of the KNMI. Used rainfall data is obtained by 2 radar stations with a temporal resolution of 5 minutes and a spatial resolution of 1 square kilometre, complemented by data sets of 32 weather stations with a temporal resolution of 1 hour, and 322 rainfall gauges with a temporal resolution of 1 day. Durations and rainfall depths of Composietbuien are also based on

insights presented in Beersma et al. (2019). Composietbuien are events designed for stress-tests as well as testing the hydraulic functioning of a sewerage system.

Sections 3.2.1.1, *3.2.1.2*, and *3.2.1.3* provide a more detailed description of rainfall event characteristics, choices to be made for modelling purposes, and comparison of design rainfall events.

3.2.1.1 Duration

Design rainfall events vary in duration, and choices regarding the duration are dependent on the study area. In rural areas, events with long durations (e.g., 48 hours) and large cumulative depths are generally normative, since those are slow responding systems with a relatively large storage capacity (Beersma et al., 2019; STOWA & RIONED, 2020). On the contrary, urban areas are fast responding systems due to relatively high percentages of paved surfaces. Therefore, short design events with high intensities are normative to identify vulnerable sections of an urban area which are prone to pluvial flooding.

When identifying vulnerable sections of an urban area, 1-hour design events are most commonly used, complemented by 2-hour events when a considerable amount of surface water is present (STOWA & RIONED, 2020), such as a dense canal system. Since only 1.1% of the study area is covered by surface water, a 1-hour rainfall design event is considered to be suitable in identifying vulnerabilities within the studied area. The duration of Bui08 is 1 hour, Bui10 has a duration of 45 minutes, and Blokbuien and Composietbuien contain a range of durations, including 1 hour rainfall events.

3.2.1.2 Rainfall depth

Another varying characteristic of design rainfall events is its cumulative depth, which indicates the total amount of rainfall. It is expressed in millimetres, indicating the number of millimetres of rain that falls onto a given area. The cumulative depth is a common indicator of the *extremeness* of a rainfall event (KNMI, 2023a). Together with the duration of an event, the cumulative depth can be expressed in a statistical recurrence time. This recurrence time gives an expected frequency of occurrence for a given design rainfall event. These recurrence times are determined based on historical rainfall measurements, being statistically valid for *a* point in the Netherlands. For instance, a one-hour rainfall event with a depth of 58 millimetres has a statistical recurrence time of 100 years under current climate conditions (denoted as T100). This indicates that such an event is expected to occur once during a 100-year period at an assessed location. A complicating element of these statistics is that recurrence times of events vary regionally across the Netherlands due to geographical factors. There is however no indication that cumulative depths of short rainfall events (< 12 hours) do vary regionally (Beersma et al., 2019). Hence, statistical recurrence times for short events are valid for the entire Netherlands, independent of the study area's geographical location.

Due to the changing climate, an increase in cumulative depths of rainfall events is expected. The KNMI has provided predictions for changes in meteorological variables for 2030, 2050, and 2085, considering four climate scenarios (Klein Tank et al., 2014). Beersma et al. (2019) deduced

expected changes in cumulative depth for rainfall events from the KNMI climate scenarios. They present changes in rainfall events with recurrence times ranging from 0.5 to 1000 years, and durations ranging from 10 minutes to 8 days. These changes should be considered when assessing measures aimed at the adaptation of urban areas to extreme rainfall events, since those measures often have a lifespan of several decades. STOWA & RIONED (2020) recommend to base cumulative depths of design rainfall events on a worst-case climate scenario for 2050 (*2050WH*). Additionally, it is advised to apply rainfall events with multiple recurrence times when assessing effects of rainfall events on urban areas (STOWA & RIONED, 2020). This increases understanding of the functioning of an urban area and its vulnerabilities.

Recurrence times for Blokbuien and Composietbuien are ranging from 0.5 to 1000 years and are in accordance with latest insights presented in Beersma et al. (2019). Moreover, Blokbuien and Composietbuien are available for future climate conditions in 2030, 2050, and 2085.

Based on climate conditions from 1955 to 1979, Bui08 has a statistical recurrence time of 2 years. The cumulative depth of Bui08 is only 1% lower than the cumulative depth of a 1-hour T=2 event for current climate conditions (shown in Table 8 in *Appendix D*). Also based on climate conditions from 1955 to 1979, Bui10 has a statistical recurrence time of 10 years. Yet, its cumulative depth is approximately 15% higher compared to cumulative depths for a 1-hour T=10 event for current climate conditions (shown in Table 8 in *Appendix D*). As of now, no equivalents of Bui08 and Bui10 are directly available for future climate conditions.

3.2.1.3 Intensity distribution

The intensity distribution of a design rainfall event indicates the distribution of cumulative rainfall depth over time (millimetres per time unit, i.e., *intensity*). The events intensity distribution is however independent of its cumulative depth (Beersma et al., 2018). The intensity distribution within a design rainfall event is particularly important for urban areas, since urban areas consist of relatively large amounts of paved surfaces (Beersma et al., 2019; STOWA & RIONED, 2020). Urban water and sewerage systems have difficulty with draining all excess rainwater on (paved) surfaces generated by high intensity rainfall. Therefore, events with short durations but high intensities are normative to test an urban area on its resilience to extreme rainfall events. Statistical analysis shows that the intensity distributions of short rainfall events (less than 4 hours) consist of one sharp intensity peak in more than 70% of the events (Beersma et al., 2019). These short and intense events are expected to occur with increased frequency due to climate change (Beersma et al., 2018; KNMI, 2022).

Intensity distributions of design rainfall events are shown in Figure 35 within *Appendix D*. The intensity distributions of Blokbuien are uniform. This is a strong simplification of reality, since most short rainfall events contain a sharp intensity peak. The underestimated maximum intensities of Blokbuien can, depending on water system characteristics, cause an underestimation of the extent and maximum depths of pluvial flooding (Beersma et al., 2019; Ten Velden et al., 2022). Intensity distributions of Bui08 and Bui10 contain skewed intensity peaks. Yet, as shown in Table 9 within *Appendix D*, Bui08 and Bui10 underestimate maximum peak intensities compared to the latest insights (Beersma et al., 2019; RIONED, 2020). Composietbuien have intensity distributions

that are normally distributed, and are based on latest insights presented in Beersma et al. (2019). They are composed to satisfy the condition that cumulative depths within the peak of an event matches its recurrence time. For instance, within a 1-hour Composietbui with a recurrence time of T=100, the maximum cumulative depths for 10- and 30-minute periods within that event do also have a recurrence time of T=100. This is shown in Table 9 within *Appendix D*.

3.2.1.4 Selection of design rainfall events

Table 4 presents an overview of characteristics of used design rainfall events within the Netherlands.

Table 4: Overview of characteristics from different design rainfall events

Design Event	***Duration***	***Depth***	***Intensity distribution***	***Recurrence time***
	(minutes)	*(mm)*	*(-)*	*(years)*
Bui08	60	19.8	Left skewed	2
Bui10	45	35.7	Right skewed	10
Blokbuien	10 – 11520	Variable	Uniform	0.5 – 1000
Composietbuien	10 – 600	Variable	Normal	0.5 – 1000

To get an understanding of the functioning of an urban area when subjected to rainfall events, 1-hour events with a range of recurrence times are advised. Recurrence times of 2 and 10 years are used to test the hydraulic functioning of the (sewerage) system, and a recurrence time of 100 years will be used to stress-test the urban area. In addition, due to the life span of adaptation measures, climate change should be taken into account when assessing their effectiveness. A peaked intensity distribution of design rainfall events is also advisable when assessing urban areas.

Advantages of Bui08 and Bui10 are that they are well-known amongst both engineers and policy makers, and are relatively up-to-date regarding latest insights on cumulative depths of short rainfall events. Yet, maximum rainfall intensities are underestimated, and no equivalents of Bui08 and Bui10 are available for future climate conditions. Blokbuien have as an advantage that those are available for a range of recurrence times in future climate conditions. But Blokbuien underestimate maximum rainfall intensities since they have a uniform intensity distribution. Composietbuien are composed so that all durations within a rainfall event have its recurrence time, hence they contain normative peak intensities. Moreover, they are composed for all climate scenarios, for a range of recurrence times. A disadvantage of Composietbuien is that they are not well-known among policy makers. Yet, this disadvantage does not outweigh the advantages of using Composietbuien, hence those will be used as rainfall event input for this study (also advised in Ten Velden et al. (2022)). This enhances consistency as well, since Composietbuien with varying recurrence times are used to both test the hydraulic functioning of the sewerage system as well as for conducting stress-tests. To incorporate future climate conditions, Composietbuien designed for the KNMI 2050WH scenario will be used. Concluding, 1-hour Composietbuien with recurrence times of 2, 10, and 100 years for worst-case climate conditions of 2050 are used as model input to establish base scenarios.

3.2.2 Base scenarios

To establish base scenarios the T002, T010, and T100 composite events are used as rainfall event input. The events' cumulative rainfall depths are 24.3, 37.5, and 69.9 mm respectively, and their intensity distributions are shown in Figure 6.

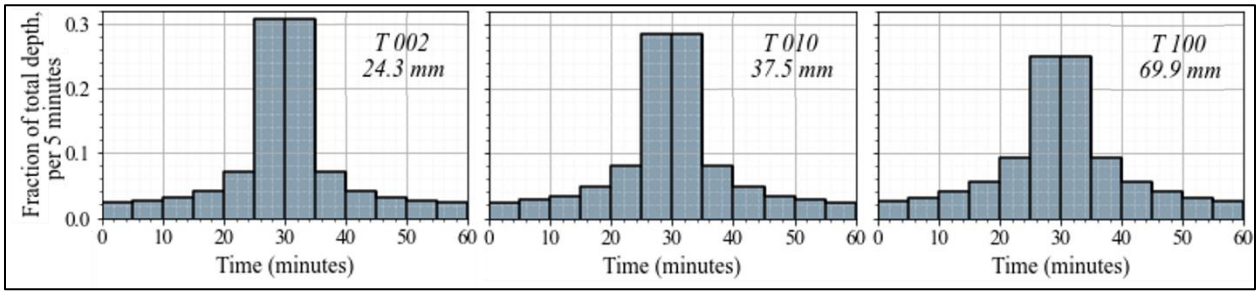

Figure 6: Rainfall intensity distribution of T002, T010, and T100 composite events for climate scenario 2050WH.

Despite the fact that used design rainfall events are based on the most recent and comprehensive statistical analysis presented in Beersma et al. (2019), the authors indicate uncertainty ranges in rainfall depths of *not known*, -4 to +5%, and -9% to +11% for T002, T010, and T100 events respectively. This represents the statistical uncertainty induced by followed statistical methods. Those current events are used as a base, whereafter those are altered based on predicted changes in meteorological conditions in 2050 due to climate change. Yet, uncertainties in predicted changes of hourly rainfall depths are between +13% and +25% for the 2050WH scenario as indicated by the KNMI (Klein Tank et al., 2014).

The use of varying rainfall depths for future climate conditions gives insight in the functioning of the study area and its sewerage system in its current state, when subjected to short intense rainfall events in 2050. The *functioning* will be quantified using water balance terms (depicted in Figure 7), mixed sewerage and storm drain overflows, and flood indicators (described in *Section 3.1.3*). Those will be deducted from raw modelling results using Python scripts. Water balance terms and sewer overflows will be expressed as percentages of the total water input (rainfall and DWF). Flood indicators will be expressed as the percentage of buildings which are vulnerable, and the percentage of roads that are (partly) inaccessible. These results, in percentages, will serve as *base scenarios* for chosen rainfall events.

When adaptation measures will be separately implemented into model schematisations in Step 3, results of model runs with measures implemented will be compared to the base scenarios. In this way the effects of adaptation measures can be studied by comparing them to the present situation (i.e., the base scenarios).

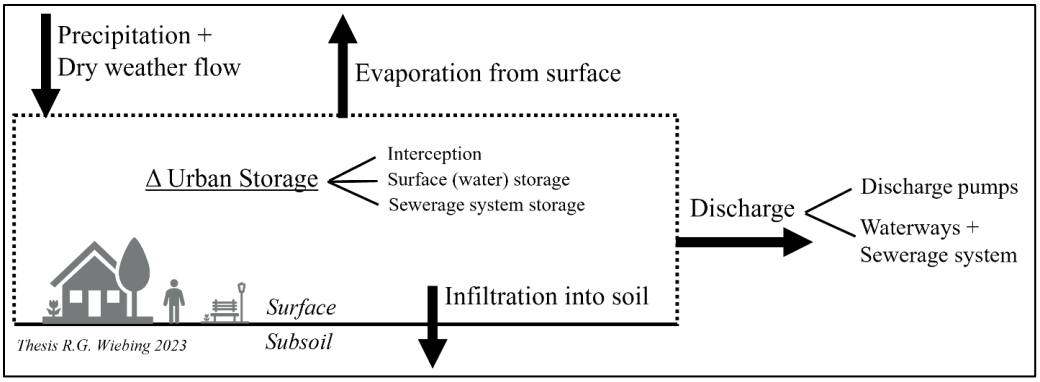

Figure 7: Water balance terms used within this study.

3.3 Studying the effects of rainwater adaptation measures

3.3.1 Selection of adaptation measures

Options to store rainwater found in Dutch literature have been listed in Table 5. First of all, it is assessed whether these options can be implemented into the used 3Di model schematisation. When, possible, the box of the column '***MS***' in Table 5 will be green, when technically infeasible it is red. This results in the exclusion of options 2, 3, 4, 12, 16 and 17, since subsoil water flow processes are not incorporated in the used 3Di model schematisation.

Next, the difficulty level of implementation in the 3Di model schematisation of the remaining options is considered with the help of an experienced 3Di modeller. Due to time constraints, options 9, 10, and 11 are excluded due to time constraints (column '***DL***' in Table 5). Those require a very detailed adjustment of the surface elevation map and computational grid. It is not feasible to implement it in the whole study area within the available time.

Lastly, a consultation was held with a landscape planner and climate adaptation manager from Doetinchem (column '***gD***' in Table 5). As a result, options 1 and 6 were excluded due to the limited available surface water. Furthermore, based on policy, it is preferred to store rainwater on permeable surfaces rather than paved surfaces, thus excluding option 5.

This results in a selection of options to retain and store rainwater which effects can be studied. Options 13, and 18 enhance the storage of rainwater on buildings and private properties. Options 7, 8, and 14 tend to increase the rainwater storage capacity by altering surface elevations of vegetated surfaces within the study area. This can also facilitate infiltration into the subsoil. Lastly, option 15 aims to facilitate infiltration by the removal of pavement on the surface area.

In consultation with the municipality, 4 measures have been proposed from the 7 implementable options. The first measure will assess the effect of decreasing impervious surfaces on private properties (option 15), while the second measure will assess effects of rainwater storage on private properties (options 13 and 18). The third and fourth measure will adjust vegetated surface area heights, to increase rainwater storage and enhance infiltration (options 7, 8, and 14). In this way, all options are represented by a measure, with a balance between two measures implemented on private property and two measures implemented in the public space.

*Table 5: List of urban water retaining options. Red boxes indicate which options are excluded due to infeasibility model-wise ('**MS**'), infeasibility difficulty level-wise ('**DL**'), or after consultation with the municipality ('**gD**').*

no.	***Rainwater retaining options***	***MS***	***DL***	***gD***	***Source***
	Measures solely for implementation in the public space:				
1	Increase maximum levels surface waters				(Brolsma et al., 2012; Hoogvliet et al., 2013, 2021; Veraart & Voskamp, 2022)
2	Repair draining sewerage pipes				(Brolsma et al., 2012; Veraart & Voskamp, 2022)
3	Increase infiltration out of waterways				(Terpstra et al., 2019)
4	Decrease groundwater seepage				(Veraart & Voskamp, 2022)
5	Storing rainwater on paved public squares				(Ministry of I&M, 2016; Terpstra et al., 2019)
6	Optimisation of draining waterways				(Brolsma et al., 2012; Hoogvliet et al., 2013, 2021)
7	Lowering of vegetated strips/verges				(Hoogvliet et al., 2013, 2021; Ministry of I&M, 2016)
8	Create retention areas (e.g., a pond)				(Dolman & Brolsma, 2023; Ministry of I&M, 2016; Terpstra et al., 2019)
9	Create obstructing road bumps				(Ministry of I&M, 2016)
10	Concaved road sections				(Rainproof Netwerk, 2023; RIONED, 2023)
11	Heighten sidewalk curbs				(Rainproof Netwerk, 2023; RIONED, 2023)
12	Create infiltrating storm drain pipes				(Rainproof Netwerk, 2023; RIONED, 2023)
	Measures for implementation in the public space or on private property:				
13	Storing rainwater in crates, (garden) tanks, or hollow spaces, possibly for domestic use				(Ministry of I&M, 2016; Rainproof Netwerk, 2023; RIONED, 2023; Terpstra et al., 2019)
14	Enlarging rainwater infiltration (e.g., disconnect roof run-off from sewerage system, wadis, infiltration crates)				(Brolsma et al., 2012; Dolman & Brolsma, 2023; Hoogvliet et al., 2021; RIONED, 2023; Terpstra et al., 2019; Veraart & Voskamp, 2022)
15	Decrease pavement on surface area				(Brolsma et al., 2012; Hoogvliet et al., 2013, 2021; Terpstra et al., 2019)
16	Improving soil structure and type				(Brolsma et al., 2012; Hoogvliet et al., 2021)
17	Create shadow on surface areas				(Hoogvliet et al., 2021; Terpstra et al., 2019)
18	Green (vegetated) roofs				(Dolman & Brolsma, 2023; Ministry of I&M, 2016; Terpstra et al., 2019)

3.3.2 Implementation of adaptation measures

As aforementioned, measure 1 and 2 are implemented within private properties, while measure 3 and 4 are implemented in the public space. The measures will be implemented into model schematisations separately, to study their isolated effects. *The effect* of measures will be assessed based on changes in water balance terms, flood indicators, and sewer overflows with reference to the base scenarios as described in in *Section 2*.

3.3.2.1 Measure 1: storing rainwater on private property.

Measure 1 will be based on the storage of rainwater on private property according to the example of Flanders. From 2005 onwards, legislation concerning the storage of rainwater falling onto buildings is implemented in Flanders, Belgium (Vlaamse Regering, 2023; Willems & Smet, 2023). When a building is newly built or its horizontal surface area is increased, it is mandatory to implement a private water storage to store rainwater. It has to be stored on private property, which can thereafter be used for practices such as washing a car or flushing toilets. This saves drinking water, contribution to a usage of only 87.5 litres per person per day in Flanders compared to 125 litres (+40%) within the Netherlands (Willems & Smet, 2023). A second advantage is that these storages store rainwater during rainfall events, alleviating the sewerage system. The minimum storage capacity is based on the horizontal surface area of a building, following:

- 5000 litres (5.0 m^3) if horizontal surface area < 80 m^2
- 7500 litres (7.5 m^3) if horizontal surface area ≥ 80 m^2 and < 120 m^2
- 10000 litres (10.0 m^3) if horizontal surface area ≥ 120 m^2 and < 200 m^2
- Tailor-made requirements if horizontal surface area ≥ 200 m^2

In a study conducted in 2021 by the Vlaamse Milieu Maatschappij (VMM), 16 years after the legislation was implemented, it was found that more than half of the buildings already had a rainwater storage facility (Willems & Smet, 2023). In addition, 32% of storage facilities had a capacity that exceeded minimal requirements. In 2013, a requirement was implemented which requires that surplus rainwater exceeding storage capacity has to be infiltrated into the soil.

Measure 1 will be based on described legislation of Flanders concerning rainwater storage on private property, to study the effect when such legislation will be implemented within the study area. For this study, effects of measures are assessed for climate conditions in 2050. Based on the study of VMM conducted in 2021, it seems reasonable to implement storage facilities meeting minimal requirements in 50% of the buildings present in the study area to study its effects for 2050 conditions. The other half of the buildings, or when a storage facility is full, will discharge rainwater into the sewerage system. In addition, buildings with an area less than 25 m^2 (e.g., car garages, garden sheds) do not get an implemented storage. Buildings with an area larger than 200 m^2 (tailor-made requirements in Flanders) get a storage facility of 10000 litres within this study. This measure will be named '*Storepp*' in figures within this study.

3.3.2.2 Measure 2: increasing infiltration on private property.

Private properties, other than buildings, make up 38.7% of the total surface within the study area. This makes it a significant large area to try to increase the retention of rainwater, for instance to promote rainwater infiltration. As seen in *Section 2.2.5*, percentages of paved surface within private properties exceed 60% on average, varying between neighbourhoods.

For measure 2 it is studied what the effect will be if 50% of current impervious surface area within private properties will become pervious, i.e., permeable. For example, a private property that is currently paved for 60% will be paved for 30% in this scenario. An exemption is the private property classified as industrial property (around 30% of the total surface of private properties), since such properties are often used as storage or parking areas for heavy traffic. It is ambitious to assume a decrease of 50% of paved surfaces within private properties, since the trend within is the Netherlands is to increase paved surfaces (Mulder, 2020). When this measure sorts a significant influence on the model outcomes, less ambitious percentages will be assessed on their effects as well. This measure will be named '*Erf50p*' in figures.

3.3.2.3 Measure 3: storing and infiltrating rainwater along roads.

Numerous vegetated verges are present alongside roads, generally higher or equally elevated with reference to adjacent road lane surfaces. For measure 3, named *'Road10'* within figures, these vegetated verges will be lowered. In consultation with a landscape planner from Doetinchem, the verges will be lowered to a commonly used average of 10 cm under the surface level of adjacent road section.

The verges which will be lowered are selected from vegetated surfaces within the Basis Registration Topography (BGT (PDOK, 2022c)). No general directives are present to identify which vegetated surfaces are suitable for lowering. Thus, conditions to identify a vegetated surface as verge to be lowered are based on visual inspection and trial-and-error. This is thus an arbitrary process. In the end, vegetated surfaces from the BGT satisfying the following conditions are identified as verges which will be lowered:

- The assessed surface <u>is not</u> classified as *'forest'* or *'agriculture'* in the BGT, <u>and</u>:
- The assessed surface <u>is</u> adjacent to a BGT road section surface (bicycle lane, car lane, pavement, parking space), <u>and</u>:
    - The assessed surface area is smaller than 400 square metres, <u>or</u>:
    - The assessed surface area has a ratio of area/perimeter < 2.5 (since a significant part of vegetated verges along roads are narrow but stretched, resulting in a large area)

Vegetated surfaces satisfying these conditions are given in Figure 33 in *Appendix C*, as well as a more detailed description on the method of determining the new height level of selected surfaces. The total area of these vegetated verges is 0.475 km^2 within the study area, making it a potentially significant area to store rainwater.

After lowering selected surfaces, it was found that those surfaces were lowered 25 cm on average. This is not surprising since most verges are currently elevated compared to the adjacent road surface, and will be lowered to 10 cm below it.

3.3.2.4 Measure 4: storing and infiltrating rainwater within larger green spaces.

Public spaces within urban areas contain numerous spacious vegetated surfaces, although not evenly spread across an urban area due to neighbourhood characteristics. Those surfaces combined are a substantial area for potential rainwater storage. Such lowered rainwater storages are commonly called a *wadi* in the Netherlands, and *bioswales* internationally. Here, excess rainwater can be stored whereafter it can gradually infiltrate into the soil (RIONED, 2022). For safety reasons it is often 30 cm deep at maximum. For the 4th measure, named *'Wadi30'*, every height cell within selected surfaces will be lowered 30 cm in reference to its current height. The surfaces used to create wadis are selected from vegetated surfaces within the Basis Registration Topography (BGT (PDOK, 2022c)). There are no general directives present for which surfaces are suitable for constructing a wadi. Thus, conditions for the suitability for wadi construction are based on trial-and-error and visual inspection. This is therefore an arbitrary process. For the implementation of a wadi on a vegetated surface, the BGT vegetated surface has to satisfy the following conditions:

- The assessed surface is not classified as *'forest'* or *'agriculture'* in the BGT, and:
- The assessed surface area is larger than 400 square metres, and:
- The assessed surface area has a ratio of area/perimeter > 2.5 (since a significant part of vegetated surfaces are narrow but stretched, resulting in a large area but are deemed too narrow for the construction of a wadi)

Vegetated surfaces that satisfy these conditions are reduced with a 1 metre buffer on the whole perimeter, to account for a 1:3 sloping embankment on wadis that is commonly applied for wadis (RIONED, 2022). Wadis which will be lowered in scenario *Wadi30* are indicated in Figure 33 within *Appendix C*. These wadis have a total area of 0.820 square kilometre within the study area.

4 Results

4.1 Evaluation of model performance after historic rainfall events

Figure 8, 9, 10, 11 show modelled versus measured water levels for the two assessed events. Those 4 measuring locations have been selected since they represent the four different structures in the sewerage system. Other locations area shown in *Appendix B* to save space in this section.

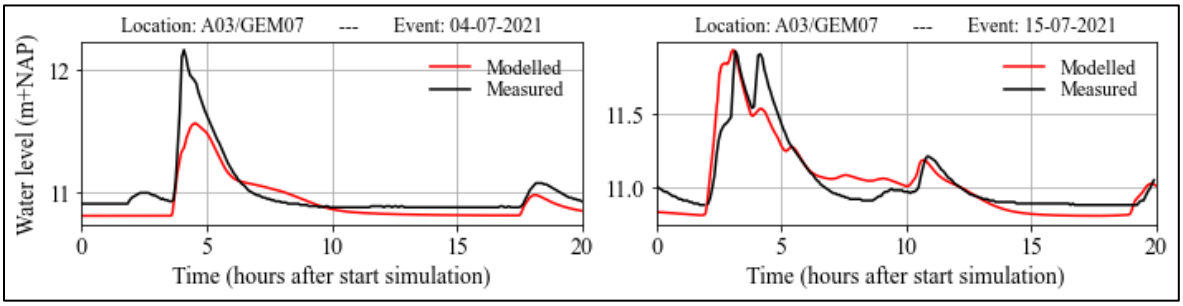

Figure 8: Modelled versus measured water levels at a mixed sewerage overflow.

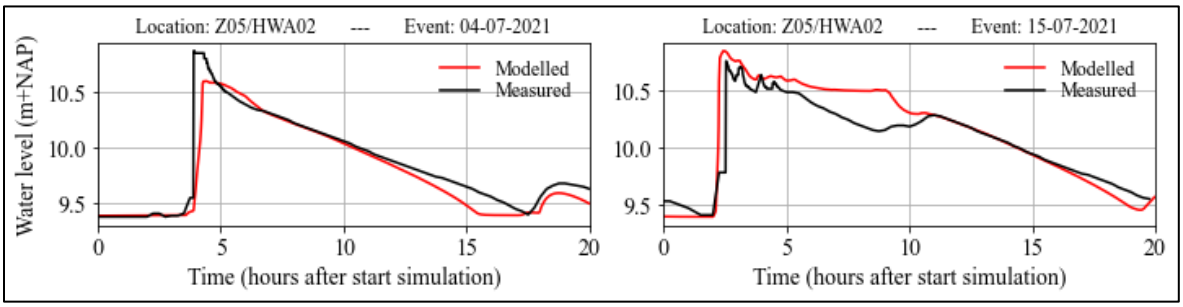

Figure 9: Modelled versus measured water at a storm drain overflow.

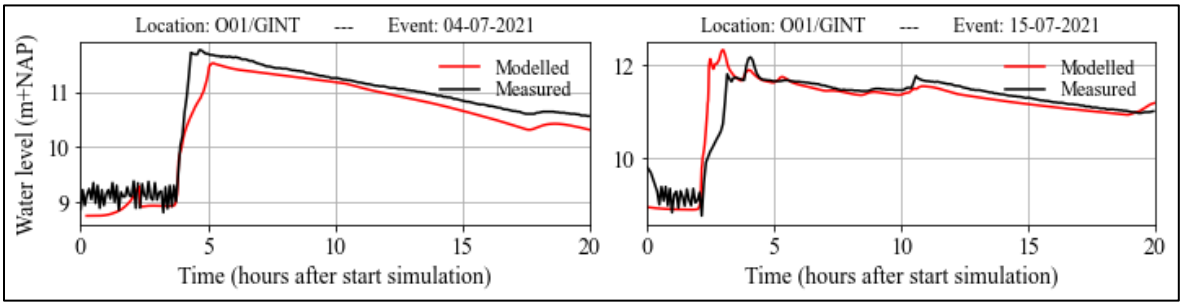

Figure 10: Modelled versus measured water levels at an intern discharge pump.

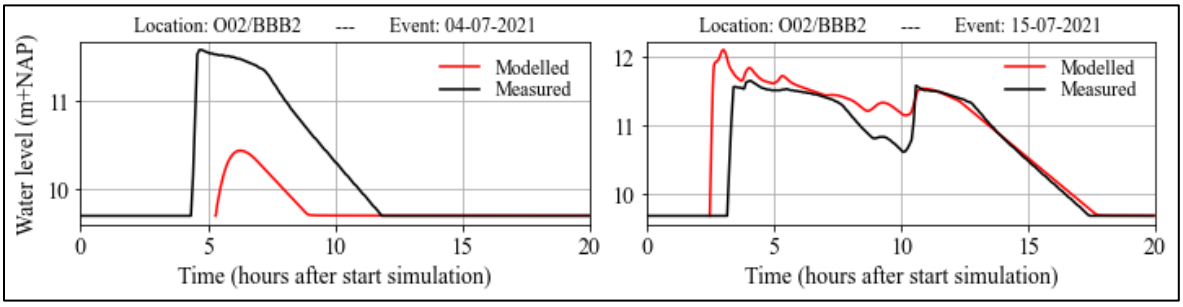

Figure 11: Modelled versus measured water levels within an internal storage tank.

It is challenging to determine the causes of differences between modelled and measured water level values, since numerous factors can cause deviations. Causes of inaccuracy can lie in both the real-world as well as in model schematisations.

Next to uncertainty in input data about the sewerage system, the model represents an *optimal* draining situation, while in reality it is generally not. For example, measured discharges within sewerage pipes can be influenced by broken sewerage pipes or clogged sewerage system in- and outlets. In addition, measuring sensors contain systematic and stochastic uncertainties.

Next to the real-world processes which influence measured water levels, modelled water levels with which they are compared also contain inherent uncertainties. This is caused by both inaccurate input data as well as modelling parameters and setups. Although a lot of open-source data of good quality about the physical environment is present, information about private properties is absent, and so is data about infiltration rates, interception values, bottom friction et cetera. Additionally, the *equifinality* concept comes in play when modelling a complex system, such as an urban area where features vary on small spatial scales (Beven & Freer, 2001). This concept states that many different parameters sets and many model structures may be acceptable to reproduce measured observations. Hence, finding the *correct* model is challenging given limited input and measurement data. In addition, Doetinchem has a *branched* sewerage system, indicating that sub-catchments of sewerage systems within the city are interconnected. Hence, inaccuracies in one sub-catchment of the modelled system propagates to other sub-catchments.

Due to all aforementioned reasons, it is challenging to comprehensively assess causes of deviations between modelled and measured water levels, particularly at the scale of the study area using a high-resolution 1D-2D model. Despite all inherent uncertainties within the model and its input, figures indicate that the model replicates timing of peaks, increasing and decreasing slopes, and durations of peaks considerably well.

Yet it is seen that, particularly in the beginning of rainfall events, measured water levels deviate from modelled water levels. Modelled water levels on the 4th of July are consistently underestimated, while modelled water levels on the 15th of July are consistently overestimated. So, the 4th and 15th of July express opposite signals. The two model runs were setup identically with reference to model schematisation and scenario information, except for rainfall input data. This suggests that rainfall input data is largely causing the deviations between modelled and measured water levels.

This is not surprising however, while assessed rainfall events happened in summer conditions, and were short and intense. Rain radars are less accurate in capturing such convective rainfall events. This is due to the fact that radar signals are attenuated by heavy rainclouds (also promoting occultation, i.e., rainfall clouds *hiding* behind other rainclouds), together with uncertainties in the vertical profiles of rainfall reflection and raindrop sizes (Holleman et al. 2006; Overeem et al., 2009). Besides, corrections with gauge stations are less accurate in summer conditions, due to generally high spatial variability in summer rainfall events (Holleman et al.,

2006). Therefore, it is expected that the used rainfall event input data contains significant uncertainties in rainfall depth and intensities.

Yet, the importance of rainfall event input data is stressed by multiple studies performing sensitivity analysis on model inputs of 2D hydrodynamic models based on the full SWE within urban areas (Alipour et al., 2021; Xing et al., 2021). Although no sensitivity analyses were found for particularly the water levels in sewerage systems, analysis found are an indication about the sensitivity of water flows in an urban area to different model inputs.

Alipour et al. (2021) show that modelled flood extent and depth are predominantly sensitive to rainfall event input, with about a 4 times lower influence of the combined influence of roughness coefficients, infiltration rates, and computational grid sizes. Xing et al. (2021) also shows a dominant role for rainfall input for calculated flood extent and depth, showing on average 3 to 6 times more influence than the computational grid size, Manning roughness coefficients on permeable and impermeable surfaces, infiltration rates, and drainage loss due to the sewerage system. Only when assessing maximum flow speeds the computational grid size has more influence than rainfall input. Additionally, at smaller spatial scales influences of inputs can differ due to local characteristics, but the relative importance of rainfall is generally maintained (Xing et al., 2021).

Modelled inundation depths and extents cannot be evaluated straightforwardly since no measurements of it are available, which is a common problem (de Arruda Gomes et al., 2021; Mihu-Pintilie et al., 2019). A hindrance map based on pluvial flood indicators is made, to evaluate the model performance in modelling inundation depth and extent by expert judgment. Yet, some drawbacks are present for this approach. The used hindrance map is based on maximum water depths which is dependent on modelled water levels and surface elevation data. These both contain uncertainties, contributing to uncertainty in the hindrance map. Inaccuracies in the surface elevation map can also under- or overestimate the flood extent (de Arruda Gomes et al., 2021). In addition, the hindrance map only assess modelled maximum water depths, thus does not incorporate the duration for which hindrance occurred. When this duration is taken into account, this could limit the hindrance for road sections.

Figure 12 shows the hindrance maps for both evaluated rainfall events, as well as renowned locations where hindrance due to pluvial flooding often occurs according to the experts. It is seen that the event on the 4th of July is producing less hindrance locations than the 15th of July. This was expected since the event of the 4th had a lower cumulative rainfall depth and rainfall intensity than the event on the 15th. After the modelled event of the 4th, some individual road sections are indicated as only accessible for emergency vehicles, but no clusters are seen. On the contrary, some clusters are seen after the event of the 15th. It shows that this hindrance map based on modelled water depths indicate hindrance in 5 of the 7 known hindrance locations. Yet, some hindrance locations are shown which are not indicated as well-known hindrance locations. Overall, the hindrance maps do not indicate extraordinary results according to the two experts from Doetinchem.

Concluding, the model performs well in calculating rainwater distribution across the urban area when subjected to historic short and intense rainfall events. Modelled water levels within the sewerage system showed high similarity with measured water levels. Moreover, deviating water levels are assumed to be predominantly caused by inaccuracies in rainfall event input. A closed water balance could however not be evaluated, since measurements in numerous sewer outflows and waterways are absent. Besides, it proved difficult to evaluate the model performance regarding inundation depths and extent due to the lack of data. Yet, experts judged that the hindrance map due to pluvial flooding did not indicate extraordinary results, and were in line with expectations. Moreover, it was found in literature that flood depth and extent are predominantly influenced by rainfall event input and the digital elevation model. Digital elevation models are accurate and available on high spatial resolutions within the Netherlands. Moreover, designed rainfall events are used for scenario modelling within this study, eliminating uncertainty in rainfall input. Thus, although uncertainties remain present in particularly in the water balance part of the model, the used model is deemed suitable for this study.

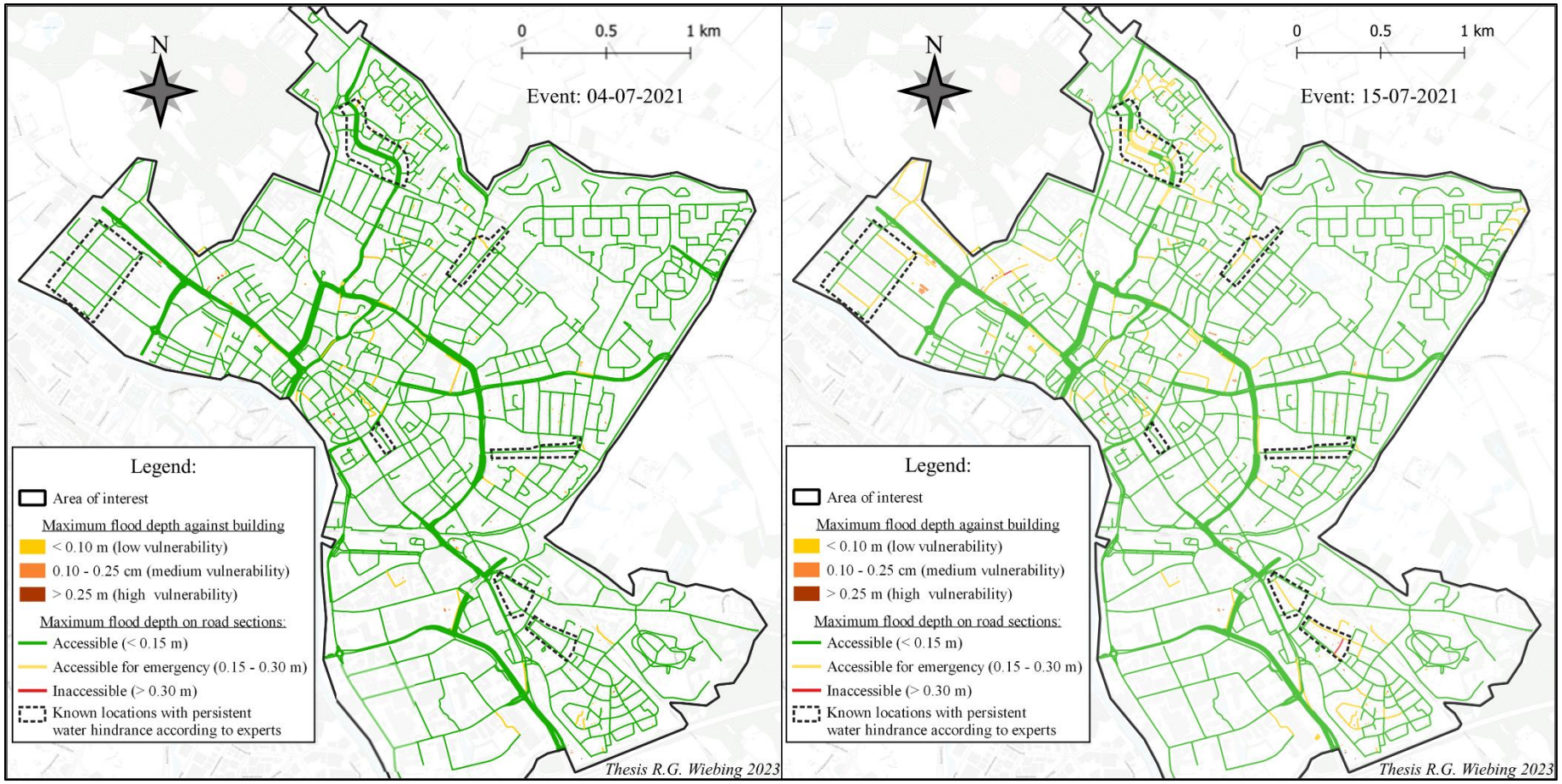

Figure 12: Map of water hindrance after evaluated events, together with known hindrance locations based on expert judgement.

4.2 Base scenarios

A simulation time of 24 hours was used, where assessed design rainfall events occurred in the first hour of the simulation. Figure 13 presents the water balance terms, flood indicators and sewerage system overflows for assessed rainfall events with recurrence times of 2 (T002), 10 (T010), and 100 (T100) years. The balance terms in Figure 13 represent the following:

- ***Total input***: total input volume within the study area for the given rainfall event, which is either stored or discharged at the end of a model simulation. The total input consists mostly of rainfall input. *Made up of:*
- ***Rain on surface***: rain falling on surface areas other than buildings.
- ***Rain on buildings***: rain falling on buildings.
- ***Dry weather flow***: wastewater flow from buildings into the sewerage system.
- ***Total stored***: total percentage of input volume that is still present within the study area at the end of the simulation. *Made up of:*
- ***Infiltration***: infiltrated water into the subsoil.
- ***Δ Surface storage***: change in storage on surface area (ponding rainwater, waterways, lakes)
- ***Interception***: rain intercepted by surfaces such as grass, trees, flat roofs.
- ***Δ System storage***: change in storage within sewerage system.
- ***Total discharged***: total percentage of input volume that has been discharged out of the study area at the end of the simulation. *Made up of:*
- ***Sewer/waterways***: water that has been discharged out of the study area via sewerage system overflows or via waterways.
- ***Discharge pumps***: pump stations that discharge sewage and rainwater to a wastewater treatment plant.
- ***Surface flow***: water that flows over the surface area out of the study area, e.g.: water that flows over surface area to the river Oude IJssel.
- ***Surface evaporation***: water that evaporates from surface areas.

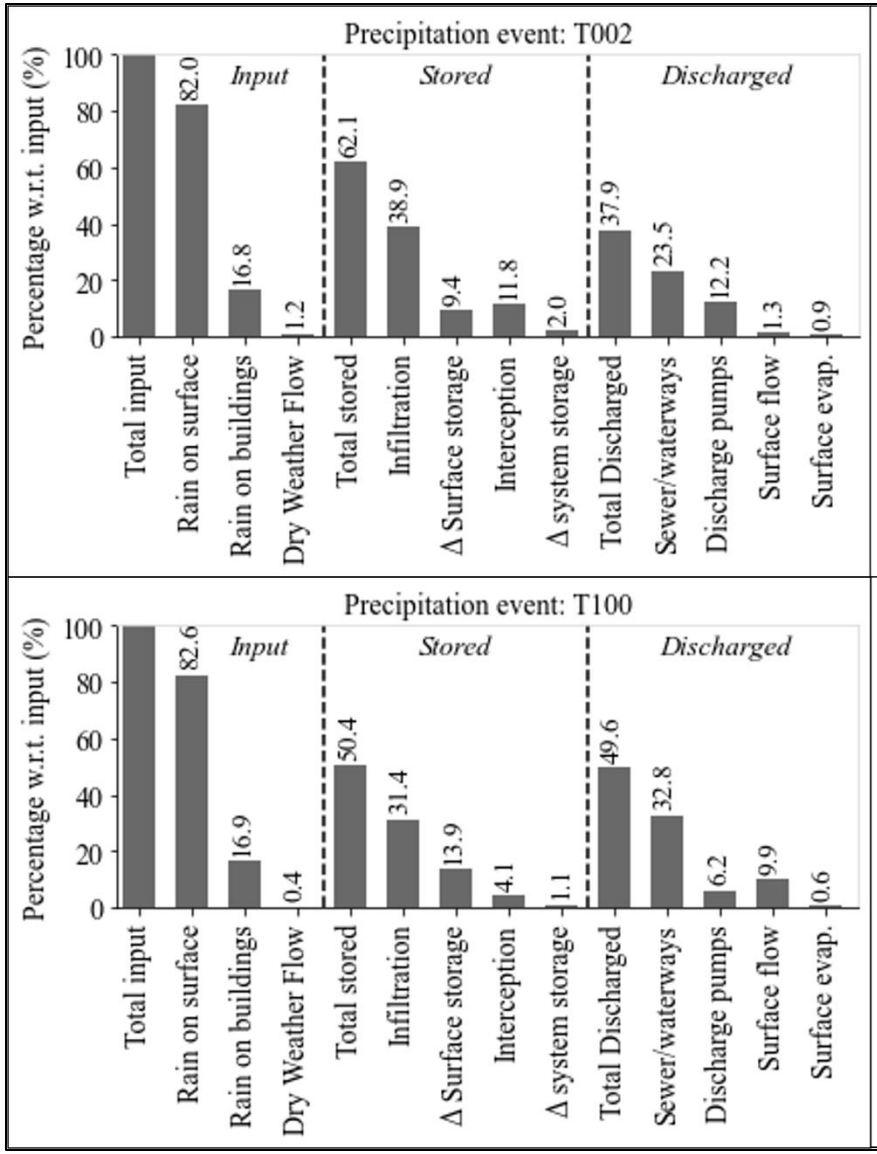

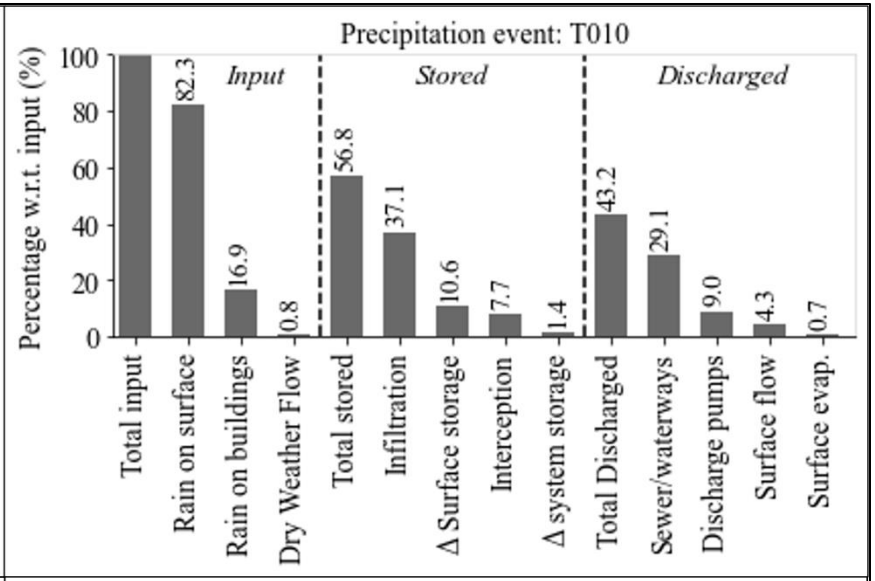

	T002	***T010***	***T100***
Roads *(170.7 km)*	*(%)*	*(%)*	*(%)*
Fully accessible *(< 15 cm)*	88.6	75.4	54.4
Acc. by Emergency only *(15-30 cm)*	10.9	21.6	36.4
Not Accessible *(> 30 cm)*	0.4	2.3	9.0
Buildings *(10.390)*	*(%)*	*(%)*	*(%)*
Low vulnerability* *(< 10 cm)*	99.6	99.0	95.4
Moderate vulnerability* *(10 - 25 cm)*	0.4	0.8	3.3
High vulnerability* *(> 25 cm)*	0.0	0.2	1.4
Overflows *(w.r.t. total input)*	*(%)*	*(%)*	*(%)*
Mixed Sewerage	11.2	14.7	17.2
Storm Drain Sewerage	6.8	9.5	10.6
2050WH climate scenario			*Thesis R.G. Wiebing 2023.*

Figure 13: Water balance terms and flood indicators for base scenarios T002, T010 and T100 (vulnerability to pluvial flooding)*

Modelling results for assessed base scenarios are in line with expectations. For instance, it is seen that DWF and evaporation from water on the surface are insignificant compared to other water balance terms, becoming increasingly insignificant with increasing rainfall depths. In addition, the total percentage of stored (i.e., retained) rainwater decreases when rainfall depth increases. This is in line with expectations, since the infiltration rate becomes an increasingly larger limitation when rainfall depth increases, while the infiltration is the largest balance term within the total amount of stored rainwater. Part of the increased amount of excess rainwater is collected by rainwater storages on the surface (e.g., surface area depressions, ponds), while another part is drained out of the area. Hence, relative amounts of discharged (i.e., drained) rainwater out of the area increases with larger rainfall depths. Discharged rainwater out of the study area via overland flow show the largest relative increase when rainfall depths increase, while drained rainwater via waterways and sewerage system show less relative increase. This is again due to the fact that more excess rainwater is present due to limitations on infiltration rate and sewerage system capacities. Rainwater volumes discharged via waterways and sewerage overflows does increase, but show less relative increase compared to overland flow. In addition, the percentage of rainwater that is discharged out of the study area by discharge pumps decreases significantly. This is consistent with the fact that the sewerage system's maximum capacity is designed for a T002 event (current climate conditions), thus playing a less important role when assessing T010 and T100 events.

Subsequently, percentages of sewer overflows also show limited relative increase with reference to rainfall depth increases. It should be noted however that one sewer overflow was found to be schematised 1 m too high, and 1 overflow was schematised 0.5 m too low, shown *Appendix B*. This results in inaccurate overflow volumes at these locations, as well as inducing under- or overestimated sewerage discharges in sewerage pipes downstream. However, part of the induced inaccuracy may be mitigated, as downstream overflow locations will experience under- or overestimated sewerage discharges, resulting in under- or overestimated sewerage overflow volumes. Thus, larger overflow volumes upstream are expected to be (partly) compensated by lower overflow volumes downstream, and vice versa.

Flood indicators also indicate an increase in vulnerability and inaccessibility with increasing rainfall depth. This is expected since a larger volume of rainwater needs to be stored or discharged with increased rainfall depths, while maximum storage and drainage capacities are limited. This results in pluvial flooding, which can lead to inaccessibility of roads and vulnerability of buildings. Low percentages of inaccessible roads and vulnerable houses are present at the T002 event. This was expected since municipal policy demands that the drainage capacity of the urban water system is such that no hindrance will occur at a T002 event for current climate conditions. The results presented indicate some hindrance, which is not remarkable since those are obtained by using a predicted T002 event for climate conditions in 2050. This event contains 23% more cumulative rainfall and higher intensities than the T002 event used for designing the urban water system.

4.3 Studying the effects of proposed measures

This section provides quantitative results of the effects of proposed measures to make the spatial rainwater distribution more robust. Rainwater retention is quantified by the amount of stored rainwater, limiting pluvial flooding by flood indicators on vulnerable buildings and inaccessibility of roads, and limiting overflows by a percentage of sewerage overflows compared to rainfall input. It is given for each measure separately, together with the relative change compared to the base scenario. *Section 5.1* gives an overview of the proposed measures after which they are compared to each other to assess their effectiveness.

4.3.1 Measure 1: storing rainwater on private property.

When implementing private rainwater storages on half of the private properties, based on implemented legislation in Flanders, the cumulative volume of these storage facilities would be 32000 m^3. In theory, this is 14%, 9%, and 5% of cumulative rainfall depths for the T002, T010, and T100 events respectively. However, these storage facilities are only filled by a building's roof runoff (i.e., rain which falls onto the building's roof). This roof runoff volume is often not sufficient to utilise all potential storage of the connected storage facilities. Figure 14 shows the cumulative distribution function (cdf) of implemented storage capacity at buildings, expressed as the maximum number of millimetres which can be stored in reference to the connected roof surface area, following:

$$max.storage\ capacity\ (mm) = 1000 * \frac{\text{implemented storage capacity at building } (m^3)}{\text{square surface area of building's roof } (m^2)}$$

Figure 14 also indicates rainfall depths corresponding to the T002, T010, and T100 events with vertical dotted lines. It is seen 94%, 92%, and 72% of implemented storages can store all rainfall runoff from its connected roof for the T002, T010, and T100 event respectively.

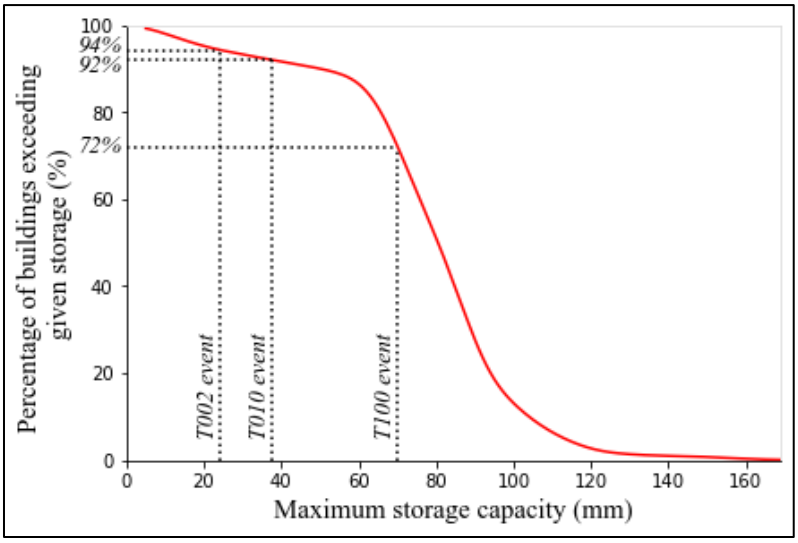

Figure 14: Maximum storage capacity of implemented storage facilities, expressed in mm in reference to the connected roof from the building.

Outcomes of the effects of rainwater storage from building roofs on half of the private properties are shown in Figure 15.

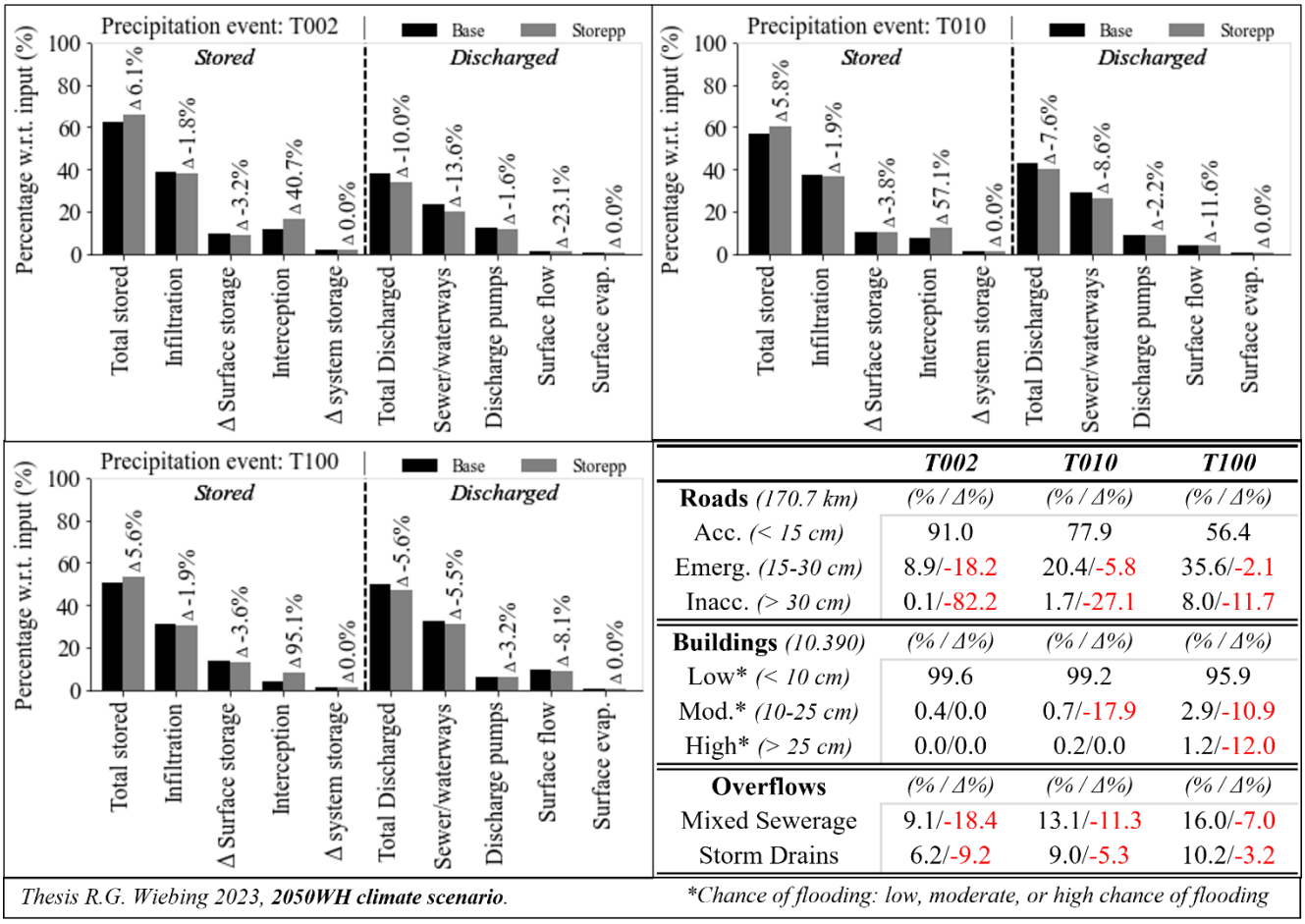

	T002	*T010*	*T100*
Roads *(170.7 km)*	*(% / Δ%)*	*(% / Δ%)*	*(% / Δ%)*
Acc. *(< 15 cm)*	91.0	77.9	56.4
Emerg. *(15-30 cm)*	8.9/-18.2	20.4/-5.8	35.6/-2.1
Inacc. *(> 30 cm)*	0.1/-82.2	1.7/-27.1	8.0/-11.7
Buildings *(10.390)*	*(% / Δ%)*	*(% / Δ%)*	*(% / Δ%)*
Low* *(< 10 cm)*	99.6	99.2	95.9
Mod.* *(10-25 cm)*	0.4/0.0	0.7/-17.9	2.9/-10.9
High* *(> 25 cm)*	0.0/0.0	0.2/0.0	1.2/-12.0
Overflows	*(% / Δ%)*	*(% / Δ%)*	*(% / Δ%)*
Mixed Sewerage	9.1/-18.4	13.1/-11.3	16.0/-7.0
Storm Drains	6.2/-9.2	9.0/-5.3	10.2/-3.2

Thesis R.G. Wiebing 2023, ***2050WH climate scenario****.*

**Chance of flooding: low, moderate, or high chance of flooding*

Figure 15: Effects of measure 'Storepp', given in percentages and as relative change (Δ%) compared to the base scenario. The additional created storages on private property are schematised as 'Interception' model-wise. As a result, the interception term increases due to this measure.

In Figure 15 it is seen that the total retained rainwater increases with 6.1%, 5.8% and 5.6% for the T002, T010, and T100 events respectively. This is the net result of increased storage capacities on private properties (model-wise implemented as additional *Interception* on buildings' roofs). It is seen that surface storage and infiltration show a decrease, presumably since private storages reduces the amount of rainwater which has to be discharged via the sewerage system. Hence, less sewerage system capacity is used to discharge rainfall runoff from buildings' roofs, increasing the discharge of excess rainwater from other surfaces via the sewerage system. In addition, since this measure alleviates the sewerage system, sewage flowing out of the sewerage system onto the surface area is presumably limited. This effect is also seen in the reduction of sewage overflows.

Interestingly, this measure also shows a significant decrease in the amount of (partly) inaccessible roads, particularly for smaller rainfall depths. This can be caused by the combined effect of alleviating the sewerage system and the fact that sewerage system pipes are often located under roads. Therefore, drainage of excess rainwater on roads is drained faster. In Figure 15 it is also seen that the increased percentage of stored rainwater remains relatively stable with increasing rainfall depths. This complies with the fact that maximum storage capacities of facilities get increasingly utilised with increasing rainfall depths.

It has to be noted however that it is assumed that the storage facilities are empty at the start of the assessed rainfall event. This assumption is particularly influencing outcomes for larger rainfall depths, since an increasing number of storage facilities are used at their maximum storage capacity. Nevertheless, used storage facilities are implemented at their minimum required storage in the schematisation, but it was found in Flanders that 1/3rd of storages had a storage capacity larger than the minimum. Moreover, assessed T100 events are typical for summer conditions where less rainfall occurs and water demands are high, resulting in largely empty rainwater storages. Due to these reasons, the assumption of an empty storage facility seems reasonable.

Concluding, this measure has a significant contribution to rainwater retention, for all assessed rainfall depths. As a secondary effect, stored rainwater can thereafter be used to decrease the drinking water consumption per person. Moreover, it significantly contributes to less sewage overflows and (partly) inaccessible roads. Yet, the sewerage system plays a less important role when assessing large rainfall depths due to its limited draining capacity, designed for a T002 event. Thus, this measure becomes less effective in limiting sewer overflows and pluvial flooding with increased rainfall depths.

4.3.2 Measure 2: infiltration private property.

Outcomes of the effects of removing half of the pavement on private properties are shown in Figure 16.

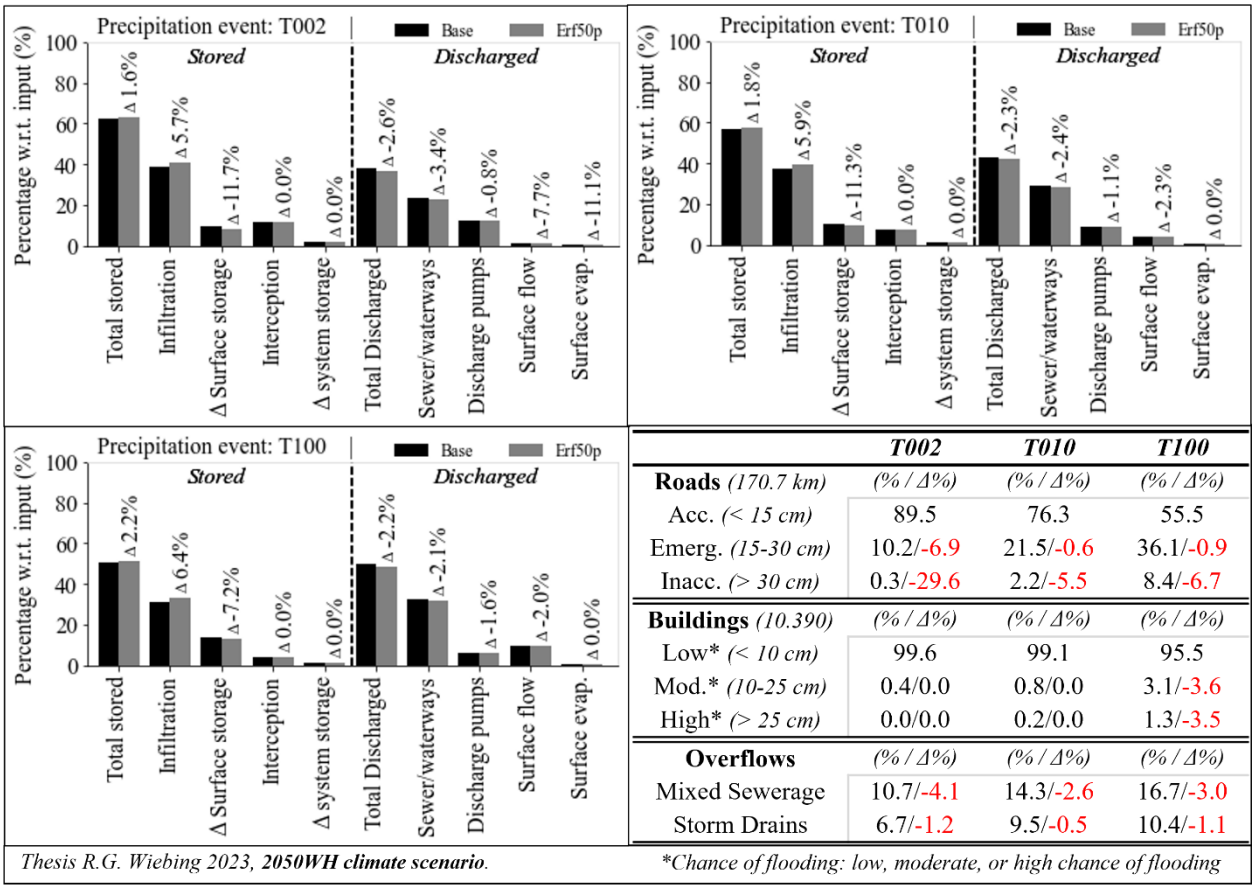

	T002	*T010*	*T100*
Roads *(170.7 km)*	*(% / Δ%)*	*(% / Δ%)*	*(% / Δ%)*
Acc. *(< 15 cm)*	89.5	76.3	55.5
Emerg. *(15-30 cm)*	10.2/-6.9	21.5/-0.6	36.1/-0.9
Inacc. *(> 30 cm)*	0.3/-29.6	2.2/-5.5	8.4/-6.7
Buildings *(10.390)*	*(% / Δ%)*	*(% / Δ%)*	*(% / Δ%)*
Low* *(< 10 cm)*	99.6	99.1	95.5
Mod.* *(10-25 cm)*	0.4/0.0	0.8/0.0	3.1/-3.6
High* *(> 25 cm)*	0.0/0.0	0.2/0.0	1.3/-3.5
Overflows	*(% / Δ%)*	*(% / Δ%)*	*(% / Δ%)*
Mixed Sewerage	10.7/-4.1	14.3/-2.6	16.7/-3.0
Storm Drains	6.7/-1.2	9.5/-0.5	10.4/-1.1

Thesis R.G. Wiebing 2023, ***2050WH climate scenario****.*

**Chance of flooding: low, moderate, or high chance of flooding*

Figure 16: Effects of measure 'Erf50p', given in percentages and as relative change (Δ%) compared to the base scenario.

In Figure 16 it is seen that removing half of the paved area on private properties sorts limited effects on rainwater retention. It is seen that rainwater retention increases with 1.6%, 1.8% and 2.2% for the T002, T010, and T100 events respectively. This is the net result of increased infiltration but decreased surface storage. Its effectiveness in retaining rainwater becomes slightly more effective with increasing rainfall depths. This is expectedly due to the fact that more newly created pervious surface is inundated due to increased inundation extents when rainfall depths increase. This is effect is also found by Haghighatafshar et al. (2018). Nonetheless, this measure shows a very limited effectiveness.

This is presumably due to multiple reasons. Firstly, this measure only has effect on approximately 15% of the study area. Infiltration rates are increased solely for this part. Secondly, infiltration is still limited due to these infiltration rates since maximum rainfall intensities are higher than infiltration rates. Lastly, surface elevations of private properties are generally designed with gradients, with higher elevated buildings with respect to the public space such as public pavements (Bügel et al., 2010). Consequently, excess rainwater during intense rainfall events flows

from the private properties to the public space. This prevents rainwater from being gradually infiltrated on private properties.

Moreover, the infiltration rate on a private property is now multiplied by a perviousness factor which represent the average percentage of vegetated area on neighbourhood scale. Hence, it implies impervious land covers on non-vegetated areas while this is not necessarily the case. Moreover, this approach erases spatial variability on pervious and impervious sections on both neighbourhood and private property scale, since it is using a spatially averaged factor. Furthermore, small scale geographical features (e.g., perennial borders) are not modelled since it is based on a DEM with a spatial resolution of 0.5m. The computational grid with a spatial resolution of 8 meters exacerbates this effect since the area of individual gardens are commonly within that order of magnitude. On a more practical side, this measure would also require a lot of effort to implement since the trend is to increase paved surfaces rather than decreasing it (Mulder, 2020).

All in all, this measure shows limited effectiveness to make the spatial rainwater distribution more robust on municipal scale. Expectedly, it is a more viable approach to try to create rainwater storages on private properties which prevent swift rainfall run-off to the public space, whereafter it can infiltrate over longer time periods. These measures can however be beneficial for other municipal objectives, such as reducing heat stress or strengthening biodiversity.

4.3.3 Measure 3: storing and infiltrating along roads.

Selected vegetated verges are shown in Figure 33 within *Appendix C*. When lowering the verges to 10 cm under the road surface (total area of the verges is 475000 m^2), it creates an extra surface storage of 47500 m^3 in theory. This *theoretical* rainwater storage capacity is 20%, 13%, and 7% of cumulative rainfall depths in T002, T010, and T100 events respectively.

Outcomes of the effects when vegetated verges along roads are lowered to 10 cm below adjacent road surfaces are shown in Figure 17.

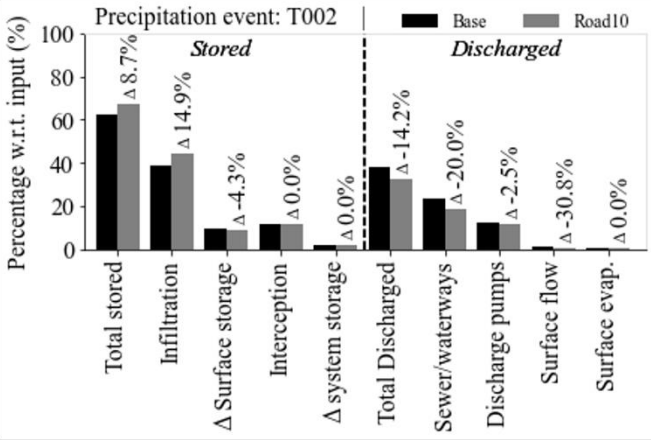

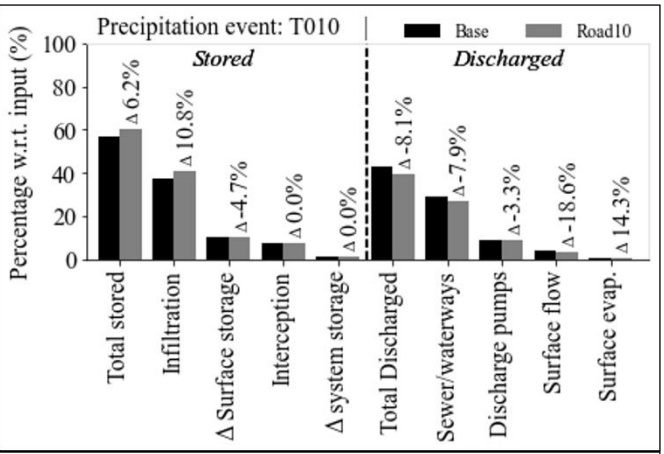

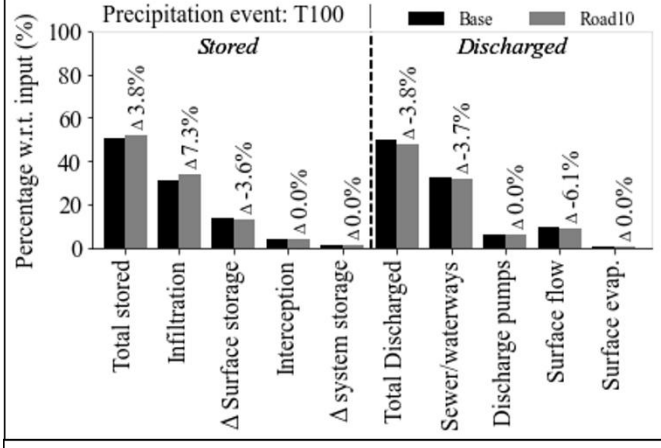

	T002	*T010*	*T100*
Roads *(170.7 km)*	*(% / Δ%)*	*(% / Δ%)*	*(% / Δ%)*
Acc. *(< 15 cm)*	93.9	81.5	62.1
Emerg. *(15-30 cm)*	5.8/-47.2	17.0/-21.4	31.0/-14.9
Inacc. *(> 30 cm)*	0.3/-36.5	1.5/-34.1	6.9/-23.7
Buildings *(10.390)*	*(% / Δ%)*	*(% / Δ%)*	*(% / Δ%)*
Low* *(< 10 cm)*	99.6	99.2	96.2
Mod.* *(10-25 cm)*	0.3/-17.1	0.7/-15.5	2.7/-16.3
High* *(> 25 cm)*	0.2/0.0	0.1/-27.8	1.1/-18.3
Overflows	*(% / Δ%)*	*(% / Δ%)*	*(% / Δ%)*
Mixed Sewerage	8.3/-25.6	13.2/-10.5	16.2/-5.6
Storm Drains	5.7/-16.6	8.5/-10.5	10.4/-1.9

Thesis R.G. Wiebing 2023, ***2050WH climate scenario.***

**Chance of flooding: low, moderate, or high chance of flooding*

Figure 17: Effects of measure 'Road10', given in percentages and as relative change (Δ%) compared to the base scenario.

In Figure 17 it is seen that the effect of this measure on the total stored rainwater is 8.7%, 6.2%, and 3.8% for assessed T002, T010, and T100 rainfall events respectively. The main cause of this water retention is the decreased amount of rainwater drained via the sewerage system and waterways. This is aligned with expectations, since sewerage system pipes are commonly located under road sections where excess rainwater is collected, while this measures also collects excess rainwater from adjacent road sections. This effect is also seen in significant decreases in sewerage overflow volumes. Nevertheless, the effect of decreased overflows and increased rainwater storage reduces significantly with increasing rainfall depths. This indicates that the extra created storage

capacity of lowered verges is a limitation, but that those verges are filled up well with rainwater during all simulations.

Besides, it is observed that percentages of (partly) inaccessible roads are decreased considerably. This is not an extraordinary result since additional rainwater storage is created directly adjacent to road sections and the verges are distributed relatively equally over the total study area. Moreover, those vegetated verges are on average 15 cm elevated in reference to the adjacent road section as of now, but are lowered to 10 cm under the elevation level of the road section. Therefore, additional *temporary* storage above the road sections surface level is created (i.e., the nowadays elevated part of the verges) when verges are lowered to 10 cm below the road section surface level. This is created next to the additionally *longer-term* storage which is created as a result of lowering the verges to 10 cm under the road surface level. Consequently, maximum inundation depths and extents on road sections will be lowered significantly.

Nonetheless, it was found that additionally stored rainwater equals 12650, 12730, and 12900 m^3 for T002, T010, and T100 events respectively. Thus, additionally stored rainwater increases with 0.6% and 1.3% for subsequent rainfall event depths, while rainfall depths increase with 53% and 86% in those events. So, this measure shows a limited rainwater storage capacity of around 12750 m^3 when implemented in the model, being only $1/4^{th}$ of the *theoretical* additional storage capacity. In theory, this could be due to the fact that rainwater is caught in the verges which would otherwise have been stored elsewhere, thus limiting the net result. This is however increasingly unlikely when assessing events with large rainfall depths due to large amounts of excessive rainwater and limited storage capacity.

Hence, most likely, it has to do with the shape of the verges and implementation into the model. Most of the verges are narrow but stretched, since they are parallel to roads. But due to surface elevation differences, the verges are sloped. This sloping causes parts of the additionally created storage in the verges to be ineffective, since rainwater will flow to the lowest elevated point in verges. When the water depth at these lowest elevated points exceeds 10 cm, rainwater flows onto the road surface again, not filling up created storage above this height level.

When implementing these verges in more detail into the model (e.g., stepped compartments), it is expected that this measure will become more effective regarding rainwater retention, reducing overflows, and limiting hindrance due to pluvial flooding. To further increase the effectiveness of this measure, ‘paved verges’ can be lowered as well. This will be adding to the potential of this measure, since ‘paved verges’ are also widely present in an urban context.

In conclusion, this measure already significantly limits pluvial flooding and sewerage overflows, and increases water retention. It is particularly suited to reduce the (partly) inaccessibility of roads within the study area. Its effectiveness does however decrease with increasing rainfall depths due to limited storage capacities. Yet, when a more detailed model implementation is used it will likely show a greater effectiveness due to increased usage of storage potential.

4.3.4 Measure 4: storing and infiltrating within larger green public spaces.

Selected vegetated surface suitable for wadis are shown in Figure 33 in *Appendix C*. In theory, the 30 cm deep wadis (total area of the wadis is 820000 m^2) create an additional surface rainwater storage of 245700 m^3. This *theoretical* rainwater storage capacity is 105%, 68%, and 36% of cumulative rainfall depths in T002, T010, and T100 events respectively.

Outcomes of the effects when wadis with a depth of 30 cm are implemented in the study area are shown in Figure 18.

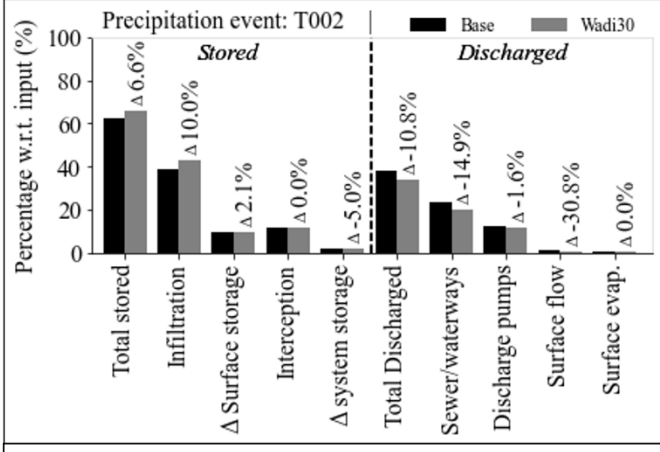

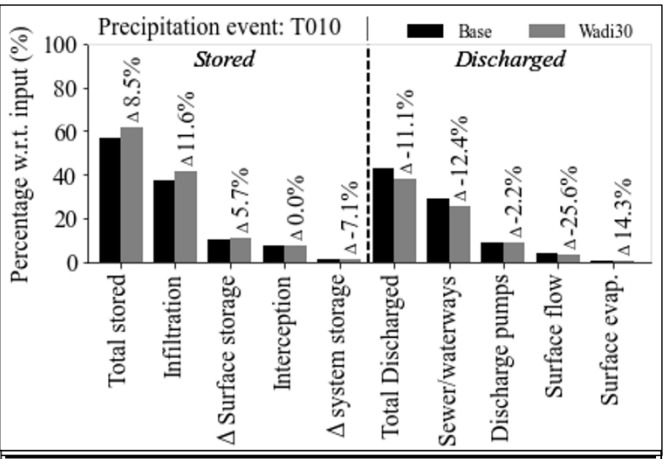

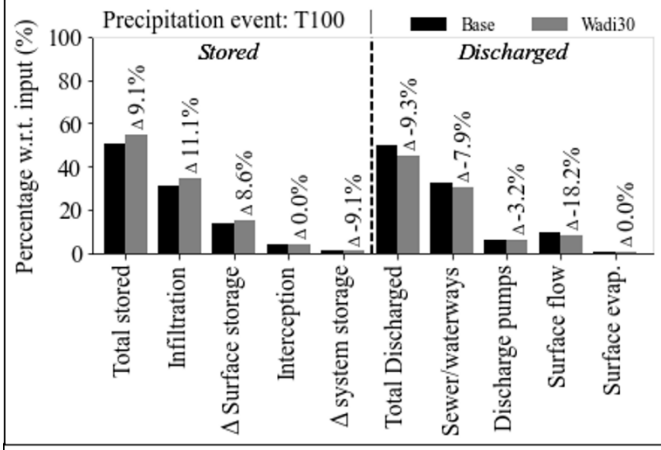

	T002	*T010*	*T100*
Roads *(170.7 km)*	*(% / Δ%)*	*(% / Δ%)*	*(% / Δ%)*
Acc. *(< 15 cm)*	91.2	81.4	59.4
Emerg. *(15-30 cm)*	8.7/-20.8	17.2/-20.3	34.1/-6.3
Inacc. *(> 30 cm)*	0.1/-72.4	1.3/-42.6	6.5/-27.6
Buildings *(10.390)*	*(% / Δ%)*	*(% / Δ%)*	*(% / Δ%)*
Low* *(< 10 cm)*	99.7	99.2	96.7
Mod.* *(10-25 cm)*	0.3/-17.1	0.7/-15.5	2.3/-27.8
High* *(> 25 cm)*	0.0/0.0	0.1/-44.4	0.9/-33.1
Overflows	*(% / Δ%)*	*(% / Δ%)*	*(% / Δ%)*
Mixed Sewerage	9.0/-19.5	12.4/-15.7	15.1/-12.1
Storm Drains	6.2/-8.4	8.7/-8.8	10.1/-4.2

Thesis R.G. Wiebing 2023, ***2050WH climate scenario.***

** Vulnerability to flooding: low, moderate, or high*

Figure 18: Effects of measure 'Wadi30', given in percentages and as relative change (Δ%) compared to the base scenario.

In Figure 18 it is seen that the effect of this measure on the total stored rainwater is 6.6%, 8.5%, and 9.1% for assessed T002, T010, and T100 rainfall events respectively. Hence, the rainwater retention increases in both relative and absolute terms. It is the result of an increase in infiltration and surface storage. A large decrease in rainwater drainage via sewerage overflows and waterways is observed, while also significantly limiting surface flows out of the study area. Relative decreases in rainwater drainage by discharge pumps are limited. In addition, this measure

shows significant decreases in (partly) inaccessible roads, vulnerable buildings, and sewerage overflows for all assessed rainfall depths.

It is seen that this measure becomes more effective in retaining rainwater when rainfall depth increases, seen in ascending percentages of stored rainwater. Nevertheless, it is seen that only $1/8^{th}$ to $1/9^{th}$ of the *theoretical* increase in rainwater retention is indeed additionally retained during the simulation runs.

This is due to multiple reasons. Firstly, wadis can catch rainwater which was otherwise stored or infiltrated elsewhere, hence limiting the net result of stored rainwater in the study area. Secondly, similar to the limitation within the *Road10* scenario, gradients in surface elevation limits the effectiveness of created storage capacity. Within created wadis, rainwater flows to the lowest elevated sections. If water depths within these sections exceed 30 cm, the wadi will be overflowing. All created storage capacity within a wadi above this water level causing overflow will thus not be utilised (i.e., ineffective storage). Since implemented wadis within the model schematisation generally consist of relatively large areas, surface elevation differences within wadis can be substantial. This reduces the *effective modelled* rainwater storage capacity, by creating storage which will not be utilised (i.e., limiting the potential use of the *theoretical* rainwater storage capacity).

Thirdly, the created wadis are not equally distributed over the study area, as seen in Figure 33 in *Appendix C*. Consequently, insufficient volumes of excess rainwater *may* be present is some parts to fill all wadis located in close proximity to each other. This effect is indeed observed by the fact that this measure becomes more effective both relatively and absolutely speaking when rainfall depth increases (i.e., increase of *excess* rainwater). In absolute terms, modelling results showed that additionally retained water equals 9600, 17500, and 31100 m^3 for T002, T010, and T100 events respectively. This indicates that the *effective modelled* rainwater storage capacity is not fully filled during the simulation runs (at least for the T002 and T010 event). Hence, the effectiveness of this measure is limited by the fact that excess rainwater is not reaching the created wadis.

Due to the large theoretical potential of this measure, it is expected that a significant increase of water retention could be achieved when this measure would be implemented in more detail. First of all, extensive wadis should be divided into multiple smaller wadis with different surface level elevations, limiting height level differences within wadis. Then, as advised by RIONED (2008), wadis in sloping areas can be constructed as *cascading wadis*. When an upstream wadi is full, it flows over to a subsequent wadi. Yet, it remains of the utmost importance to design wadis and the water draining system so that rainwater can reach those wadis. For example, storm drains or gullies could be used to facilitate the distribution of rainwater to constructed wadis.

All in all, despite being coarsely implemented in the model as of now, this measure shows great potential effectiveness for both smaller and larger rainfall depths. However, it requires a more detailed implementation to show its full potential. Nonetheless, a limitation of this measure is that wadis cannot be constructed throughout the whole study area due to neighbourhood characteristics.

5 Discussion

5.1 Comparison among assessed measures

Table 6 gives an overview of the effects of measures ordered by municipal objectives to improve rainwater retention, reducing inaccessibility of roads and vulnerable buildings, and limiting sewerage overflows. For a clearer overview, partly and fully inaccessible roads, as well as moderately and highly vulnerable buildings have been combined in Table 6. To improve clarity further, only mixed sewerage overflows are shown in Table 6 since those influence water quality the most.

Within the table, the measure which is most effective in reference to an objective for an assessed rainfall event has been coloured dark green, the second most effective is coloured light green, the third most effective has been coloured orange, and the least effective has been coloured red. Note that all measures exert a positive effect on the objectives, and that the colours only indicate the order of effectiveness of assessed measures to improve comparison.

Table 6: Overview of effects of implemented measures on municipal objectives. Note: colours indicate the effectiveness, being: dark green indicates most effective, light green indicates second most effective, orange indicates third most effective, red indicates least effective.

Scenario:	***Base***	***Storepp***	***Erf50p***	***Road10***	***Wadi30***
Metrics:	*(%)*	*(Δ%)*	*(Δ%)*	*(Δ%)*	*(Δ%)*
Rainwater retention:					
T002	62.1	6.1	1.6	8.7	6.6
T010	56.8	5.8	1.8	6.2	8.5
T100	50.4	5.6	2.2	3.8	9.1
(Partly) inaccessible roads:					
T002	11.3	-20.4	-7.1	-46.0	-22.1
T010	23.9	-7.5	-0.8	-22.8	-22.6
T100	45.4	-4.2	-2.2	-16.7	-10.8
Vulnerable buildings:					
T002	0.4	0.0	0.0	-25.0	-25.0
T010	1.0	-10.0	0.0	-20.0	-20.2
T100	4.7	-12.8	-8.5	-19.1	-31.9
Mixed sewerage overflows:					
T002	11.2	-18.4	-4.1	-25.6	-19.5
T010	14.7	-11.3	-2.6	-10.5	-15.7
T100	17.2	-7.0	-3.0	-5.6	-12.1

Table 6 shows that the measures implemented in the public space, *Road10* and *Wadi30*, show to be the most effective for all quantified objectives. Due to their large rainwater storage

capacities, they are able to store large amounts of excess rainwater which otherwise could be drained or cause hindrance. Furthermore, those measures also show even larger theoretical potential, thus likely increasing their effectiveness if this potential can be utilised with more detailed model implementations.

Road10 indicates to be the most effective measures to decrease the amount of (partly) inaccessible roads for all rainfall depths. This is not surprising, since verges adjacent to roads are equally distributed within the study area, and do create a significant amount of additional rainwater storage capacity alongside roads. For the assessed T002 event, it is found that *Road10* is most effective for all objectives as well. Expectedly, this is due to the fact that the verges are found to be already effectively filled up during the T002 event, opposed to the *Wadi30* measure. This is since they are equally distributed in the study area, while also being next to road surfaces which are mostly impervious. Thus, already at smaller rainfall depths such as the T002 event, those roads generate significant amounts of excess rainwater which can be stored in the lowered verges. In addition, it effectively alleviates the sewerage system which is located beneath roads, thus showing effectiveness in limiting mixed sewerage overflows as well.

But with increasing rainfall depths, *Road10* loses effectiveness due to its limited storage capacity. For T010 and T100 events, *Wadi30* is most effective in retaining rainwater, as well as limiting mixed sewerage overflows and number of vulnerable buildings. This is due to the large potential rainwater storage capacity of this measure compared to occurring rainfall, the main limitation being that the potential storage capacity does not get filled by rainwater. At T010 and T100 events, wadis get increasingly filled since larger volumes of excess rainwater are present which fill the wadis.

Measure *Storepp* maintains its effectiveness in rainwater retention for all rainfall depths, due to the large capacity of private storage facilities compared to the connected roof area. Hence, it the second most effective measure for rainwater retention during a T100 event. Also, it is in the same order of magnitude of *Road10* or *Wadi30* regarding rainwater retention for T002 and T010 events. Moreover, since it alleviates the sewerage system directly by reducing roof rainfall runoff into the system, it shows large effectiveness in limiting mixed sewerage overflows being in the same order of magnitude as *Road10* and *Wadi30* measures. When assessing vulnerable buildings or inaccessible roads, it is less effective compared to *Road10* and *Wadi30*.

To solely remove half of impervious surfaces on private properties *Erf50p* generally shows more effectiveness when assessing larger rainfall depths. Yet, it is the least effective measures for all assessed objectives and rainfall events, often being a couple of times less effective than other measures. This is due to the fact that the infiltration rate on adjusted surfaces is still a limiting factor. When assessing longer time scales and less extreme events, reducing the impervious surface can become more effective in retaining rainwater, as shown in Ahiablame & Shakya (2016) and Xu et al. (2023).

Studies assessing the effectiveness of measures using a fully distributed 1D-2D model on municipal scale are scarce, while most studies are using *lumped* models or very coarse 2D components in 1D-2D coupled models. Therefore, it is hard to compare those findings with

findings presented in this study, since this study shows the importance of a measures' location and implementation to study its effectiveness. This is also stressed by other studies using detailed fully distributed 1D-2D models such as Costa et al. (2021) and Haghighatafshar et al. (2018). Costa et al. (2021) performed a similar studied for the city of Eindhoven for T5, T10, and T100 events, and its conclusions support the outcomes of this study. They show limited effectiveness on reducing rainwater runoff and pluvial flooding when solely converting impervious surfaces to pervious. Storing rainfall on roofs showed more effectiveness, but creating rainwater storages in green spaces showed most effectiveness, particularly when assessing larger rainfall depths. Moreover, they showed a generally decreasing effectiveness with increased rainfall depths, except for storing rainwater in green spaces which became more effective in reducing inundation depths with increasing rainfall depths, as shown in this study as well.

5.2 Relevance and potential

First of all, it is worth noting that all studied effects of measures are conducted for worst-case climate conditions for 2050, as established in 2014. This thus provides great quantitative insight into the resilience of the urban area when subjected to future rainfall events, while also implicitly taking interconnectedness between sub-catchments into account. Therefore, such a study is a good start to guide policy makers to solutions for a more robust spatial rainwater distribution by making the effectiveness of adaptation measures more tangible. This creates confidence and familiarity with effects of adaptation measures, which can thereafter foster their implementation as common practice to increase resilience (Dolman & Brolsma, 2023). Yet, effectiveness of assessed measures on other topics for a resilient urban area, such as heat stress reduction and increased biodiversity are not assessed. This could however be incorporated in a framework where quantitative and qualitative measures can be ranked as proposed by Xiong et al. (2020), to assess the effectiveness of measures on all objectives to make urban areas climate-resilient on all policy domains. For instance, areas with cascading wadis can create multiple ecological habitats to increase biodiversity, or drinking water can be saved by implementing private rainwater storages.

Also, since multiple recurrence times are assessed, it is suited for multiple uses. It can be used for assessing the hydraulic functioning of the sewerage system as well as *stress-testing* the urban area. Yet, further analysis on water balance terms could be performed on neighbourhood scale since neighbourhoods show variations in their geographical characteristics, thus potentially influencing the effectiveness of measures within neighbourhoods (Costa et al., 2021).

Lastly, the 3Di modelling software has shown great potential for scenario modelling since it is relatively fast, simulations can run on the cloud, and scenarios can run simultaneously. This enables studies on multiple measures subjected to multiple rainfall events, while incorporating both the sewerage system as well as the surface area in high detail.

5.3 Limitations

A state-of-the-art 1D-2D hydrodynamic model is used within this study, capable of accurately calculating the distribution of *excess* rainwater within and out of the study area. Yet, some hydrological processes are incorporated in less detail, particularly regarding processes in the subsoil. While this limits the number of measures which can be assessed on their effectiveness, it can also influence the accuracy of model outcomes since calculated volumes of excess rainwater contain more uncertainty. This influences the spatial rainwater distribution and hence the magnitude of water balance terms and inundation depths and extents.

Infiltration is the largest rainwater storage term in the urban water balance while also containing multiple inherent uncertainties as described in *Section 2.2.6*. This could thus significantly influence the accuracy of modelled rainwater distributions and hence the effects of measures. Moreover, changes in infiltration rates could influence the relative effectiveness of measures (partly) depending on infiltration rates being *Erf50p*, *Road10*, and *Wadi30*, also compared to measure *Storepp*. The influence of infiltration rates on rainwater distributions within an urban area is studied in Glenis et al. (2018). The authors conclude that infiltration rates can indeed significantly influence excess rainwater volumes which influence inundation depths, but that spatial rainwater distribution patterns and locations where inundation occurs remain the same. It stresses the importance of the elevation data input (DEM) on rainwater distributions within an urban area. Furthermore, infiltration rates are particularly important *during* rainfall events but loses its importance afterwards since no additional excess rainwater is generated. de Arruda Gomes et al. (2021), McClean et al. (2020), Wei et al. (2022), and Yalcin (2020) also stress the large importance of a high-resolution DEM compared to other input data sources to accurately model spatial rainwater distributions, particularly when historic data on inundation is absent. Conveniently, this is a strong point of used modelling software 3Di, which incorporates the DEM (and other input) in its highest resolution into a model schematisation by using a subgrid technique.

Moreover, studies which assess the sensitivity of modelled spatial rainwater distribution with 1D-2D hydrodynamic models to multiple uncertainty sources, such as Alipour et al. (2021), Chen et al. (2018), and Xing et al. (2021), showed that rainfall event input is indisputably the most important factor influencing hydrodynamic modelling results. Yet, used design rainfall depths for 2050 contain uncertainty due to both used statistical methods and predicted changes due to climate change as described in *Section 3.2.2*. This uncertainty in rainfall event input can change the relative effectiveness of measures compared to each other for different rainfall events, since measures *Storepp* and *Wadi30* become more effective compared to *Road10* and *Erf50p* when rainfall depths increase and vice versa. Nonetheless, predicted cumulative rainfall depths increase with 55% going from a T002 to a T010 event, and with 86% going from a T010 to a T100 event, which is a couple of times more than uncertainty ranges as indicated in Beersma et al. (2019). Hence, changes in effectiveness of measures compared to each other due to uncertainty in rainfall event depths will likely be limited. In addition, relative effectiveness of measures compared to each other are expected to be influenced to a larger extent by the level of detail of model implementation. To this

extent, the theoretical rainwater storage of *Storepp* has been fully used in present model calculations, while the theoretical rainwater storage of *Road10* and *Wadi30* has only be used for $1/4^{th}$ and $1/9^{th}$ respectively in present model calculations due to coarse implementation.

Furthermore, as of now, the isolated effectiveness of measures to make the spatial rainwater distribution more robust has been studied. However, since all measures limit the amount of excess rainwater, their effectiveness in terms of rainwater retention can be influenced when they are combined. For instance, rainwater storages on private properties influence the amount of roof runoff. This will alleviate the sewerage system, which is generally located under road sections. Therefore, the measure of lowered verges adjacent to road sections could be less effective since more rainfall run-off can be drained by the sewerage system, affecting the filling of those verges. Moreover, it was found that potential storage of wadis was largely unused since it was not filled by excess rainwater. This effect will likely be exacerbated when other measures would be implemented which also store rainwater.

Yet, it is seen that about 35 to 55% of rainwater is still drained out of the area when proposed measures are implemented. So, interference implemented measures on their effectiveness can be limited when this drained rainwater is more efficiently routed towards the implemented storage facilities, increasing total retained rainwater. Additionally, combining proposed measures could be more effective together when assessing vulnerable buildings, inaccessible roads, and overflows, since those are based on *threshold values*. For instance, combined measures can result in water levels below the threshold value (e.g., below doorstep height) for a building to be vulnerable, while separate they would not.

5.4 Generalisation

The study area contains multiple types of neighbourhoods and industrial areas. In addition, the percentage of paved landcover within Doetinchem approximates the average paved percentages within a Dutch urban area (Mulder, 2020). It is located in the higher-elevated sandy part of the Netherlands, which is free draining. Those characteristics influence hydrodynamic and hydrological processes and are found in numerous urban areas in the southern and eastern part of the Netherlands, where shown effects and limitations of this study will be comparable.

In the lower-elevated peaty and clayey areas within the Netherlands, shown effects and limitations will not necessarily occur. First of all, peaty and clayey soils are characterised by low infiltration rates. This limits the effects of this uncertainty on outcomes, since infiltration will be less dominant on small timescales. Moreover, surface elevation gradients are less steep in those areas which is beneficial for adaptation measures which are implemented on the surface area. Yet, more surface water is present in those areas with controlled water levels. Therefore, 2-hour rainfall events should complement 1-hour events since those surface waters can have significant effects on assessed model outcomes (STOWA & RIONED, 2020). Outcomes of this study are therefore not directly representative for urban areas within the lower parts of the Netherlands. This also holds for rural areas, where different rainfall events are normative since storage capacities are

generally higher. On top of that, high amounts of paved surface and dense sewerage systems are absent.

Furthermore, the *effectiveness* of measures on a robust spatial rainwater distribution is assessed for short and intense rainfall events within this study, which are in varying extent *extreme*. This is required for assessing which sections of the urban area are vulnerable to pluvial flooding and sewerage overflows, but it is dependent on the objective whether these are the most useful events when assessing the effectiveness of measures to retain rainwater. For example, when the objective is to recharge groundwater annually, it is expectedly more convenient to assess the effectiveness of measures on larger timescales with less extreme rainfall events, such as shown in Ahiablame & Shakya (2016), and Hoogvliet et al. (2013). However, this study is useful when the objective is to retain as much rainwater as possible after short and intense events during the summer period (e.g., to reduce heat stress).

6 Conclusions and recommendations

6.1 Conclusions

The aim of this research is to assess which adaptation measures are effective to make the urban rainwater distribution more robust, making it more resilient to effects of changing rainfall patterns due to climate change. A robust distribution of rainwater after rainfall events can be achieved by increasing rainwater retention while also limiting sewerage overflows and hindrance due to pluvial flooding. These are three objectives of Doetinchem, which are quantified using state-of-the-art 1D-2D hydrodynamic model of a 9.5 km^2 study area within Doetinchem. Four measures have been assessed on their effectiveness to achieve those objectives after short and intense rainfall events. Implemented measures show varying effectiveness when studying various objectives and rainfall events depths (with recurrence times of 2 (T002), 10 (T010), and 100 (T100) years).

Lowering verges adjacent to roads (measure *Road10*) showed to be the most effective to reduce the inaccessibility of roads for all assessed rainfall depths. In addition, *Road10* showed to be the most effective for T002 events to retain rainwater, limit overflows, and limit the number of vulnerable buildings due to its swift filling. Nevertheless, the limited storage capacity of the verges causes a reduced effectiveness for larger rainfall depths, i.e., the T010 and T100 events. For those events, creating wadis (i.e., bioswales, measure *Wadi30*) showed to be the most effective in retaining rainwater, limiting sewerage overflows, and limiting the number of vulnerable buildings due to their large storage capacity. These two measures, implemented in the public space, show larger effectiveness *overall* than the two measures implemented on private properties. Nonetheless, creating rainwater storage facilities to reduce runoff from building roofs (*Storepp*) showed consistent effectiveness for rainwater retention and limiting sewerage overflows for all rainfall depths. This is due to the relatively large maximum storage capacities compared to connected roofs' surface areas. Yet, limited effectiveness was found in reducing road inaccessibility and vulnerable buildings, particularly when assessing larger rainfall depths. Solely changing impervious surfaces to pervious surfaces on private properties (measure *Erf50p*) showed minimal effects. Consequently, it showed to be the least effective measure for all assessed rainfall depths and objectives.

Furthermore, it was found that using a detailed, fully distributed and physical-based 1D-2D hydrodynamic model is suited for assessing the effectiveness of measures on a robust rainwater distribution. It showed good performance on accurately modelling historic events without calibration. This is convenient, since the validity and robustness of calibrated parameters is questionable when assessing future climate conditions or after the implementation of measures. Moreover, it was found that the effectiveness of measures is dependent on the spatial location within the urban area, thus advocating for the use of a fully distributed 1D-2D model. Both the spatial rainwater distribution (e.g., routing of rainwater, is it reaching implementation location) and local geographical features (i.e., sloping surface elevations) are shown to be important for the effectiveness of adaptation measures. Lastly, it was found that the effectiveness of measures relative to one another is varying when assessing different rainfall event depths.

6.2 Recommendations for future research and practice

This study gives rise to recommendations for future research. First of all, it should be studied if and how adaption measures whose theoretical storage is not fully utilised can be implemented in more detail. This is to ensure that the full potential effectiveness is shown, given surrounding geographical features. In addition to this, more detail can be given to rainwater routing towards those measures. But first, it must be studied how a more detailed implementation can be achieved without having to specifically design each storage location separately, which would be too time-consuming when assessing effects of adaptation measures on municipal scale. Yet, this scale is needed to show their full potential effectiveness by incorporating important exchanges of rainwater between sub-catchments (e.g., neighbourhoods).

Secondly, future adaptation plans could incorporate a combination of assessed measures to make the urban area more resilient. Yet, assessed measures could both negatively and positively influence each other's effectiveness when implemented simultaneously, expected to vary per objective and rainfall event depth. It would therefore be interesting to study their interconnectedness.

Lastly, sewerage overflows can contribute to a degrading water quality by for instance adding excessive amounts of nutrients or remnants of medicines into surface waters. However, water quality is often related to thresholds of concentrations which should not be exceeded to maintain sufficient water quality within waterbodies. Since concentrations are dependent on both the amount of a substance and the volume where it is dissolved, water quality and quantity are related. Hence, a comprehensive study on water quality related to a robust spatial rainwater distribution for the objective of improving water quality is needed, instead of solely focusing on sewerage overflow volumes. In addition, sewerage water which flows onto the surface due to the exceeding of a sewerage system drainage capacity can also create hindrance and water quality problems.

Some recommendations for future practice can also be given. First of all, comparing theoretical and modelled rainwater storage can give valuable insights in the effect of physical system characteristics on the effectiveness of adaptation measures, for both the municipal and local scales. These insights can thereafter be taken into account when developments within the urban area are designed. In addition, quantitative results provided within this study should be situated in a broader context for practical implementations, for instance by giving legal boundaries for assessed measures.

Gaining familiarity and confidence in both quantitative effectiveness and practical implementation of adaptation measures will foster their common use. Therefore, results of such a study on the effectiveness of proposed measures should also be communicated to city planners and policy makers. They can thereafter foster the implementation of adaptation measures when designing the public space, to make the urban area resilient to future climate conditions.

References

3DBAG. (2023). 3DBAG viewer v2023.10.08. Retrieved 16 November 2023, from https://3dbag.nl/en/viewer

3Di Documentation. (2023). Retrieved 14 October 2023, from https://docs.3di.live/

Ahiablame, L., & Shakya, R. (2016). Modeling flood reduction effects of low impact development at a watershed scale. *Journal of Environmental Management*, *171*, 81–91. https://doi.org/10.1016/J.JENVMAN.2016.01.036

AHN. (2022). Kwaliteitsbeschrijving. Retrieved 4 October 2023, from https://www.ahn.nl/kwaliteitsbeschrijving

Alipour, S. M., Engeland, K., & Leal, J. (2021). A practical methodology to perform global sensitivity analysis for 2D hydrodynamic computationally intensive simulations. *Hydrology Research*, *52*(6), 1309–1327. https://doi.org/10.2166/NH.2021.243

Beersma, J., Hakvoort, H., Jilderda, R., Overeem, A., & Versteeg, R. (2019). *NEERSLAGSTATISTIEK EN -REEKSEN VOOR HET WATERBEHEER 2019.* (Report no. 19). Amersfoort: STOWA.

Beersma, J., Versteeg, R., & Hakvoort, H. (2018). *NEERSLAGSTATISTIEKEN VOOR KORTE DUREN ACTUALISATIE 2018*. (report no. 12). Amersfoort: STOWA.

Bessembinder, J., Bintanja, R., van Dorland, R., Homan, C., Overbeek, B., Selten, F., & Siegmund, P. (2023). *KNMI'23 klimaat scenario's voor Nederland*. De Bilt: KNMI.

Beven, K., & Freer, J. (2001). Equifinality, data assimilation, and uncertainty estimation in mechanistic modelling of complex environmental systems using the GLUE methodology. *Journal of Hydrology*, *249*(1–4), 11–29. https://doi.org/10.1016/S0022-1694(01)00421-8

Brolsma, R., Buma, J., van Meerten, H., Dionisio, M., & Elbers, J. (2012). *Effect van droogte op stedelijk gebied*. (Report no. 1206224-000-BGS-0010). Delft: Deltares.

Brolsma, R., van Leeuwen, E., & ten Velden, C. (2016). *Circular Solutions. Part III: the Rainproof City*.

Bügel, P. J. R., Meeuwissen, A. J., & Wentink, R. (2010). *AANLEGHOOGTE VAN NIEUWE WONINGEN IN RELATIE TOT WATEROVERLAST*. (Report no. 2010-W01). Amersfoort: STOWA.

Bulti, D. T., & Abebe, B. G. (2020). A review of flood modeling methods for urban pluvial flood application. *Modeling Earth Systems and Environment*, *6*(3), 1293–1302. https://doi.org/10.1007/S40808-020-00803-Z/FIGURES/5

Carson, J. S. (2002). Model verification and validation. In E. Yüsecan, C. H. Chen, J. L. Snowdon, & J. M. Charnes (Eds.), *2002 Winter Simulation Conference* (pp. 52–58). Marietta.

Casulli, V., & Stelling, G. S. (2011). Semi-implicit subgrid modelling of three-dimensional free-surface flows. *International Journal for Numerical Methods in Fluids*, *67*, 441–449. https://doi.org/10.1002/fld.2361

Cea, L., & Costabile, P. (2022). Flood Risk in Urban Areas: Modelling, Management and Adaptation to Climate Change. A Review. *Hydrology 2022*, *9*(3), 50–85. https://doi.org/10.3390/HYDROLOGY9030050

Chen, W., Huang, G., Zhang, H., & Wang, W. (2018). Urban inundation response to rainstorm patterns with a coupled hydrodynamic model: A case study in Haidian Island, China. *Journal of Hydrology*, *564*, 1022–1035. https://doi.org/10.1016/j.jhydrol.2018.07.069

Costa, S., Peters, R., Martins, R., Postmes, L., Keizer, J. J., & Roebeling, P. (2021). Effectiveness of Nature-Based Solutions on Pluvial Flood Hazard Mitigation: The Case Study of the City of Eindhoven (The Netherlands). *Resources*, *10*(3), 24. https://doi.org/10.3390/RESOURCES10030024

Cultuurtechnische Vereniging. (1988). *Cultuur technisch vademecum; Werkgroep Herziening Cultuurtechnisch vademecum*. Utrecht.

de Arruda Gomes, M. M., de Melo Verçosa, L. F., & Cirilo, J. A. (2021). Hydrologic models coupled with 2D hydrodynamic model for high-resolution urban flood simulation. *Natural Hazards*, *108*, 3121–3157. https://doi.org/10.1007/s11069-021-04817-3

De Bruijn, K., Slager, K., Piek, R., Riedstra, D., & Slomp, R. (2018). *Leidraad voor het maken van overstromingssimulaties*. (Report no. 11200537-007-ZWS-0004). Delft: Deltares.

de Oliveira Campos, P. C., da Silva Rocha Paz, T., Lenz, L., Qiu, Y., Alves, C. N., Simoni, A. P. R., … Paz, I. (2020). Multi-criteria decision method for sustainable watercourse management in Urban Areas. *Sustainability (Switzerland)*, *12*(16). https://doi.org/10.3390/su12166493

Dolman, N. J. J., & Brolsma, R. J. (2023). Groenblauwe maatregelen en nature-based solutions voor de waterrobuuste en klimaatbestendige stad. *Water Governance*, *1*, 40–47.

Folkesson, A. (2020). The route of stormwater through Augustenborg. In M. Månsson & B. Persson (Eds.), *Green roofs, stormwater and sustainability: Augustenborg as a research site* (1st ed., pp. 187–213). Malmö, Sweden: Arkus.

Gaznayee, H. A. A., Zaki, S. H., Al-Quraishi, A. M. F., Aliehsan, P. H., Hakzi, K. K., Razvanchy, H. A. S., … Mahdi, K. (2023). Integrating Remote Sensing Techniques and Meteorological Data to Assess the Ideal Irrigation System Performance Scenarios for Improving Crop Productivity. *Water*, *15*(8). https://doi.org/10.3390/w15081605

Geologische Dienst Nederland. (2023). Grondwaterstanden in Beeld. Retrieved 4 August 2023, from https://www.grondwatertools.nl/gwsinbeeld/

Glenis, V., Kutija, V., & Kilsby, C. G. (2018). A fully hydrodynamic urban flood modelling system representing buildings, green space and interventions. *Environmental Modelling & Software*, *109*, 272–292. https://doi.org/10.1016/J.ENVSOFT.2018.07.018

Guo, K., Guan, M., & Yu, D. (2021). Urban surface water flood modelling-a comprehensive review of current models and future challenges. *Hydrology and Earth System Sciences*, *25*(5), 2843–2860. https://doi.org/10.5194/HESS-25-2843-2021

Haghighatafshar, S., Nordlöf, B., Roldin, M., Gustafsson, L. G., la Cour Jansen, J., & Jönsson, K. (2018). Efficiency of blue-green stormwater retrofits for flood mitigation – Conclusions

drawn from a case study in Malmö, Sweden. *Journal of Environmental Management*, *207*, 60–69. https://doi.org/10.1016/J.JENVMAN.2017.11.018

He, B. J., Zhu, J., Zhao, D. X., Gou, Z. H., Qi, J. Da, & Wang, J. (2019). Co-benefits approach: Opportunities for implementing sponge city and urban heat island mitigation. *Land Use Policy*, *86*, 147–157. https://doi.org/10.1016/J.LANDUSEPOL.2019.05.003

Heinen, M., Brouwer, F., Teuling, K., & Walvoort, D. (2021). *BOFEK2020 - Bodemfysische schematisatie van Nederland: update bodemfysische eenhedenkaart*. (Report no. 3056). Wageningen: Wageningen Environmental Research.

Henckens, G., & Engel, W. (2017). *Benchmark inundatiemodellen. Modelfunctionaliteiten en testbank berekeningen*. (Report no. 34). Amersfoort: STOWA.

Holleman, I., Michelson, D., Galli, G., Germann, U., & Peura, M. (2006). *Quality information for radars and radar data*.

Hoogvliet, M., Buma, J., Brolsma, R., de Lange, G., Landwehr, H., Coenders-Gerrits, M., … Landa, P. (2013). *Naar een bestendige stedelijke waterbalans*. (Report no. 1206329-000-BGS-0013). Delft: Deltares.

Hoogvliet, M., Spijker, J., Noome, W., Slingerland, E., & de Groot-Reichwein, M. (2021). *Droogte en stedelijk groen*.

Hu, R., Fang, F., Salinas, P., Pain, C. C., Sto.Domingo, N. D., & Mark, O. (2019). Numerical simulation of floods from multiple sources using an adaptive anisotropic unstructured mesh method. *Advances in Water Resources*, *123*, 173–188. https://doi.org/10.1016/j.advwatres.2018.11.011

Huang, S., Tang, L., Hupy, J. P., Wang, Y., & Shao, G. (2021). A commentary review on the use of normalized difference vegetation index (NDVI) in the era of popular remote sensing. *Journal of Forestry Research*, Vol. 32, pp. 1–6. https://doi.org/10.1007/s11676-020-01155-1

Iliadis, C., Glenis, V., & Kilsby, C. (2023). Representing buildings and urban features in hydrodynamic flood models. *Journal of Flood Risk Management*, 1–21. https://doi.org/10.1111/JFR3.12950

Jeevalakshmi, D., Reddy, S. N., & Manikiam, B. (2016). Land cover classification based on NDVI using LANDSAT8 time series: A case study Tirupati region. *International Conference on Communication and Signal Processing, ICCSP 2016*, 1332–1335. https://doi.org/10.1109/ICCSP.2016.7754369

Jiang, Z., Huete, A. R., Chen, J., Chen, Y., Li, J., Yan, G., & Zhang, X. (2006). Analysis of NDVI and scaled difference vegetation index retrievals of vegetation fraction. *Remote Sensing of Environment*, *101*(3), 366–378. https://doi.org/10.1016/j.rse.2006.01.003

Klein Tank, A., Beersma, J., Bessembinder, J., Van den Hurk, B., & Lenderink, G. (2014). *KNMI '14: Klimaatscenario's voor Nederland*. De Bilt: KNMI.

Klimaatatlas Doetinchem. (2022). Retrieved 10 May 2023, from https://storymaps.arcgis.com/stories/411ba21b52d64bff990a281e5b71c904

KNMI. (2020). KNMI - Klimaatviewer. Retrieved 21 June 2023, from https://www.knmi.nl/klimaat-viewer/grafieken-tabellen/meteorologische-stations/stations-maand/stations-maand_1991-2020

KNMI. (2021). Buien groeien in intensiteit en omvang. Retrieved 25 March 2023, from https://www.knmi.nl/over-het-knmi/nieuws/buien-groeien-in-intensiteit-en-omvang

KNMI. (2022). Als het regent, gaat het plenzen. Retrieved 25 March 2023, from https://www.knmi.nl/over-het-knmi/nieuws/als-het-regent-gaat-het-plenzen

KNMI. (2023a). Extreme neerslag. Retrieved 9 March 2023, from https://www.knmi.nl/kennis-en-datacentrum/uitleg/extreme-neerslag

KNMI. (2023b). Neerslagindex (SPI). Retrieved 9 August 2023, from http://knmi-spi-monitor-frontend-prd.s3-website-eu-west-1.amazonaws.com/

Kuiry, S. N., Sen, D., & Bates, P. D. (2010). Coupled 1D–Quasi-2D Flood Inundation Model with Unstructured Grids. *Journal of Hydraulic Engineering*, *136*(8), 493–506. https://doi.org/10.1061/(ASCE)HY.1943-7900.0000211

Li, C., Liu, M., Hu, Y., Gong, J., & Xu, Y. (2016). Modeling the Quality and Quantity of Runoff in a Highly Urbanized Catchment Using Storm Water Management Model. *Polish Journal of Environmental Studies*, *25*(4), 1573–1581. https://doi.org/10.15244/pjoes/60721

Li, C., Liu, M., Hu, Y., Han, R., Shi, T., Qu, X., & Wu, Y. (2018). Evaluating the Hydrologic Performance of Low Impact Development Scenarios in a Micro Urban Catchment. *International Journal of Environmental Research and Public Health*, *15*(2), 273. https://doi.org/10.3390/IJERPH15020273

Lizard. (2023a). Meetstation Doetinchem, 667, KNMI. Retrieved 11 May 2023, from https://nens.lizard.net/viewer/map

Lizard. (2023b). Neerslag (mm), Lizard, NRR. Retrieved 11 May 2023, from https://nens.lizard.net/viewer/map

Luijmes, R. (2023). Waterbergend vermogen van zandgronden beperkt. *Staf*, *13*, 18–21.

McClean, F., Dawson, R., & Kilsby, C. (2020). Implications of using global digital elevation models for flood risk analysis in cities. *Water Resources Research*, *56*(e2020WR028241). https://doi.org/10.1029/2020WR028241

Mihu-Pintilie, A., Cîmpianu, C. I., Stoleriu, C. C., Pérez, M. N., & Paveluc, L. E. (2019). Using High-Density LiDAR Data and 2D Streamflow Hydraulic Modeling to Improve Urban Flood Hazard Maps: A HEC-RAS Multi-Scenario Approach. *Water*, *11*(9), 1856. https://doi.org/10.3390/W11091832

Ministry of I&M. (2016). *Stad In Het Nieuwe Klimaat*. Amersfoort.

Ministry of I&W. (2022). *Water en Bodem sturend*. (Report no. IENW/BSK-2022/283041). 's-Gravenhage.

Mitsopoulos, G., Panagiotatou, E., Sant, V., Baltas, E., Diakakis, M., Lekkas, E., & Stamou, A. (2022). Optimizing the Performance of Coupled 1D/2D Hydrodynamic Models for Early Warning of Flash Floods. *Water (Switzerland)*, *14*(15). https://doi.org/10.3390/w14152356

Mondeel, H., & Drost, M. (2022). *Studiegroep Grondwater: Verdroging Hoog Nederland*. (Report no. 128667/21-018.897).

Mulder, F. (2020). 'Een tuin is een aanval'. *Grijze Tuinen*. Retrieved from https://www.groene.nl/artikel/een-tuin-is-een-aanval

NASA. (2023). Measuring Vegetation (NDVI&EVI). Retrieved 7 June 2023, from https://earthobservatory.nasa.gov/features/MeasuringVegetation/measuring_vegetation_2.php

Nash, S., Comer, J., Olbert, A., & Hartnett, M. (2018). High Resolution Urban Flood Modelling: A Case Study of Cork City, Ireland. *EPiC Series in Engineering*, *3*, 1495–1504.

Nelen&Schuurmans. (2023). 3Di documentation: Computational grid. Retrieved 2 October 2023, from https://docs.3di.live/h_computational_grid.html

Overeem, A., Holleman, I., & Buishand, A. (2009). Derivation of a 10-year radar-based climatology of rainfall. *Journal of Applied Meteorology and Climatology*, *48*(7), 1448–1463. https://doi.org/10.1175/2009JAMC1954.1

Patra, J. P., Kumar, R., & Mani, P. (2016). Combined Fluvial and Pluvial Flood Inundation Modelling for a Project Site. *Procedia Technology*, *24*, 93–100. https://doi.org/10.1016/J.PROTCY.2016.05.014

PDOK. (2022a). Dataset: Actueel Hoogtebestand Nederland (AHN). Retrieved 4 October 2023, from https://www.pdok.nl/introductie/-/article/actueel-hoogtebestand-nederland-ahn

PDOK. (2022b). Dataset: Basisregistratie Adressen en Gebouwen (BAG). Retrieved 6 October 2023, from https://www.pdok.nl/introductie/-/article/basisregistratie-adressen-en-gebouwen-ba-1

PDOK. (2022c). Dataset: Basisregistratie Grootschalige Topografie (BGT). Retrieved 3 April 2023, from https://www.pdok.nl/introductie/-/article/basisregistratie-grootschalige-topografie-bgt-

PDOK. (2022d). Dataset: Basisregistratie Topografie (BRT) TOPNL. Retrieved 6 October 2023, from https://www.pdok.nl/introductie/-/article/basisregistratie-topografie-brt-topnl

PDOK. (2022e). Dataset: BRO Bodemkaart (SGM). Retrieved 4 October 2023, from https://www.pdok.nl/introductie/-/article/bro-bodemkaart-sgm-

PDOK. (2022f). Dataset: Nationaal Wegen Bestand (NWB). Retrieved 6 October 2023, from https://www.pdok.nl/introductie/-/article/nationaal-wegen-bestand-nwb-wegen

Qin, H. peng, Li, Z. xi, & Fu, G. (2013). The effects of low impact development on urban flooding under different rainfall characteristics. *Journal of Environmental Management*, *129*, 577–585. https://doi.org/10.1016/j.jenvman.2013.08.026

Rainproof Netwerk. (2023). Amsterdam Rainproof. Retrieved 27 April 2023, from https://www.rainproof.nl/

Rijksoverheid. (2023). Samenvatting kwaliteitsinformatie per basisregistratie. Retrieved 2 August 2023, from https://www.digitaleoverheid.nl/overzicht-van-alle-onderwerpen/stelsel-van-basisregistraties/kwaliteit-en-terugmelden/kwaliteitsinformatie-per-basisregistratie/

RIONED. (2008). Kennisbank RIONED: Wadi. Retrieved 18 September 2023, from https://www.riool.net/wadi

RIONED. (2019a). Kennisbank RIONED: Bui01 - Bui10. Retrieved 25 April 2023, from https://www.riool.net/bui01-bui10

RIONED. (2019b). Kennisbank RIONED: Ontwerpbuien met statistische herhalingstijd. Retrieved 25 April 2023, from https://www.riool.net/ontwerpbuien-met-statistische-herhalingstijd

RIONED. (2019c). Kennisbank RIONED: Standaard inloopmodel. Retrieved 2 May 2023, from https://www.riool.net/standaard-inloopmodel

RIONED. (2020). Kennisbank RIONED: Composietbuien in vergelijking met de Leidraadbuien. Retrieved 26 April 2023, from https://www.riool.net/composietbuien-in-vergelijking-met-de-leidraadbuien

RIONED. (2022). Kennisbank RIONED: Wadi ontwerpen. Retrieved 25 October 2023, from https://www.riool.net/wadi-ontwerpen

RIONED. (2023). Kennisbank RIONED: Stedelijk Water. Retrieved 13 October 2023, from https://www.riool.net/kennisbank

Schuurmans, H., & van Vossen, J. (2013). *Nationale Regenradar: Toelichting operationele neerslagproducten*. (Report no. LW-AF20112987MSW). Royal HaskoningDHV, Nelen&Schuurmans.

Schuurmans, W., & van Leeuwen, E. (2017). 3Di: Hollands glorie in watermodellering. *Stromingen*, *29*(3), 51–64. Retrieved from https://edepot.wur.nl/461505

Sidi Almouctar, M. A., Wu, Y., Kumar, A., Zhao, F., Mambu, K. J., & Sadek, M. (2021). Spatiotemporal analysis of vegetation cover changes around surface water based on NDVI: a case study in Korama basin, Southern Zinder, Niger. *Applied Water Science*, *11*(1). https://doi.org/10.1007/s13201-020-01332-x

STOWA. (2021). *WATERKWANTITEIT EN WATERBEHEER*. (Report no. 23a). Amersfoort: STOWA.

STOWA, & RIONED. (2020). *Standaarden voor de stresstest wateroverlast (herzien o.b.v. nieuwe neerslagstatistiek 2019)*.

Stumpe, J., & Tielrooij, F. (2000). Waterbeleid voor de 21e eeuw: Geef water de ruimte en de aandacht die het verdient. Advies van de Commissie Waterbeheer 21e eeuw. In *Advies aan de Staatsecretaris van Verkeer en Waterstaat en aan de voorzitter van de Unie van Waterschappen*. Commissie WB21.

Ten Velden, C., Koekoek, A., De Groot - Reichwein, M., Keizer, R., Taanman, M., & Steenstra, M. (2022). *NKWK-KBS, Monitoren lokale klimaatbestendigheid*. (Report no. 11208355-006-BGS-0002). Delft: Deltares.

Teng, J., Jakeman, A. J., Vaze, J., Croke, B. F. W., Dutta, D., & Kim, S. (2017). Flood inundation modelling: A review of methods, recent advances and uncertainty analysis. *Environmental Modelling & Software*, *90*, 201–216. https://doi.org/10.1016/J.ENVSOFT.2017.01.006

Terpstra, T., Huizinga, J., Hurkmans, R., & Jacobs, C. (2019). *Hitte en droogte in de kleine kernen en het landelijk gebied van Overijssel*. (Report no. PR3936.10). HKV, Wageningen Environmental Research.

Thacker, B. H., Doebling, S. W., Hemez, F. M., Anderson, M. C., Pepin, J. E., & Rodriguez, E. A. (2004). *Concepts of Model Verification and Validation*. 27. https://doi.org/10.2172/835920

van Wieringen, H. (2009). *HAAS - HEMELWATERAFVOER ANALYSE SYSTEMATIEK*. (Report no. 24). Amersfoort: STOWA.

Veraart, J., & Voskamp, I. (2022). *Droogte en hitte in de stad*. Amersfoort, STOWA Deltafact.

Viero, D. P. (2019). Modelling urban floods using a finite element staggered scheme with an anisotropic dual porosity model. *Journal of Hydrology*, *568*, 247–259. https://doi.org/10.1016/j.jhydrol.2018.10.055

Vlaamse Regering. (2023). *Hemelwaterverordening: VR 2023 1002 DOC.0135/2*.

VNG. (2017). *Klimaatbestendige gemeenten*.

Volp, N. D., Van Prooijen, B. C., & Stelling, G. S. (2013). A finite volume approach for shallow water flow accounting for high-resolution bathymetry and roughness data. *Water Resources Research*, *49*(7), 4126–4135. https://doi.org/10.1002/wrcr.20324

Wei, H., Zhang, L., & Liu, J. (2022). Hydrodynamic Modelling and Flood Risk Analysis of Urban Catchments under Multiple Scenarios: A Case Study of Dongfeng Canal District, Zhengzhou. *International Journal of Environmental Research and Public Health*, *19*(22), 1–18. https://doi.org/10.3390/ijerph192214630

Willems, P., & Smet, K. (2023). Vlamingen kampioen recupereren regenwater. *H2O*, *12*(1), 37–40.

WRIJ. (2023a). Meetgegevens: Brug Doetinchem. Retrieved 9 May 2023, from https://waterdata.wrij.nl/grafiek-kiwis-multi.php?graphid=&tsid=12354042&periode=1jaar&eind=14

WRIJ. (2023b). Waterschap Rijn en IJssel - Open data portaal. Retrieved 6 October 2023, from https://opendata-wrij.opendata.arcgis.com/

Xing, Y., Shao, D., Ma, X., Zhang, S., & Jiang, G. (2021). Investigation of the importance of different factors of flood inundation modeling applied in urbanized area with variance-based global sensitivity analysis. *Science of the Total Environment*, *772*, 145327. https://doi.org/10.1016/j.scitotenv.2021.145327

Xiong, H., Sun, Y., & Ren, X. (2020). Comprehensive assessment of water sensitive urban design practices based on multi-criteria decision analysis via a case study of the university of Melbourne, Australia. *Water (Switzerland)*, *12*(10), 1–37. https://doi.org/10.3390/w12102885

Xu, J., Dai, J., Wu, X., Wu, S., Zhang, Y., Wang, F., … Tan, Y. (2023, February 7). Urban rainwater utilization: A review of management modes and harvesting systems. *Frontiers in Environmental Science*, Vol. 11. Frontiers Media S.A. https://doi.org/10.3389/fenvs.2023.1025665

Yalcin, E. (2020). Assessing the impact of topography and land cover data resolutions on two-dimensional HEC-RAS hydrodynamic model simulations for urban flood hazard analysis. *Natural Hazards*, *101*(3), 995–1017. https://doi.org/10.1007/s11069-020-03906-z

Zeleňáková, M. (2021). Urban rainwater and flood management. *Water (Switzerland)*, Vol. 13, p. 974. https://doi.org/10.3390/w13070974

Zischg, J., Zeisl, P., Winkler, D., Rauch, W., & Sitzenfrei, R. (2018). On the sensitivity of geospatial low impact development locations to the centralized sewer network. *Water Science and Technology*, *77*(7), 1851–1860. https://doi.org/10.2166/wst.2018.060

Zuzulova, V., & Vido, J. (2018). Normalized difference vegetation index (NDVI) as a tool for the evaluation of agricultural drought. *Ecocycles*, *4*(1), 83–87. https://doi.org/10.19040/ecocycles.v4i1.124

Appendices

Appendix A: Classification of vegetation within private properties

Within this study the landcover of private properties is differentiated on neighbourhood scale in vegetated and non-vegetated landcover. This is done by classifying vegetated surfaces within the private property with the Normalised Difference Vegetation Index (NDVI).

The NDVI is a commonly used index to classify vegetated surfaces, due to its effectiveness and incomplexity (Huang et al., 2021). The index is based on the ratio between reflected red (RED) and near-infrared (NIR) light, since plants leaves strongly absorb red light while strongly reflecting near-infrared light. This property is used to classify vegetation. The NDVI can range between -1 and 1, where values below and around zero indicate non-vegetated surfaces, while the closer to 1 the denser the surface is vegetated (Huang et al., 2021; Jiang et al., 2006; NASA, 2023; Sidi Almouctar et al., 2021; Zuzulova & Vido, 2018). Both RED and NIR images needed are available within the Netherlands with a spatial resolution of 25 centimetres for the years 2016, 2017, 2018, 2019, 2020, and 2022. The areal images are obtained by planes during summer conditions. These images are used to calculate the NDVI using Equation (1):

$$NDVI = \frac{NIR - RED}{NIR + RED} \quad (1)$$

Multiple minimal thresholds for the NDVI to classify an area as vegetated are found in literature, such as 0, 0.1, 0.16 and 0.2 (Gaznayee et al., 2023; Huang et al., 2021; Jeevalakshmi et al., 2016; Jiang et al., 2006; NASA, 2023; Sidi Almouctar et al., 2021; Zuzulova & Vido, 2018). This is due to the fact that NDVI values responds linearly with properties of vegetation such as density, health, and growing status, next to uncertainties like scattering, quality of equipment, and alignment of images (Huang et al., 2021; Jiang et al., 2006). For example, Jeevalakshmi et al. (2016) present differing NDVI values for the same surfaces during differing seasons. Therefore, minimal thresholds of NDVI values to classify vegetation can differ for different data sources, seasons, or assessment objectives.

Initial NDVI classification of vegetated and paved surfaces within private properties was conducted using the most recent data from 2022. Nevertheless, it was found by visual comparison between aerial images and surfaces classified as vegetated and paved that a lot of misclassifications was present. This is presumably due to the fact that NIR images are taken in summer, while 2022 did have a dry summer. Since NIR reflectance of plants correlates linearly with health, vegetation under drought stress reflects significantly less NIR light. This negatively affects NDVI value accuracy, resulting in misclassification. Unfortunately, during the period from 2016 to 2022, summers have been (*yet* unusually) dry, with 2016 and 2021 as exceptions (KNMI, 2023b).

Unfortunately, no NIR image is available for the year 2021. Therefore, a comparison between 2022 and 2016 has been made, which had a dry and wet summer respectively.

To test NDVI classification accuracy, it is tested against BGT data (PDOK, 2022c). BGT surfaces contain vegetated surfaces within the public space as well as surfaces classified as buildings, with a classification accuracy of 99% (Rijksoverheid, 2023). For both 2016 and 2022, it is assessed what percentage of BGT vegetated and building surfaces is classified correctly by the NDVI. It is worth noting that barren soil is classified as vegetated in the BGT, but will be classified non-vegetated by the NDVI. Results are shown in Table 7 in the form of a *confusion matrix*. Here, every row adds up to 100%, indicating how much percent is classified correctly (green) by the NDVI with reference to the BGT, and how much percent is classified incorrectly (red).

Table 7: percentages of BGT surfaces correctly (green) and incorrectly (red) classified by the NDVI, for years 2022 and 2016 using different NDVI thresholds values.

		BGT classification			
		Vegetated	*Paved*	*NDVI threshold value*	*Year*
NDVI classification	*Vegetated*	*90.9%*	*9.1%*	*0.10*	*2016*
		90.1%	*9.9%*	*0.16*	
		85.9%	*14.1%*	*0.20*	
		56.6%	*43.4%*	*0.10*	*2022*
		42.4%	*57.6%*	*0.16*	
		26.8%	*73.2%*	*0.20*	
	Paved	*4.0%*	*96.0%*	*0.10*	*2016*
		3.2%	*96.8%*	*0.16*	
		2.2%	*97.8%*	*0.20*	
		14.3%	*85.7%*	*0.10*	*2022*
		10.4%	*89.6%*	*0.16*	
		8.1%	*91.9%*	*0.20*	

In Table 7 it is observed that the accuracy of NDVI classification with reference to BGT classification varies significantly for different years and threshold values. This particularly applies for 2022 which had a dry summer (less NIR reflectance), showing poor performance of the NDVI classification. Therefore, it is decided to use RED and NIR images captured in 2016 to classify private properties into percentages of vegetated and non-vegetated surface, using the 0.1 threshold value. Those images are from 7 years ago, so changes within private properties have occurred inevitably. However, accuracy of the NDVI is considered sufficient on neighbourhood scale.

Appendix B: Model evaluation

This appendix contains figures not shown in *Section 4.1* to save space, which generally show the same patterns as described in *Section 4.1*. Some additional information is given on measurement points and possible reasons why some graphs show consistent differences between measured and modelled values. Generally, it is challenging to determine reasons for differences, since a lot of factors can cause it, in both the real-world (e.g., a broken sewerage pipe) as well as model schematisations (e.g., missing pipes within input data). Moreover, most storm drain outlets are not measured, making an evaluation of a closed water balance impossible. In addition, Doetinchem has a *branched* sewerage system, indicating that sub-catchments of sewerage systems within the city are interconnected.

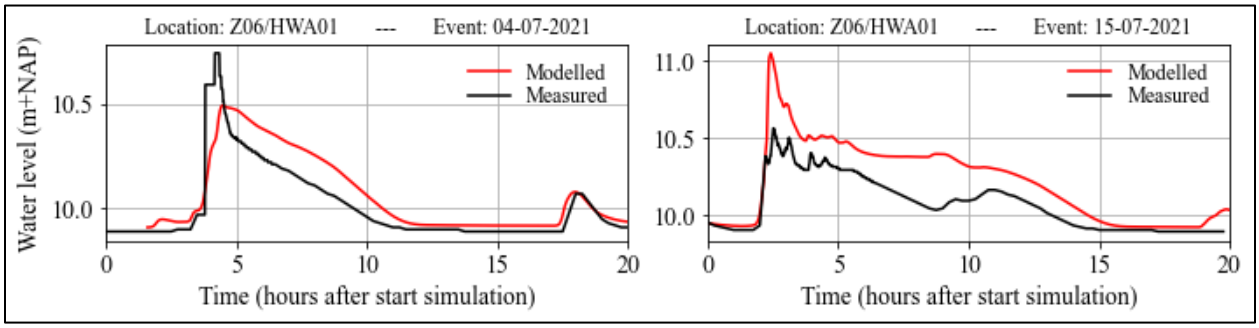

Figure 19: Modelled versus measured water at a storm drain overflow.

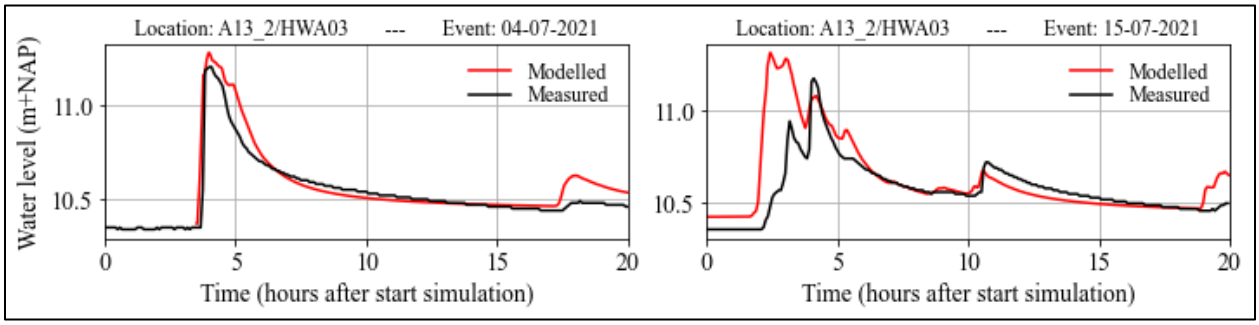

Figure 20: Modelled versus measured water at a storm drain overflow.

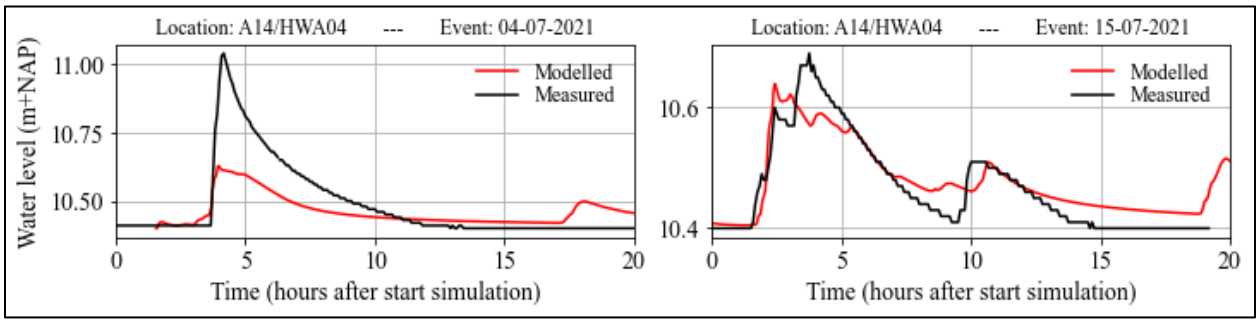

Figure 21: Modelled versus measured water at a storm drain overflow.

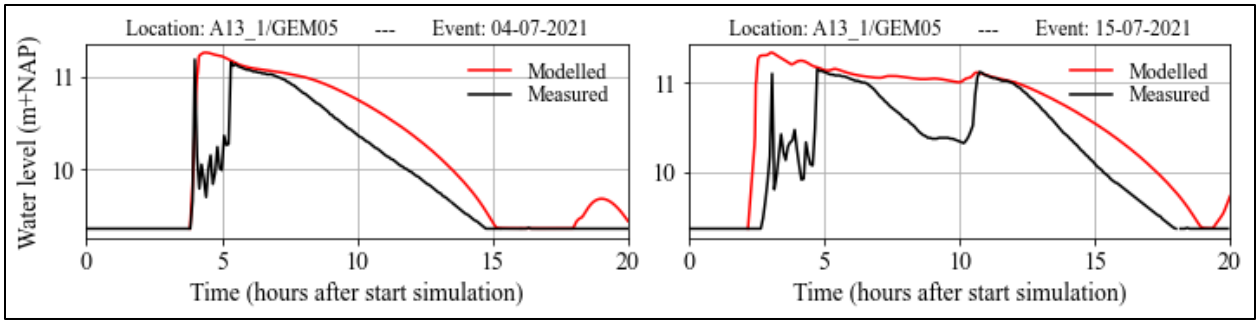

Figure 22: Modelled versus measured water at a mixed sewer overflow.

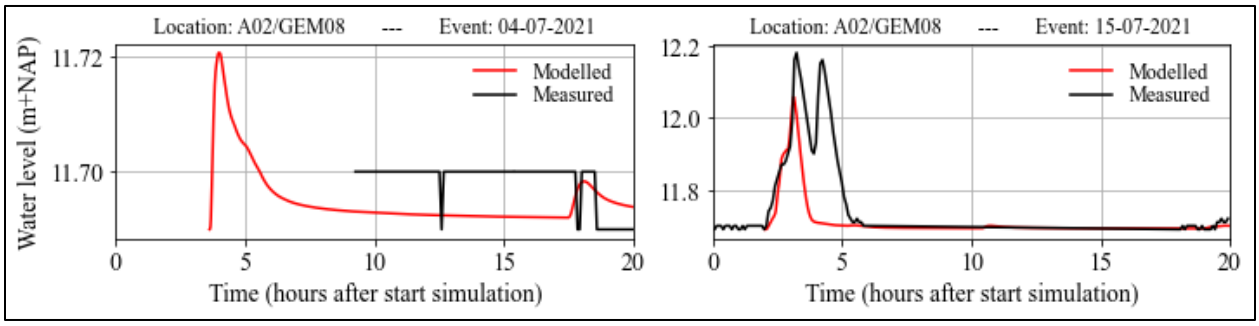

Figure 23: Modelled versus measured water at a mixed sewer overflow.

Figure 24 shows an internal sewerage storage tank *Z04/BB1*, used when the capacity of pipes is insufficient to discharge the amount of excessive rainwater. This storage tank is then temporarily filled with sewage and rainwater to prevent sewer overflows. It is pumped back into the sewerage pipes at a later moment. Within the model it is schematised as 1 compartment, while in reality it consists of four compartments with differing internal weir crest levels and pumps. So, water levels can be deviating due to this reason. Yet, the maximum volume that can be stored by the storage tank is the same.

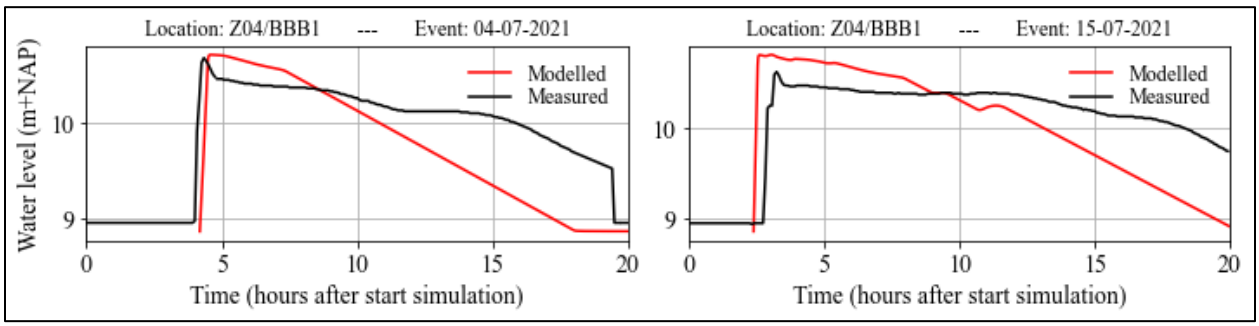

Figure 24: Modelled versus measured water in an internal storage tank.

While following patterns of peaks and decreasing water levels, measurement locations *A04/GEM06* and *A05/GEM09* show consistent deviation of modelled values with reference to measured values. This suggests either a fault in the measuring sensor, or a fault in heights of sewerage pipes within the model. Therefore, height levels of pipes at measurement location within the model and the administrative data of *Telecontrolnet* is compared.

At location *A04/GEM06* pipes within the model lie 1 metre lower than found in administrative data within the municipal database *Telecontrolnet*. This is likely a fault in input data when the model was constructed. To support this observation, modelled values have been heightened by 1 metre in Figure 25, indicated by a dotted line. The new dotted line is close to the measured line, and shows the generally consistent pattern of under- and overestimation at the 4th and 15th respectively. It indicates that the deviation is caused by wrong input data of by pipe height for this location.

At location *A05/GEM09* pipes within the model lie 90 centimetres higher than found in administrative data within *Telecontrolnet*. Pipes lie at 9.28 m+NAP within *Telecontrolnet*, with a sensor height of 9.62 m+NAP. Differences between modelled and measured graphs can be explained by discrepancies between modelled and real-world pipe bottom heights at this location. This has to be taken into account when interpreting outcomes with reference to sewerage outflows on these locations. The sewerage system manager is looking into the source data used for model building after those findings.

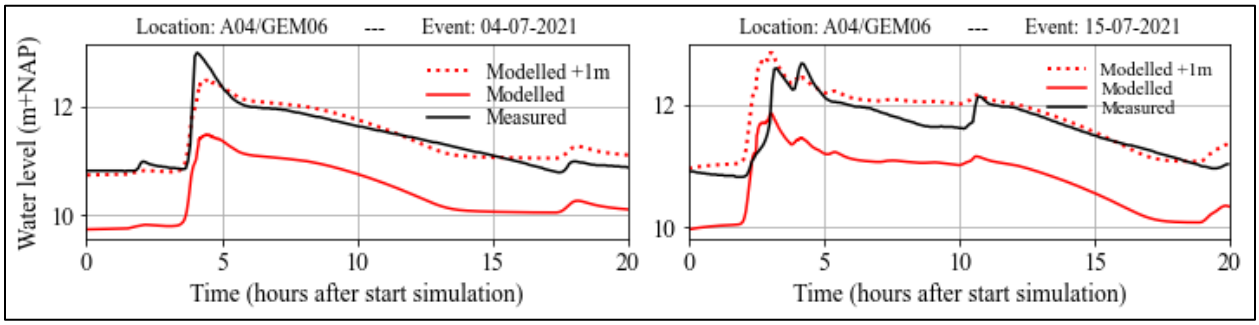

Figure 25: Modelled versus measured water at a mixed sewer overflow.

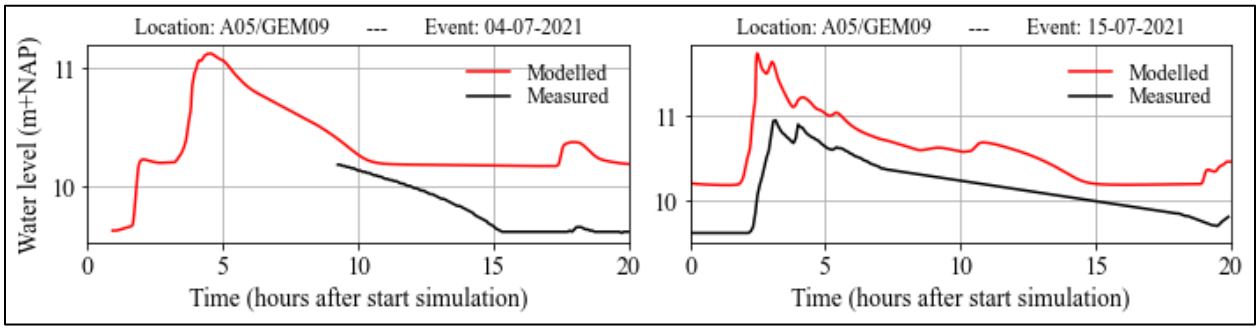

Figure 26: Modelled versus measured water at a mixed sewer overflow.

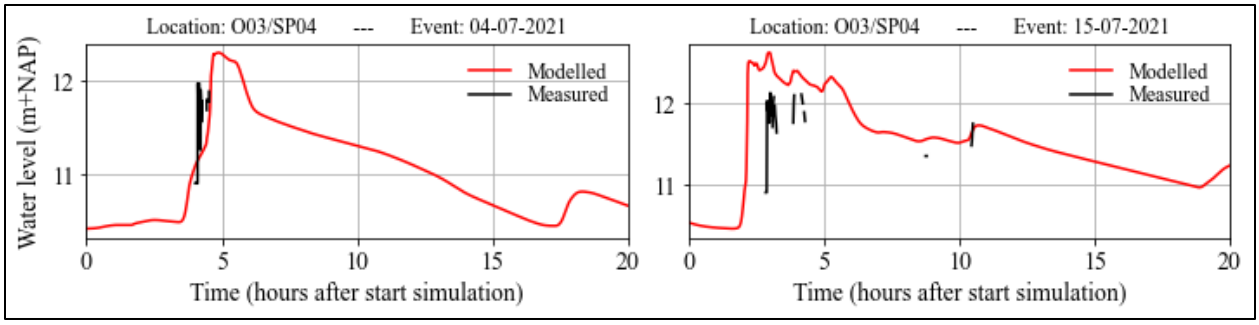

Figure 27: Modelled versus measured water at an internal weir.

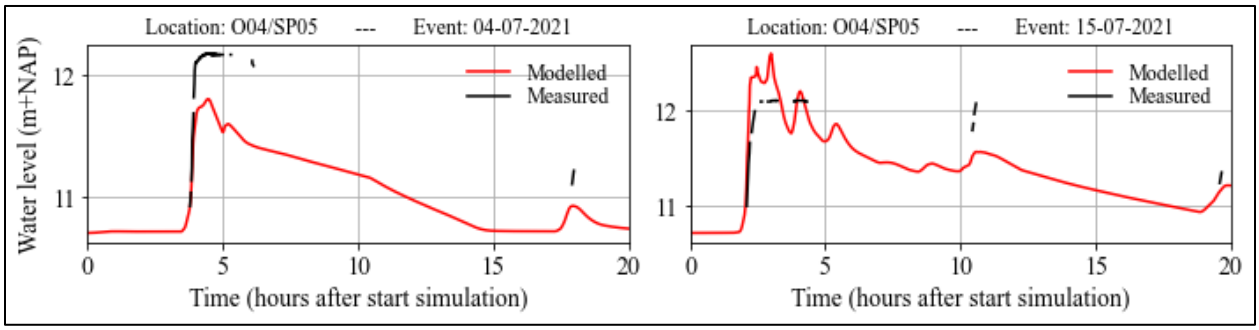

Figure 28: Modelled versus measured water at an internal weir.

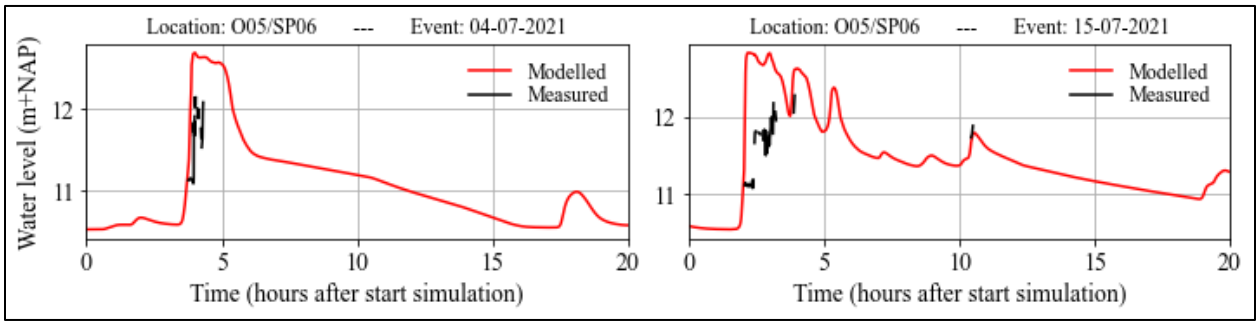

Figure 29: Modelled versus measured water at an internal weir.

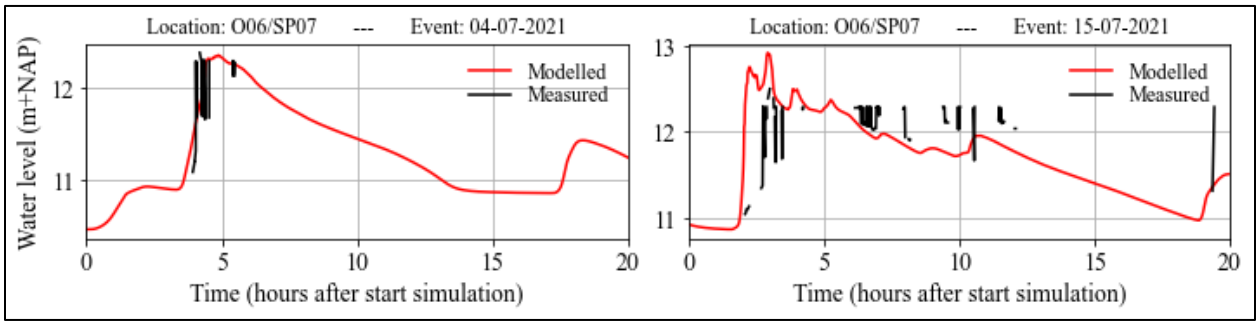

Figure 30: Modelled versus measured water at an internal weir.

Minimum water levels consistently deviate between measured and modelled values at locations *Z07/SP03* and *Z08/SP02*. Measured water levels do not go below 10.03 and 10.4 m+NAP respectively, while modelled values do. This is due to the fact that measurement devices at these

locations are not placed on the bottom of pipes, but halfway. Modelled values can indicate values below bottom levels of measurement devices.

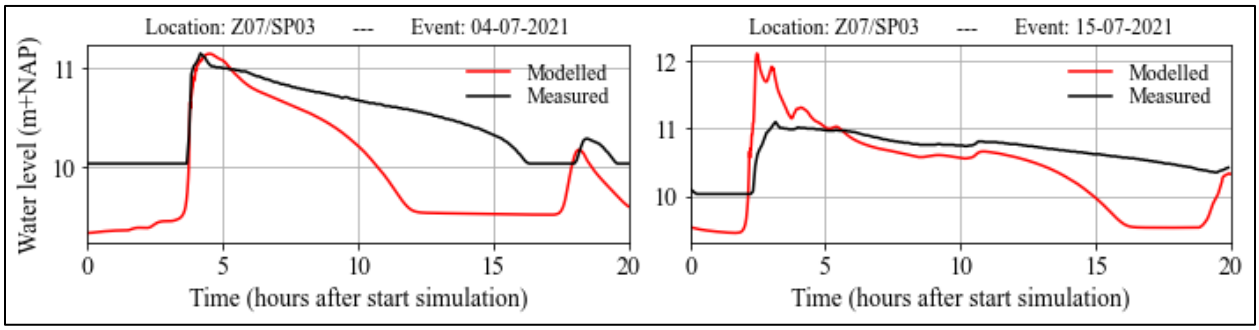

Figure 31: Modelled versus measured water at an internal weir.

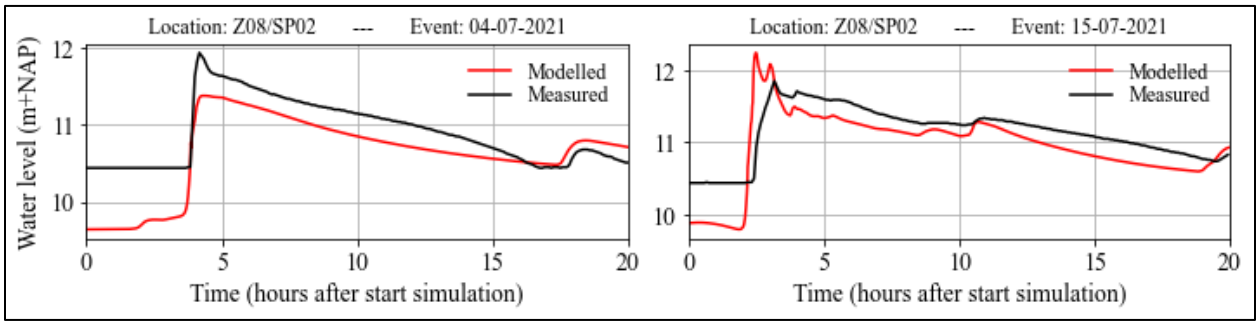

Figure 32: Modelled versus measured water at an internal weir.

Appendix C: Adaptation measures

Figure 33 presents the locations of the vegetated parts which will be lowered to schematise scenarios ‘Road10’ and ‘Wadi30’, together with their cumulative surface area. It is seen that lowered surfaces are not evenly distributed throughout the study area.

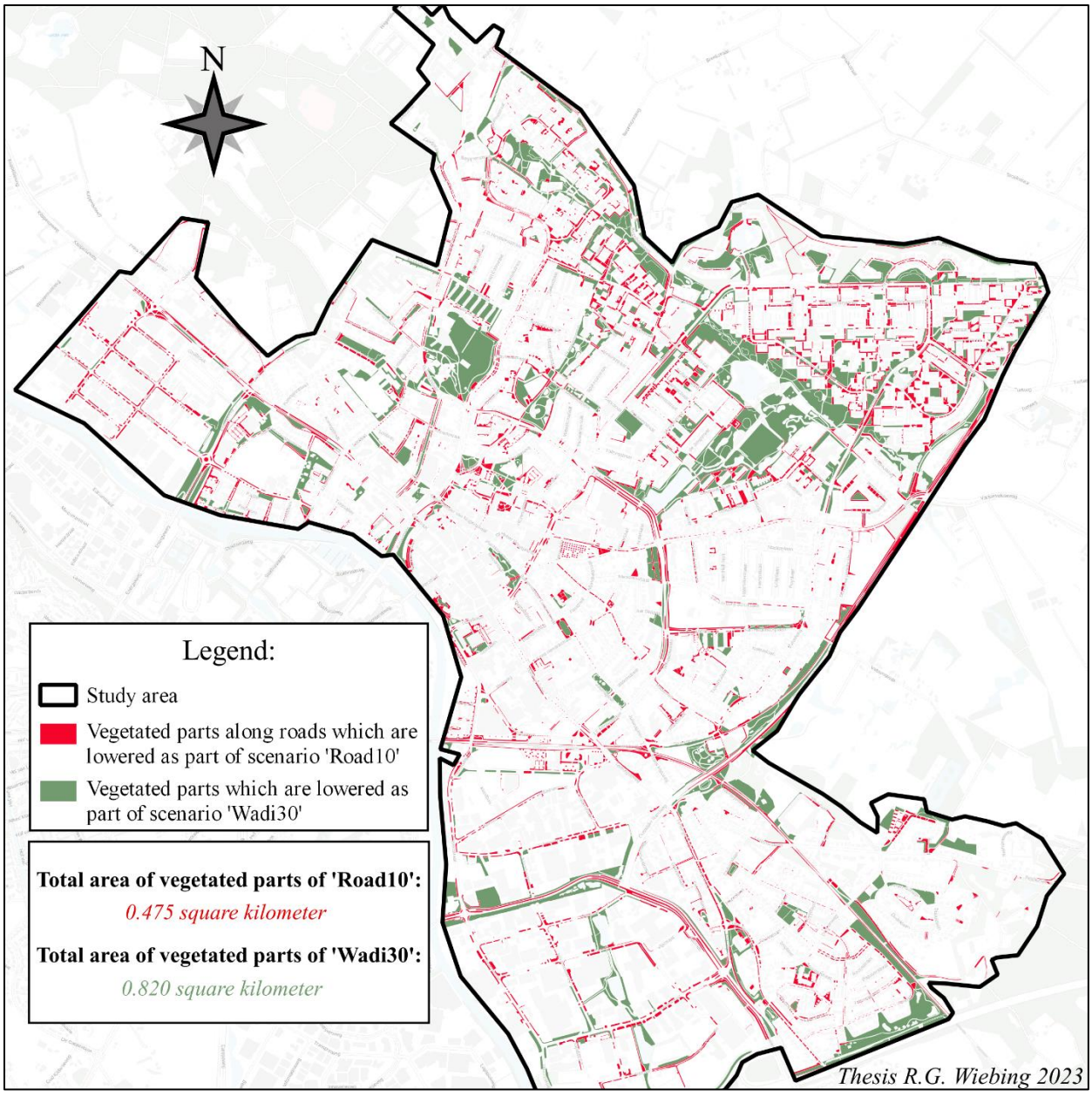

Figure 33: Vegetated parts which are lowered as a result of scenario 'Road10' and 'Wadi30'.

Vegetated parts along roads

Vegetated parts along roads will be lowered to 10 centimetres below adjacent road surface elevation, thus relating them to the nearest height level of road surfaces. Since a significant portion

of vegetated parts along roads are narrow but stretched, maximal height level differences within those parts can be significant due to a (mildly) sloping landscape. Therefore, surfaces which will be lowered are divided into smaller sections of maximal 8 by 8 metres (computational cells). These sections are lowered to the lowest height level of a road surface within the same computational cell (see Figure 34). For example, section 1b, 2b, and 3b will be lowered to the lowest height level within section 1a, 2a, and 3a respectively. Section 4, where a road surface is not present within the computational cell, will get a height value of the average of adjacent cells which are adjacent to road surfaces. So, section 4 will get a height value which is the average height value of sections 2b and 3b.

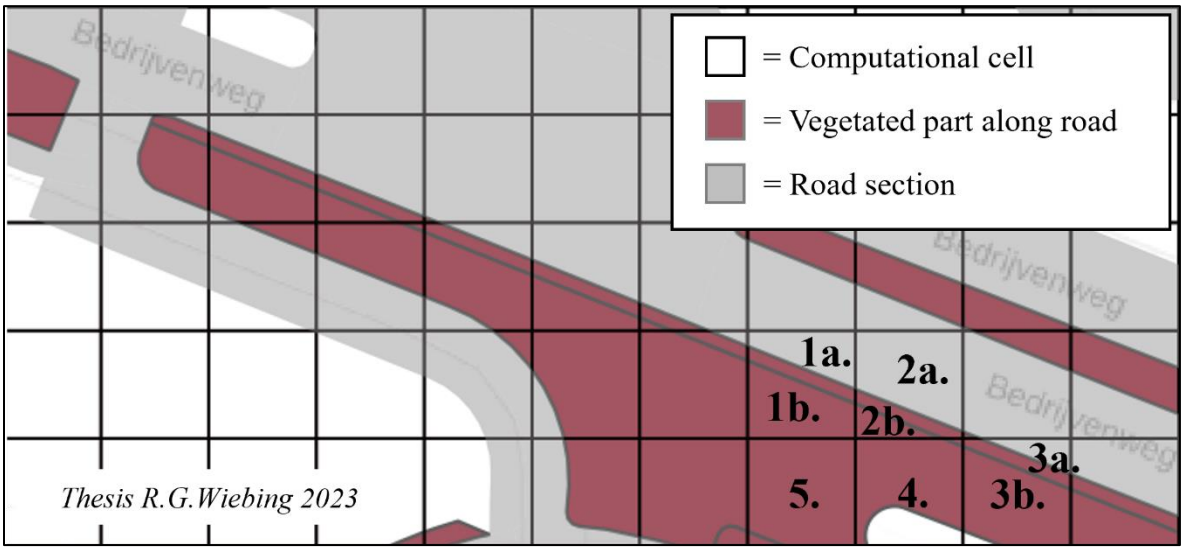

Figure 34: Computational grid overlapping vegetated surfaces along road sections.

Appendix D: Design rainfall events

Table 8 shows rainfall depths per timestep for 1-hour design rainfall events that are commonly used within the Netherlands. Depths of Composite and Uniform events are based on current climate conditions (they are also available for climate scenarios).

Table 8: rainfall depth per 5-minute time step for 1-hour design rainfall events (composite events are based on current climate conditions)

Time (minutes):	*0-5*	*5-10*	*10-15*	*15-20*	*20-25*	*25-30*	*30-35*	*35-40*	*40-45*	*45-50*	*50-55*	*55-60*	*Total*
	(mm)	*(mm)*	*(mm)*	*(mm)*	*(mm)*	*(mm)*	*(mm)*	*(mm)*	*(mm)*	*(mm)*	*(mm)*	*(mm)*	*(mm)*
						T = 2:							
Composietbui	0.4	0.5	0.7	0.9	1.4	6.1	6.1	1.4	0.9	0.7	0.5	0.4	20.0
Bui08	0.3	0.6	0.9	1.2	1.5	2.1	2.7	3.3	3.3	2.1	1.2	0.6	19.8
						T = 10:							
Composietbui	0.7	0.9	1.1	1.5	2.5	8.8	8.8	2.5	1.5	1.1	0.9	0.7	31.0
Bui10	1.8	3.6	6.3	6.3	5.7	4.8	3.6	2.7	1.2	0.0	0.0	0.0	35.7
						T = 100:							
Composietbui	1.5	1.9	2.4	3.2	5.5	14.4	14.4	5.5	3.2	2.4	1.9	1.5	57.8
Uniform	4.8	4.8	4.8	4.8	4.8	4.8	4.8	4.8	4.8	4.8	4.8	4.8	57.6

Figure 35 shows the intensity distributions of commonly used design rainfall events within the Netherlands. The distributions are given as a fraction of the total depth of the event. The Composite intensity distribution shown is valid for an event with a recurrence time of 10 years, for current climate conditions. Composite events with a different recurrence time or for other climate scenarios will differ slightly in terms of fractions per timestep.

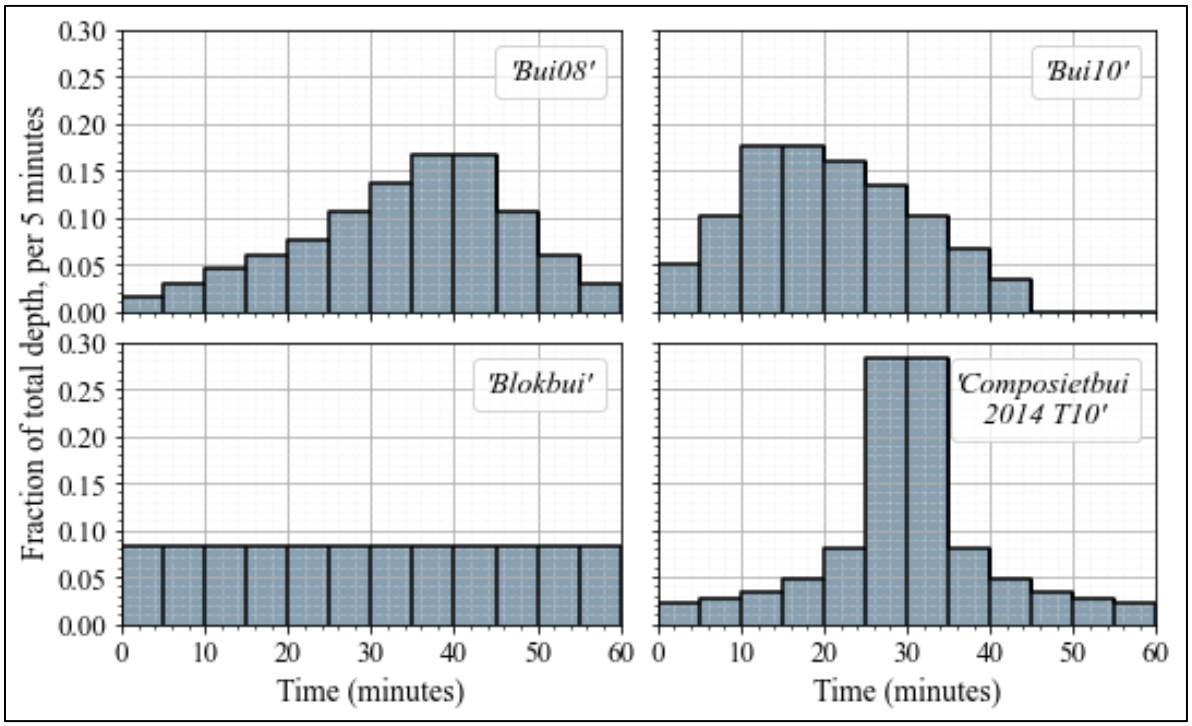

Figure 35: Rainfall intensity distributions of design events

Table 9 shows a comparison among maximum rainfall depths of 10-, 30-, and 60-minute periods of commonly used design rainfall events with latest insights presented in Beersma et al. (2019). All values are based on current climate conditions. It is seen that all durations within composite events match their recurrence time. On the contrary, Bui08, Bui10, and the Blokbui underestimate maximum intensities for shorter durations within a rainfall event.

Table 9: Comparison among design rainfall events and found literature values of Beersma et al. (2019).

	Maximum in 10 minutes	Maximum in 30 minutes	Maximum in 60 minutes
	T = 2:		
Beersma et al. (2019)	12.2 mm	16.6 mm	20.0 mm
Composietbui	12.2 mm	16.8 mm	20.0 mm
Bui08	6.6 mm	15.0 mm	19.8 mm
	T = 10:		
Beersma et al. (2019)	17.5 mm	25.3 mm	31.0 mm
Composietbui	17.6 mm	25.6 mm	31.0 mm
Bui10	12.6 mm	30.3 mm	35.7 mm
	T = 100:		
Beersma et al. (2019)	28.7 mm	45.8 mm	57.7 mm
Composietbui	28.8 mm	46.2 mm	57.8 mm
Blokbui	9.6 mm	28.8 mm	57.6 mm